NASA TECHNICAL MEMORANDUM

NASA TM-88531

ZHAMANSHIN METEOR CRATER

P.V. Florenskiy and A.I. Dabizha

Translation of "Meteoritniy krater Zhamanshin," Moscow, Nauka Press, 1980, pp. 1-127.

NATIONAL AERONAUTICS AND SPACE ADMINISTRATION
WASHINGTON, D.C. 20546 JANUARY 1987

STANDARD TITLE PAGE

1. Report No.	2. Government Accession No.	3. Recipient's Catalog No.
NASA TM-88531		

4. Title and Subtitle	5. Report Date
ZHAMANSHIN METEOR CRATER	January 1987
	6. Performing Organization Code

7. Author(s)	8. Performing Organization Report No.
P.V. Florenskiy and A.I. Dabizha	
	10. Work Unit No.

9. Performing Organization Name and Address	11. Contract or Grant No.
Leo Kanner Associates Redwood City, California 94063	NASW-4005
	13. Type of Report and Period Covered
	Translation
12. Sponsoring Agency Name and Address	
National Aeronautics and Space Administration, Washington, D.C. 20546	14. Sponsoring Agency Code

15. Supplementary Notes

Translation of "Meteoritniy krater Zhamanshin," Moscow Nauka Press, 1980, pp. 1-127.

16. Abstract

A historical survey and geographic, geologic and geophysical characteristics, the results of many years of study of the Zhamanshin meteor crater in the Northern Aral region, are reported, from which data the likely initial configuration and cause of formation of the crater are reconstructed. Petrographic and mineralogical analyses are given of the brecciated and remelted rocks, of the zhamanshinites and irgizite tektites in particular. The impact melting, dispersion and quenching processes resulting in tektite formation are discussed.

17. Key Words [Selected by Author(s)]	18. Distribution Statement
	Unclassified-Unlimited

19. Security Classif.(of this report)	20. Security Classif. (of this page)	21. No. of pages	22.
Unclassified	Unclassified	136	

ANNOTATION

The results of many years of study of the Zhamanshin meteor crater (Northern Aral region) by a set of geological and geophysical methods are reported in the work. A petrographic and mineralogical analysis is given of the brecciated and remelted rock found in the crater. The presence of irgizite tektites, found for the first time in the meteor crater, is of particularly great importance.

The publication is intended for investigators of meteorites and meteor craters on the earth and other planets, as well as for people engaged in mineralogy, petrography and geology.

FROM THE EDITOR

Forty years ago in 1939, while working in the Northern Aral region, which is composed of gently sloping Tertiary sedimentary rocks, I noticed a small section where Paleozoic metamorphic basement rocks were found on the surface **(133)**. This place, then called Zhibinyn-Tau is designated the Zahamanshin natural landmark on modern maps.

It has been shown by the work of the last 15 to 20 years that, approximately 700,000 years ago, a gigantic meteorite fell here and the basement rock was ejected from a 700 meter crater as the result of an explosion, the energy of which reached that of tens of thousands of megaton bombs. The pressure increased to hundreds of kilobars and megabars, when high pressure minerals (coesite, shtishovite) and even high pressure carbon (lonsdaleite, found in particular in Ries meteor crater (FRG)) can be formed **(138)**. The temperature in the region of the explosion was several thousand degrees, which caused melting and vaporization of substantial rock masses.

Although more than a hundred explosive meteor craters have been found on the earth, Zhamanshin meteor crater is a unique phenomenon even among them, because of the presence of tektites around it, which are called irgizites in this place. As is shown in this book, tektites are among the most final products of ultrahigh temperature differentiation of matter. An incandescent cloud is formed in an explosion, which contains silicate vapors and aerosol and can move a substantial distance, after which the condensation and falling out of glassy drops to the earth occur. Actually, tektites have so far been found scattered among young sedimentary rocks and their paragenesis with meteor craters has been demonstrated only indirectly. A series is present in Zhamanshin crater from basement sedimentary and metamorphic to calcined and remelted rocks (impactites and further to irgizite tektites).

Direct planetological studies have permitted demonstration of the leading role of meteor bombardment in the formation of various shells of a planet in early stages of its development, as well as in the formation of the surfaces of small (without atmosphere) planets and their satellites. Moreover, glasses similar to those found in Zhamanshin crater have been found in the lunar regolith, study of which is being conducted in parallel with study of irgizites (a series of methods applied to study of the regolith was worked out on irgizites). The tektite problem is therefore both a geological and physical chemistry problem and a planetological and space problem.

Zhamanshin meteor crater naturally attracted great interest of

both domestic and foreign investigators. Immediately after identification of its glassy irgizite droplets with tektites **(42-44, 50-53)**, a combined program of study of Zhamanshin crater and irgizites was developed, which now is being carried out under the direction of the Committee on Meteorites, USSR Academy of Sciences. Samples and necessary information have been made available to all organizations which have expressed a desire to participate in the study of irgizites. As a result, study of them is being conducted by more than 25 scientific organizations of the USSR, Australia, GDR, USA, FRG, and Czechoslovakian SSR and the number of published articles is several tens. By the efforts of the authors, an international group of investigators has been created, which is occupied in study of irgizites and problems connected with them. Besides, student geologists of the Moscow Institute of the Petrochemical and Gas Industry im. I.M. Gubkin and the Moscow State University im. M.V. Lomomosov have been attracted to the studies, since the training of future scientists should be carried out on the most interesting and timely material.

The present book presents a summary of 20 years of study of the Zhamanshin structure as a meteor crater and of its irgizite tektites. However, the answers found to a series of questions permitted the raising of fundamentally important problems, the solutions of which go far beyond the framework of the book. These are practically important geological problems of structure and mineralogy of explosive craters, physical chemistry problems of the behavior of matter at ultrahigh temperatures and pressures and cosmogonic problems of the histories of formation of the planets, their satellites, asteroids and meteoroids, especially in early stages of their histories.

A.L. Yanshin

PREFACE

Individual "hot" points can be noted in the history of science, which give rise to particuarly sharp disputes, questions and contradictory interpretations. This is not accidental. In searching for answers to just such, sometimes mysterious questions, many fundamental problems are posed to investigators, in which the most important, sometimes unexpected problems, the importance of which goes far beyond the framework of the initial discussion, are grouped at the focus. The object of such studies stand as a rule on the dividing line between different processes, different phenomena and different forces, but the most puzzling and mysterious questions of all are those where terrestrial materials and phenomena meet space energies and matter. Gigantic volumes of energy are liberated here, which permit the study of matter and processes under extreme conditions. Thus for example, because of the superpower of cosmic ray energies, success has been achieved in both obtaining information on the universe and in the discovery in a number of fundamental regularities of the structure of matter.

The agelong controversy in geology of the Neptunists and Plutonists which, after being modernized is again flaring up in the problem of the origin of granites or the formation of petroleum or in discussion of the polycyclic nature and periodicity or causes of tectogenesis, is not accidental. Such a universal and at the same time unique position of the study of the role of internal and external factors in geology is natural, since it reflects the main conflict which moves geologic processes, the conflict of internal and external factors of the development of the planet. B.L. Lichkov **(90)** showed the decisive role of this conflict. Where terrestrial forces (gravity) and extraterrestrial energy, the energy of repulsion (heat, solar) are found, very interesting geological processes occur.

The tendencies of evolution of surface matter of small planets without atmospheres and large earth type planets surrounded by a hydrosphere and atmosphere are diametrically opposite **(132)**. On small planets which do not have these active shells, like the moon and Mercury for example, transformation occurs very slowly. On the other hand, the surfaces of large planets change continually and are renewed by processes which occur because of a mobile, active atmosphere and hydrosphere. On small planets which, because of weak gravity, are not capable of holding gases, water, as well as many light elements, the material balance of the surface is negative. Matter sublimes, vaporizes, is lost in the eruptions of volcanos and by meteor bombardment. K.P. Florenskiy first noted this **(109)** in descriptively comparing the surface of the moon with the surface of the thawing and subliming Martian snow. Heating up by day, the surfaces of small planets are cooled at night, completely losing the accumulated heat and endogenous heat is lost. Thus, the material and energy balances of the surfaces of small

planets where vacuum reigns is negative.

On large planets such as earth, because of considerable gravity, volatile compounds are retained, and the mobile atmosphere and hydrosphere, products of vulcanism and the results of meteor bombardment are preserved. Minerals are formed in the weathering process which are saturated with these volatile compounds, primarily oxygen, carbon dioxide and water, and carbonates and organic compounds are formed. By destroying and transporting material, water and air fix solar energy in sedimentary formations. More than that, sedimentary minerals fix this space energy in their crystal lattices. Heat which has reached the earth from the sun and been "petrified" in the geologic past is extracted directly from such compounds as petroleum and coal. The material and energy balances of the lithosphere of the earth relative to space is consequently positive. This is the fundamental difference of the surfaces of large and small planets of the terrestrial group.

A completely different, catastrophic type of interaction of a planet and space is the collision of space bodies. Besides the abovementioned cosmic rays, the planet is struck by space dust, micrometeoroids, meteroids of various sizes, and the collision of gigantic meteroids which are essentially asteroids with the planet also occur. Energetic and thermodynamic anomalies occur at the collision sites which frequently exceed conventional geologic processes in scale. For example, in the formation of the more than 5.5 km diameter Zhamanshin crater, a practically instantaneous explosion occurred, in which energy of 10^{25} ergs was released in 1 s. We note that the explosion of a megaton bomb releases 10^{22} ergs, approximately as much as was released during the most immense volcanic explosions. The crater from a megaton bomb has only a 200 m diameter **(42)**. The pressure and temperature are just as high in a meteorite explosion. The pressure is over hundreds of kilobars and even megabars, and the temperature is more than many thousands of degrees, when complete vaporization of rock material is possible. The pressure only rarely reaches a kilobar in volcanic eruptions, and the lava temperature is 1200 °C. The processes therefore occur under extreme conditions at the sites of explosions of gigantic meteors, when new minerals are formed, for example coesite, stishovite, lonsdalite and diamond, which cannot be formed in conventional geologic processes. At the points of impact of gigantic meteors, ultrahigh temperatures develop and normally relatively immobile substances prove to be volatile. From rocks subjected to high temperature treatment, not only are gases and water volatilized, but even potassium, sodium, silicon and other elements, i.e., matter does not evolve by the terrestrial pathway but by the pathway of evolution of matter on the surfaces of small planets. Therefore, such local areas shed light not so much on terrestrial as on other planet phenomena or phenomena characteristic of the earth in the initial stages of its accretion. Study of meteor craters and the final products of evolution of their matter (tektites) is a planetological and more than that

cosmogonic problem. This approach was formulated by K.P. Florenskiy **(41)** in setting up problems of study of the consequences of the Tungusska meteor explosion. He showed that gigantic volumes of matter melted and vaporized at the time of meteor explosions transformed both the appearance and the composition of the protoplanet surface material and could have formed the atmosphere and hydrosphere in the early stages. A similar extremely general formulation of the problem of study of meteor explosions and their products permits them to be considered on the one hand as a unique phenomenon on the surface of the earth and on the other hand by contrast, phenomena common to all planets which determine their evolution to be seen in them. The positions indicated were taken as the initial positions in the present work.

Interest in meteorite structures increased sharply at the end of the 1950's, and the number of craters discovered and the number of publications increased **(135)**. The study of meteor craters is one of the most timely problems of geology, interest in which is due to three factors which coincide in time: 1) a new stage of direct study of other planets and their satellites, the surfaces of which were formed to a considerable extent by crater formation processses; 2) the development of experimental studies when ultrahigh pressures and temperatures close to those generated in meteor explosions are obtained in laboratory conditions; 3) the discovery of a large number of structures, the formation of which could be understood only from the point of view of the impact meteorite hypothesis. (The contradictory nature of explanation of the genesis of these structures has long been well known as a rule and was noted earlier from the point of view of the endogenous hypothesis.)

In the light of what has been said, the Zhamanshin meteor crater, located in the Northern Aral region (its coordinates are 61° East Longitude and 48° 20' North Latitude) was not an exception. V.A. Vakhrameyev and A.L. Yanshin **(133)** first drew attention to it in 1939, when they noted the presence of Paleozoic rocks in a field of widespread Cenozoic rocks in the Zhibynin-Tau mountain region. This site later began to be called the Zhamanshin natural landmark on topographic maps. Twenty years later in 1960 during survey work, B.V. Piliya found glass here **(86)**, which P.V. Florenskiy then began to study. The natural landmark region was first examined from the point of view of the meterorite hypotheis in 1966. Field observations have been conducted nearly annually since then. L.G. Kiryukhin, V.P. Kryuchkov and N.M. Skobeleva participated in them during this time. The structurally anomalous nature of the natural landmark, the extremely unusual composition of the glasses and scoria, among which pure lechatelierite was found, and glass drops similar in composition to tektites, permitted expression of the hypothesis of the explosive origin of the structure. The first article devoted to this question was entitled "The Zhamanshin riddle" **(82)**.

Information on the crater was included in surveys and catalogs of impact meteorite structures **(150, 95-97, 17, 26, 34, 56, 94, 104, 119, et al.).** However, Zhamanshin continued to be considered on geologic maps and in publications to be an isometric local uplift **(11, 60, et al.)** and the glasses to be considered the product of Cenozoic volcanism **(86, 88).**

The explosive origin of the Zhamanshin crater structure, classification as impact slags which were called Zhamanshinites and identification of glass jets with tektites, which received the name "irgizites" from the name of the Irgiz River flowing 15 km from the crater were successfully demonstrated by 1975 **(42, 43).** Tektites were discovered thus right in a meteor crater for the first time in the world. A report of this was published in the press here and abroad. Interest is continually increasing in irgizite tektites **(134, 69, 44, 45, 50-53, 16, 75, 28, et al.).**

A combined study of material from Zhamanshin crater was begun by both domestic and foreign organizations. Irgizites and Zhamanshinites were sent to many scientific institutions of the USSR, GDR, Czechoslovakian SSR, Australia, India, USA, FRG and other countries.

An extensive international group of investigators is occupied in study of the crater and the material found in it. Work is being conducted by an approved program coordinated by the Committee on Meteorites, USSR Academy of Sciences. In 1977-1978, the Committee on Meteorites organized a combined geological and geophysical expedition to study Zhamanshin crater **(46).** The role of USSR Academy of Sciences Associate Member V.V. Fedynskiy was invaluable in organization of this expedition.

Beside the authors of the present monograph, A.O. Aaloe, A.V. Alyunin, O.I. Alyunina, V.I. Vlasov, E.S. Gorshkov, B.A. Datsuk, S.V. Isayeva, P.K. Kirillov, S.K. Kistaubayev, V.N. Krupko, V.I. Miklyayev, L.A. Nazarova, V.A. Nikonov, V.I. Nikonova, A.P. Pushel', B.S. Sadykbayev, V.A. Fedorov, Ye.M. Florenskaya, V.P. Florenskiy, Ye.Ye. Chernenko, L.A. Chuyanova, O.M. Shipilov and others participated in the work of the expeditions. Special studies have been conducted since 1977 by the Western Kazakhstan Geologic Administration (Director B.Ye. Miletskiy, Chief Geophysicist A.P. Bachin). A core drilling well has been drilled in the center of the crater (1977), and detailed geological and geophysical surveys are being conducted. In 1978, the Kustanay expedition of the Kazakhstan SSR Ministry of Geology made two seismic profiles through the crater. The soil science survey was conducted in this same year by G.V. Zonov (Institute of Soil Science, Kazakhstan SSR Academy of Sciences), and archeological observations were made in 1976 by V.D. Aubekerov and A.G. Medoyev (Kazakhtan SSR Academy of Sciences Institute of Geological Sciences im. K.I. Satpayev).

Studies of material from the crater are being conducted simultaneously. N. Short (NASA, Greenbelt, USA) has described planar structures from breccias and the petrography of individual samples **(55)**. Determination of the rock forming elements in different samples was made by Yu.F. Pogrebnyak (Institute of Geology and Geophysics, Siberian Section, USSR Academy of Sciences), I.M. Varentsov (GIN* USSR Academy of Sciences), N.Ch. Mavyyev (Turkmen Polytechnic Institute, Ashkhabad), V.L. Masaytis (VSEGEI,* Leningrad), W.D. Ehmann, W.B. Stroube, Jr., M.Z. Ali and T.I.M. Hossain (University of Kentucky, USA) **(33)** and K. Fredricsson (Smithsonian Institution, USA) **(57)**.

Determination of minor and rare earth elements was done by J.A. Philpotts and S. Schuhmann (NASA, Greenbelt, USA), S.R. Vintser (Baltimore, USA), R.K.L. Lum (University of Maryland, USA) **(110)**, H. Palme (MAX Planck Institute, Mainz, FRG), R. Wolf and R.A.F. Grieve (Ottawa, Canada) **(105)**, S.R. Taylor and S.M. McLennan (Australian Natl. Univ., Canberra) **(129)**, V. Boushka (Charles Univ., Prague, Czechoslovakian SSR) and Z. Rzhanda (Kutna Hora, Czechoslovakian SSR).

The water content of irgizites was determined by E.A. King and J. Arndt (Tubingen University, FRG) **(80)**. The gas composition of the rocks was studied by Yu.F. Pogrebnyak and L.V. Firsov (Institute of Geology and Geophysics, Siberian Section, USSR Academy of Sciences) and K. Heide and H.-G. Schmidt (Jena University, GDR) **(74)**. The absolute age of glasses from the crater was established by the fission track method by D. Storzer (Paris Mineralogical Museum France) and G.A. Wagner (Heidelberg University, FRG) **(128)** and V.P. Perelygin, D. Lkhagvasuren and S.G. Stetsenko (Joint Institute of Nuclear Research, Dubna), by the paleomagnetic method by L.M. Bazhenov (GIN, USSR Academy of Sciences) and by the potassium-argon method by L.V. Firsov (Institute of Geology and Geophysics, Siberian Section, USSR Academy of Sciences.) The magnetic properties of the rocks were determined by A.de Gasparis (NASA, Greenbelt, USA) **(57)** and E.S. Gorshkov (Institute of Terrestrial Magnetism, The Ionosphere and Radiowave Propogation, USSR Academy of Sciences, Leningrad). Irgizite glass surfaces and chips were photographed under a scanning electron microscope by R.A. Bochko and V.A. Kuz'min (Moscow Institute of the Petrochemical and Gas Industry im. I.M. Gubkin) and K. Heide (Jena University, GDR). Particuarly interesting and fundamentally important results were obtained in study of the atomic and molecular structure. T.S. Gendler and R.N. Kuz'min (Institute of Physics of the Earth, USSR Academy of Sciences) applied Mossbauer spectroscopy for study of the iron in tektites **(62)**, and Yu.P. Dikov (IGEM, USSR Academy of Sciences) conducted X-ray spectral studies of a number of tektite and breccia specimens which, in particular, permitted the finding of high pressure phases of silica (coesite and stishovite) **(47, 55)**. Coesite in Zhamanshinites was determined later by S.A. Vishnevskiy and N.A. Pal'chik (Institute of Geology and Geophysics, USSR Academy of Sciences) **(137)**. Great good in continuous discussions

* Translator's note: GIN, Institute of Geology; VSEGEI, All-Union Scientific Research Institute of Geology.

on the origin of tektites was brought in by J. O'Keefe (NASA, Greenbelt, USA).

The Historical Survey, Geophysical Characteristics of the Crater (except the Seismic Survey subsection) and Crater Reconstruction sections were written by A.I. Dabizha and the remainder by P.V. Florenskiy. During work on the book, the authors repeatedly discussed material with A.V. Ivanov and O.A. Yakovlev (Institute of Geochemistry, USSR Academy of Sciences), B.A. Ivanov (Institute of Physics of the Earth, USSR Academy of Sciences), V.L. Masaytis (VSEGEI, Leningrad) and many others. K.P. Florenskiy (Institute of Geochemistry, USSR Academy of Sciences), Yu.P. Dikov (IGEM* USSR Academy of Sciences), and the scientific editor of the book, Academician A.L. Yanshin, under whose direction studies of Zhamansin crater are coordinated, showed particularly great help with their advice and criticism.

A.D. Vishnevskaya, N.I. Zaslavskaya, V.M. Liskina and Ye.I. Malinkin provided great help in preparation of the book for publication.

The authors thank everyone who collaborated to some extent in study of Zhamanshin meteor crater and the formations found in it.

* Translator's note: IGEM, Institute of Geology of Ore Deposits, Petrography, Mineralogy and Geochemistry.

TABLE OF CONTENTS

ZHAMANSHIN METEOR CRATER

P.V. Florenskiy and A.I. Dabizha

HISTORICAL SURVEY

The history of study of meteor craters on the earth can be /10* arbitrarily broken down into three stages: the first, from the end of the 19th century to 1950; the second, from 1950 with the discovery of meteor craters in Canada and their active study in this country; modern, the last one and a half to two decades, connected with space methods of study of the planets and their satellites (Earth, Moon, Mars, Mercury, Phobos, Deimos and even Jupiter with its satellites).

Even as far back as the 17th century, Robert Hooke (1665) proposed an explanation of the origin of lunar craters as a result of meteorite impacts, which he reinforced with modeling tests by the impacts of peas on wet clay. Only at the end of the last century however was the hypothesis advanced that the formation of some depressions on the surface of the earth was connected with the collisions of meteorites. G.K. Gilbert **(64)** proposed such a hypothesis for the Arizona Crater in the USA and for the Lonar Crater in India, but he discarded this hypothesis because of the lack of understanding at the time of the possibility of the generation of tremendous explosive force (energy) in the collisions of bodies flying at speeds of 15-25 km/s.

The beginning of a scientific approach to study of the features of a meteorite impact on the earth was connected with the appearance with the works of D.M. Barringer **(6)** and B.S. Tilghman **(131)**, in which the Arizona Crater was considered meteoritic and not the result of volcanic activity or a vapor explosion. In 1939, L.J. Spencer **(125)** brought the number of craters which he considered meteoritic to 14. All these craters are presently considered to be of meteoritic origin, and meteoritic matter has been found in nearly all of them. J.D. Boon and C.C. Albritton **(12)** attempted to give an explanation of why specific circular structures previously called crypto volcanos are impact structures. The arguments here were not so clear as in the case of the individual craters pointed out by L.J. Spencer, since the ages of these structures is hundreds of millions of years and the initial shape and meteoritic matter in them were not preserved. The obviousness of a strong explosion in an epoch which does not coincide with the age of the surrounding rocks was common to these circular structures. These opinions were developed only in recent decades in connection with thorough study of rocks which have experienced impact action. At the present time, eight of the nine structures specified by J.D. Boon and C.C. Albritton are considered meteoritic impact structures.

* Numbers in the margin indicate pagination in the foreign text.

Craters were found in the 1930's in Australia (Henbury), Saudi Arabia (Vabar), USA (Odessa) and Estonia (Kaali).

The most vigorous rise in study of ancient meteor craters began in 1950, when V.B. Meen **(99)** studied circular Lake Quebec in Canada, which appeared to be a geologic anomaly, and he /11 demonstrated its meteoritic origin. A systematic study of circular structures suspected of being meteoritic by various methods has been conducted since that time in Canada. More than 20 meteor craters have been discovered and demonstrated there up to the present.

The modern stage is characterized by elevated interest in circular structures on planets including the earth. Studies of meteor craters are being developed in several directions: 1) theoretical research; 2) experimental work connected with modeling the impact of bodies at high speeds and studies of changes in properties of materials as a result of high pressures and temperatures; 3) the development of diagnostic indicators for separation of meteor structures on the terrestrial group of planets from the tremendous number of circular formations of varied origin, as well as the solution of a number of other problems (for example, questions of tektite origin) which are components of these basic questions.

Work in the field of physical theory of the collision of bodies at high velocities and crater formation theory was begun much earlier by Soviet scientists, and considerably more has been done here in this field than abroad. First and foremost, one of the first studies of K.P. Stanyukovich and V.V. Fedynskiy, which they performed immediately after the fall of the Sikhote-Alinskiy meteor shower in 1947, must be pointed out **(126).** In this work, for the first time, a complete theoretical description was given of the phenomena which arise in meteor impacts and the presence of craters on Mars was predicted, which is now generally well known. In subsequent works of K.P. Stanyukovich et al. (1950's-1960's), further development of the theoretical questions of the collision of bodies at space velocities and crater formation processes is given.

The dynamics of volumetric dispersion of fragments from a crater, as well as the size distribution function of fragments as a function of distance from the center of the explosion were examined by A.K. Mukhamedzhanov and K.P. Stanyukovich **(102).** It was shown that individual fragments can be scattered great distances from the center of the explosion. In recent years, ejecta from craters have been found at a number of large terrestrial astroblems, such as Boltysh, Ries and others.

The processes of crack development coupled with the stress and strain field were examined by a number of investigators **(3).** They showed that there is a special crack system near the explosion

center or point of application of a load, which indicates the direction of the stresses.

Various mechanisms of crater formation have been extensively examined in recent years from the analytical, mathematical and experimental points of view in numerous studies of foreign scientists. The work of E.M. Shoemaker **(122)** contains calculations on the reduction of impact parameters and fragment scattering from a crater with the examples of the Arizona Crater and photographic processing data of the Lunar Copernicus Crater. The method of the calculations conducted is similar to the method developed by K.T. Stanyukovich. R.L. Bjork **(10)** carried out the basic calculation of the complete two-dimensional hydrodynamic theory of crater formation, and he gave a three-dimensional representation based on symmetry considerations. The results coincide quite well with experimentally produced craters and terrestrial meteor craters. In the work of D.E. Gault et al. **(61)**, approximate estimates are given of the portions of energy connected with different crater forming processes. /12

Much attention was given to experimental laboratory studies of crater formation by both foreign and Soviet scientists. Especially great progress was achieved in experiments on the formation of impact craters. The difficulty in obtaining explosion craters in the collisions of bodies consists of the development of high velocities in laboratory conditions (over 6 km/s). However, the craters produced in nuclear explosions can be an analog of the explosion craters. The earliest crater modeling work was conducted by A. Wegener **(143)**, by dropping lumps of cement in a powdered layer of matter. A.M. Benevolenskiy **(9)** dropped dense particles into a layer of a semiliquid hardening mass (cement or gypsum), and he produced microcraters of the same shape as lunar craters. The experimental work of P.F. Sabaneyev **(118)** also showed the morphological similarity of lunar craters and craters produced in laboratory conditions. A.C. Charters **(15)** describes a sequence of phenomena which occur upon impact at low speed, and he illustrates three types of impact, at velocities of less than 500 m/s, up to 2.5 km/s and up to 6.0 km/s. Higher velocities could not be reached at the time but, even at velocities of 2.5-6.0 km/s, the projectile and parts of the target began to flow like a liquid.

The basic information on theoretical and experimental studies in the field of crater formation were generalized in the collections "High Velocity Impact Phenomena" **(140)** and "Mechanics of Crater Formation by Impact and Explosion" **(101)**.

Numerous studies on crater formation as a result of nuclear explosions assist in better analysis in those physical conditions which can arise in the formation of meteor craters **(117)**.

It has been shown in a large number of studies that tremendous pressures and temperatures develop in the crater formation process,

which cannot fail to be reflected in the physical properties of the rock. It has been established that a large, rapidly moving body, in a sudden stop, develops a temperature on the order of 1,000,000 ° C and that the maximum possible pressure is over 100 Mbar.

The work of N.M. Short **(123)** showed the changes in physical properties of rocks as a result of nuclear explosions. It was found that, in rocks which experienced sudden radial stresses in excess of the dynamic elastic limit, distinctly expressed changes in porosity, permeability, strength and the speed of sound occur. The classificatiion of rocks which contain progressive impact metamorphism has been the subject of active studies of a large number of scientists.

E. Chao **(14)** examined temperature-pressure curves based on petrographic observations of progressive impact metamorphism for individual dark colored minerals and showed that all iron containing silicates, which are initially paramagnetics, become ferromagnetics after impact heating. Pecularities of impact remagnetization connected with a meteor impact were dealt with in the work of P.J. Wasilewski **(142)**, where he examines all aspects connected with these questions, and he proposes a hypothetical model of a crater which shows the changes in magnetic vectors within the material subjected to the meteor impact. Some investigators have attempted to explain the connection between the molten volume and the diameter of the crater **(27)**, as well as of the volume of breccia and diameter. This aspect of crater shape is particularly important in the interpretation of magnetic and gravity anomalies, as well as seismic data, since the magnitudes of geophysical (and geological) anomalies will ultimately be determined by the volume of molten rock (for large craters) and the volume of breccia. /13

M.J.S. Innes **(76)**, C.S. Beals **(8)**, N.M. Short **(123)** and others have been engaged in study of changes of target rock density. M.J.S. Innes showed that a consequence of the dispersion of rocks is the presence of a negative gravity anomaly above meteor structures due to a lens of brecciated, shattered rock. V.G. Pashkovskiy et al. **(107)** conducted investigations to study the changes of physical properties of target rocks from the Sikhote-Alinskiy Crater.

As a result of comprehensive studies of a large number of meteor structures, diagnostic indicators were found which are characteristic just of craters formed by a meteor impact. Many studies devoted to diagnostics, **(141)** for example, are valuable because of the specific nature of the use of empirical material and order of magnitude estimates. Works are of interest which contain specific descriptions of ancient meteor craters, **(100)** for example.

In the field of morphological, geological and petrographic

study of ancient meteor craters, much work has been done by USA and Canadian investigators in the classification of lunar crater parameters. R.B. Baldwin **(5)** should be noted here first and foremost. He pointed out that the proportions of the morphological elements (crater depth, size, wall height, its width, etc.) of meteor craters are completely different from the proportions of conventional volcanic cones and calderas. Small and medium size craters are relatively deeper than large ones, since the depth to diameter ratio in them is larger. The similarity between explosion craters and terrestrial and lunar meteor craters is illustrated by Fig. 1 from the work of R.B. Baldwin **(5)**, in which crater depth h vs. diameter D is shown. With continuous variation of the lunar crater diameter vs. depth curve, this curve passes through a similar curve for terrestrial meteor craters, and it passes into the correspnding curve for explosion craters on the surface of the earth. This fact is one argument in favor of their common origin as a result of an explosion, and it was concluded in particular /14 that the earth and the moon were subjected to powerful meteor bombardment.

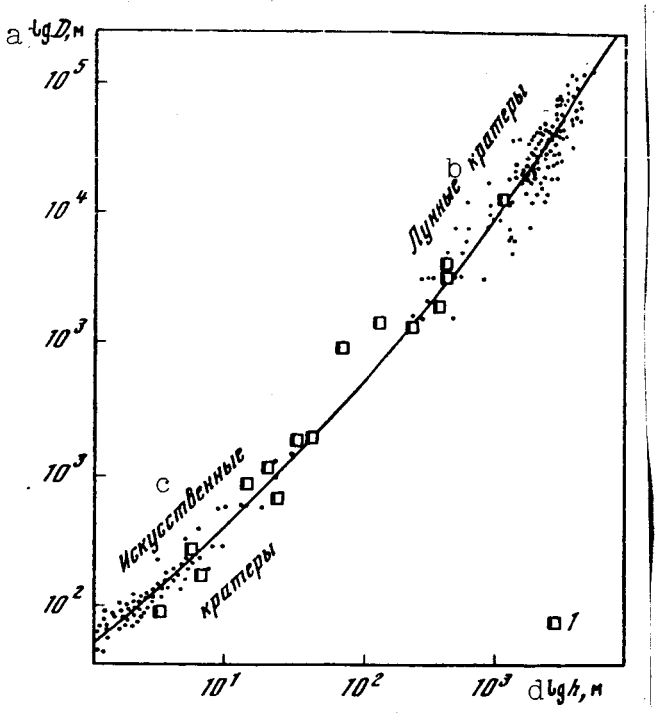

Fig. 1. Crater depth h vs. dimensions D (from **(5)** with additions by the authors): 1. terrestrial meteor craters.

Key: a. log D, m; b. lunar craters, c. artificial craters; d. log h,m

The outward characteristics of terrestrial meteor craters can be obliterated by processes of erosion and sedimentation. Knowledge of the internal structure of the crater, i.e., of that which may be preserved longer, is therefore necessary. The internal structure **of** the crater is being examined in many studies, especially in the **work** of C.S. Beals and M.J.S. Innes **(8)**, where the relationships are shown between crater diameter, brecciated zone thickness and depth of propagation of the fracture and breakup zone.

Together with the morphology and plutonic structure of the crater, diagnostic indicators in the selection of meteor craters from the tremendous number of circular structures are phase changes at high pressures (coesite, stishovite), changes in crystal structure which can

be used for calibration of impact stress magnitude (thermoluminescence, fluorescence, infrared absorption spectroscopy, X-ray structural analysis, optical axis orientation, etc.).

With the discovery of coesite and stishovite and their detection in meteor craters and astroblems, the problem of crater identification was simplified. The finding of stishovite, a structurally dense substance formed from quartz as a result of the instantaneous action of great pressure and high temperature, is /15
convincing proof of the meteoritic origin of the circular structure.

The petrographic features of rocks subjected to shock are the most interesting and diagnostically useful. Foreign scientists have done much work in this area. Classification of the degrees of shock metamorphism was developed in detail by E. Chao **(13)**. In the work of N.M. Short **(123)**, all the characteristic signs of meteor craters were examined. Based on studies of nuclear explosion craters and authentic meteor craters, he proposes criteria for meteor crater identification. The results of these works were correlated in the proceedings of two conferences **(121, 78)**.

Much work was done to compare lunar craters and craters of the earth **(5, 29, et al.)**. G. Green **(68)** proceeds from the hypothesis that the craters of the moon are of volcanic origin and shows their external similarity with terrestrial circular structures of volcanic origin. He was the first to propose that geophysical characteristics on the moon should be different for meteor craters than craters of volcanic origin. In their works on the other hand, R. Dietz and R.B. Baldwin **(5, 29)** proceed from the meteoritic origin hypothesis and compare the lunar craters with the astroblems of the earth.

The work of L.V. Firsov **(38)** is especially singled out from the works of Soviet investigators. It is devoted to a many-sided analysis of the origin of the Puchezh-Katun structure. The studies of Ye.L. Krinov **(87)**, I.T. Zotkin and V.I. Tsvetkov **(150)**, A.O. Aaloe **(1)** and others should be pointed out. Much research was conducted under the direction of Ye.L. Krinov in the Sikhote-Alin craters and, under the direction of A.O. Aaloe in the Kaali and Ilumets craters in Estonia.

An impetus in the field of geologic and petrographic study of ancient meteor craters in the Soviet Union was the work of V.L. Masaytis **(95, 97, 98)**, in which he for the first time among Soviet geologists with sufficient conclusiveness demonstrates the meteoritic nature of several circular structures in the USSR. V.L. Masaytis made a great contribution to study of the largest, 100 kilometer Popigay meteor structure.

Considerable progress has been achieved by Ukrainian geologists in study of craters in the area of the Ukrainian shield,

within which the meteoritic origin of six structures was discovered and demonstrated **(135)**. Interesting hypotheses on the meteoritic origin of large circular structures of Kazakhstan have been advanced by B.S. Zeylik and E.Yu. Seytmuratova **(149)**.

GEOLOGIC AND GEOGRAPHIC DESCRIPTION OF CRATER AND ITS VICINITY

CRATER VICINITY

The Northern Aral region is a hilly, semiarid land which is clayey but rocky and sandy in places and with vegetation which dies out in the summer. It is dissected by shallow ravines, and isolated mesas rise 50-100 m above it. In this region, the structural-tectonic zones of the Premesozoic dislocated basement have a north to northeast strike and are buried under a mantle of Cretaceous and Tertiary deposits. They are traced far to the north, where they are joined with the Paleozoic complexes of the Urals and Turgay depression (Fig.2). The following zones are distinguished in the basement from west to east: Uralo-Tobol; Priirgiz; Aya; Kustanay **(60)**. These zones, separated by faults, were predetermined by the inherited structure of the Middle Cenozocic mantle, which forms extended submeridional folds **(146)**. /16

The Zhamanshin uplift itself is in the extreme east of the Priirgiz zone, which is made up basically of Lower Paleozoic rocks and which is separated by a fault from the Aya zone, where Middle and Upper Paleozoic deposits predominate. It is confined to the eastern part of the Transural anticlinorium or even, in the opinion of A.T. Bachin **(83)**, to the extreme western part of the Tyumen-Kustanay depression. The basement depth (Fig. 3) increases from tens of meters in the north to 0.5-1.0 km or more near the Aral Sea **(146, 81)**.

More than ten holes which revealed the basement have been drilled in the crater region. A series of extended north to northeasterly folds of 100-150 m amplitude is visible along its surface. The basement is at a depth of 100-250 m from the surface in the crater region. It is made up of Lower Paleozoic metamorphic shales and Middle Paleozoic volcanogenic sedimentary molassas. Two narrow submeridional extended ultrabasic rock intrusions, traced by bands of magnetic field anomalies, pass right through the crater.

Middle Cenozoic deposits unconformably overlap the Paleozoic with profound erosion. Cretaceous rocks are represented by Senoman sandstones (30-40 m thick), dark gray Turonian clays and light gray Maastrichian marls and limestones with crinoid and bivalve fragments (15-20 m).

The Tertiary deposits are represented (from bottom to top) by greenish gray, brown, opoko-like clays of the Tasaran series of

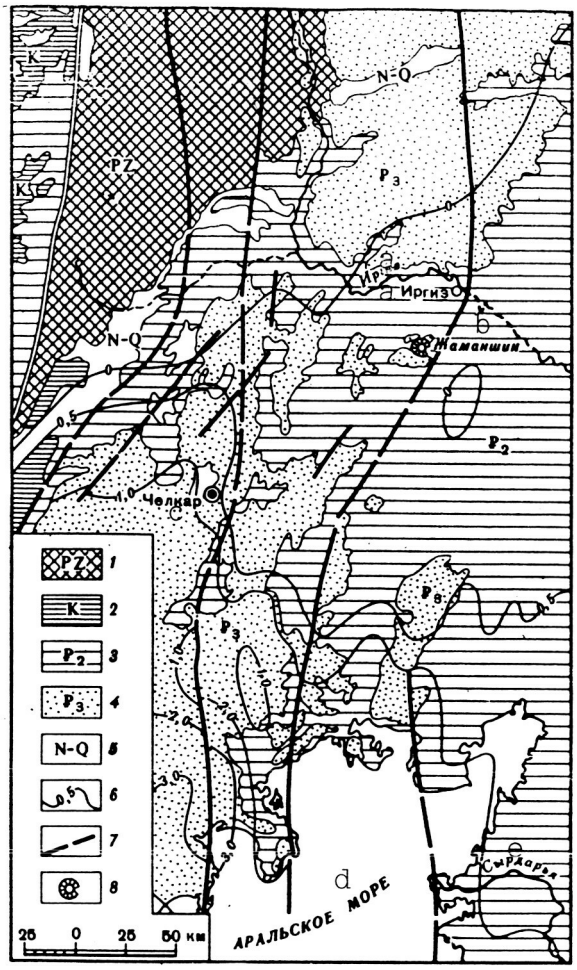

Fig. 2. General map of Northern Aral region: 1. Urals Paleozoic deposits: 2. Cretaceous deposits; 3. Eocene; 4. Oligocene; 5. Neogene-Quaternary deposits; 6. Basement roof isopachs; 7. Faults; 8. Zhamanshin Crater and its wall.

Key: a. Irgiz
b. Zhamanshin
c. Chelkar
d. Aral Sea
e. Syrdarya

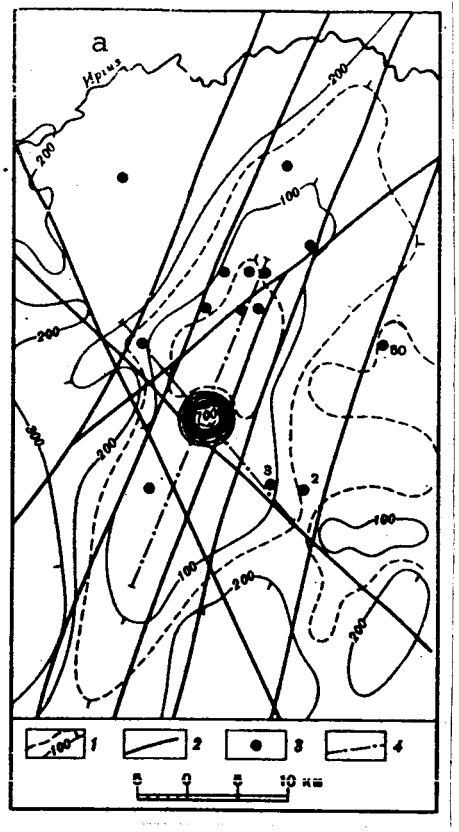

Fig. 3. Diagram of depth of occurrence of basement in Zhamanshin uplift region, compiled by A.P. Bachin:

1. Basement surface isohypses;
2. Predominant faults;
3. Drill holes revealing Paleozoic basement;
4. Seismic profile locations.

Key: a. Irgiz

the Middle Eocene (120-150 m), gray quartz sands and clays of the Saksaul series of the Upper Eocene (15 m), gray and greenish gray clays of the Chegan series of the Upper and Lower Oligocene (45 m); gray clays occur higher, overlain by sands and sandstones of the Chiliktin series of the Middle Oligocene (15 m), which jacket the surfaces of the uplands ringing the natural landmark. Monadnocks of brown and gray sandstones and gritstones of the Chagray series of the Upper Oligocene are preserved in the highest sections (up to 5 m). /17

Quaternary deposits are thin and of negligible extent, and they are represented by gray lake clays and loesses which fill isolated depressions and by barchan sands which are widespread far outside the crater to the northeast at Irgiz settlement. The deposits which fill the crater wil be discussed separately.

Drill hole materials give a more detailed characterization of the platform portion of the cross section. Drill hole No. 50 of the Turgay party was drilled 15 km northeast of the crater (see Fig. 3). The wellhead marker was approximately 115 m; the following were found from bottom to top in the drillhole cross section: /18

183-203 m, quartz porphyries, greenish gray, Paleozoic age; the top 12 m is a humid weathering crust;

147-183 m, greenish gray, dense, opoko-like clay of Senoman stage 36 m thick;

140-147 m, nearly white marl of Maastrichian stage 7 m thick;

120-140 m, gray, dense opoko, Lower Tertiary age 20 m thick;

13-120 m, gray, opoko-like clays of Tasaran series of Middle Eocene 107 m thick;

0-13 m, Quaternary gypsum containing clays.

The characteristic two layer structure of platform regions is thus characteristic of the Northern Aral region cross section (a mantle of sedimentary rock which is underlain by metamorphosed, dislocated Paleozoic basement formations). A similar (two layer) structure is characteristic of the region of the Nordlinger Ries Crater and of the regions of a number of other impact structures.

Speaking of the crater surroundings, the history of the oldest settlement in the Northern Aral region, Irgiz, should be discussed. It was reported by G.V. Zonov. In the middle of the last century, the Russian government decided to build fortresses in the Kazakh steppe for the conduct of pacification. On the right bank of the Irgiz River on 19 July 1845, Traubenberg set up fortifications which were built by the Urals Cossack forces. It was therefore called Uralsk. The settlement moved to Irgiz in 1868. This settlement played a large part in the study of Kazakhstan and Central Asia, since numerous expeditions used it as a base.

STRUCTURE OF CRATER AND ITS WALL

The immediate Zhamanshin meteor crater itself has the form of /19
a flat circular depression 6.5 km in diameter, slightly inclined to the east and cut by intermittent waterways (Fig. 4). In images obtained from the Salyut-4 orbital space station (Plate 1) and the American Landsat-1 unmanned satellite (46), this depression is seen as a regular circle surrounded by a wall, the width of which is 3 km in the northwest, but it is absent in the southeast. In addition, a 30 km radius anticlinal uplift is visible around the crater. It is not excluded that, after formation of the crater, the block surrounding it was raised inversely. The wall is formed by breccia made up of rocks which occurred inside the crater but now is laid over Tertiary deposits. The allogenic breccia makes up a unique formation of mixed, shattered Mesozoic, Cenozoic and Paleozoic rocks, as well as remelted glasses and scoria (impactites). Because of the presence of dark Paleozoic fragments, the upper portion of the allogenic breccia appears dark (Plate 2a,b). The nature of the breccia distribution in the crater is asymmetric relative to a plane oriented to the northwest, and the crater structure therefore has a "butterfly" shape (Fig. 5).

The crater wall has a marked two segment structure. Its lower portion is made up of blocks and lenses of Tertiary, Cretaceous and Paleozoic rock (Plate 3a,b). These massive lenses up to 15 m thick and up to 100 m in extent, "moved out" from the crater and "overthrust" on the surrounding rocks, were found together with A.O. Aaloe on the northwest, southwest and on the east walls of the crater. A block of mixed rock containing a continuous cross section of Paelozoic, Cretaceous and Tertiary deposits was mapped in detail in the northwest (Fig. 6, Plate 3a). The Paelozoic rocks in it are highly brecciated (Plate 3c, d), the quartz in them contains planar elements (Plate 4a), coesite and stishovite, frequently made

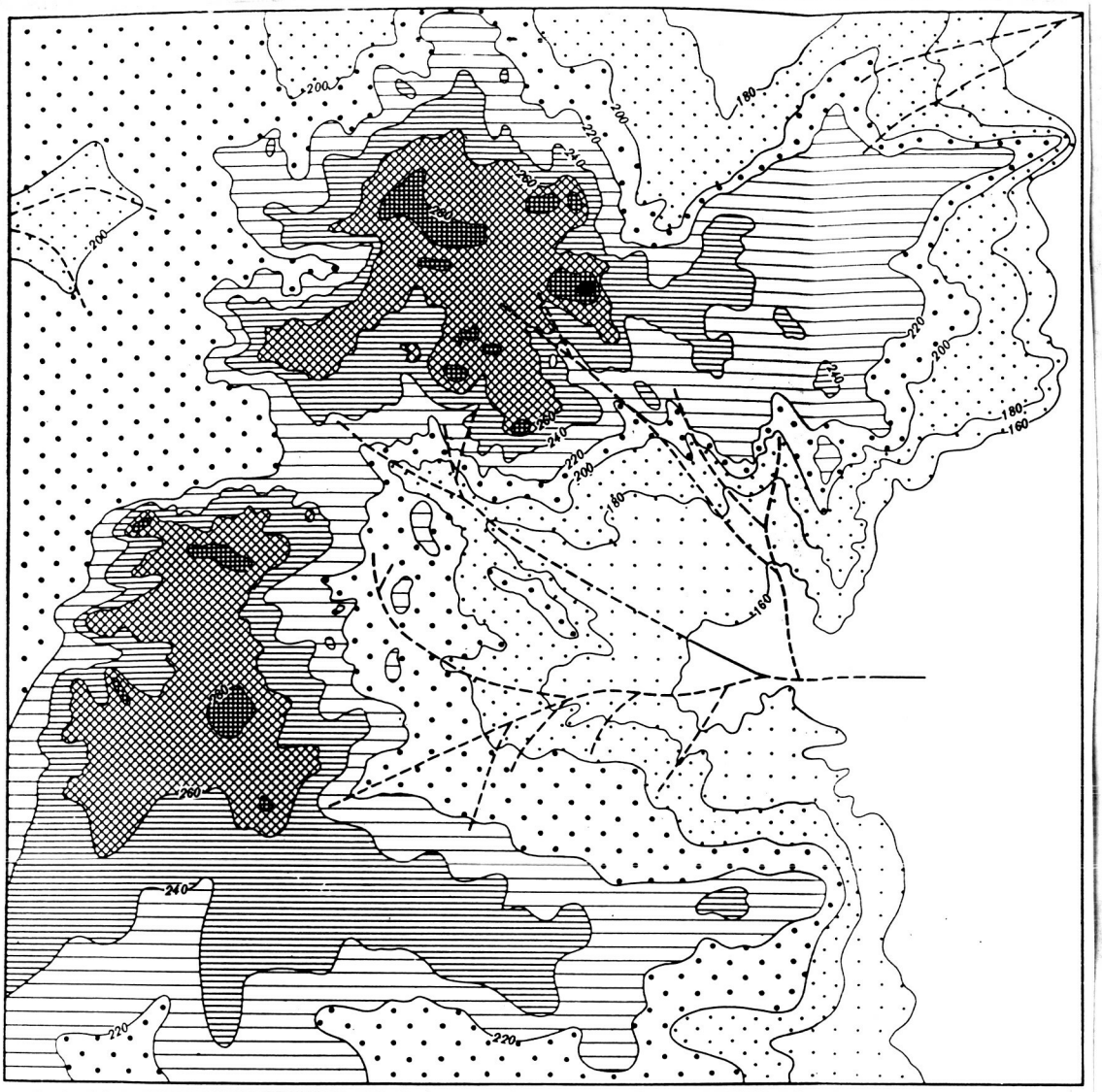

Fig. 4. Hypsometric chart of Zhamanshin Crater.
Cross hatching density corresponds to relative altitude.
Isohypse interval is 20 m **(43)**.

isotropic, but the feldspars are maskelynitized and shattered to flour. Outside the crater in the southeast, uplifted, vertically standing Tertiary sandstones are exposed, forming a series of sublatitudinal ridges more than 100 m long (Plate 3b).

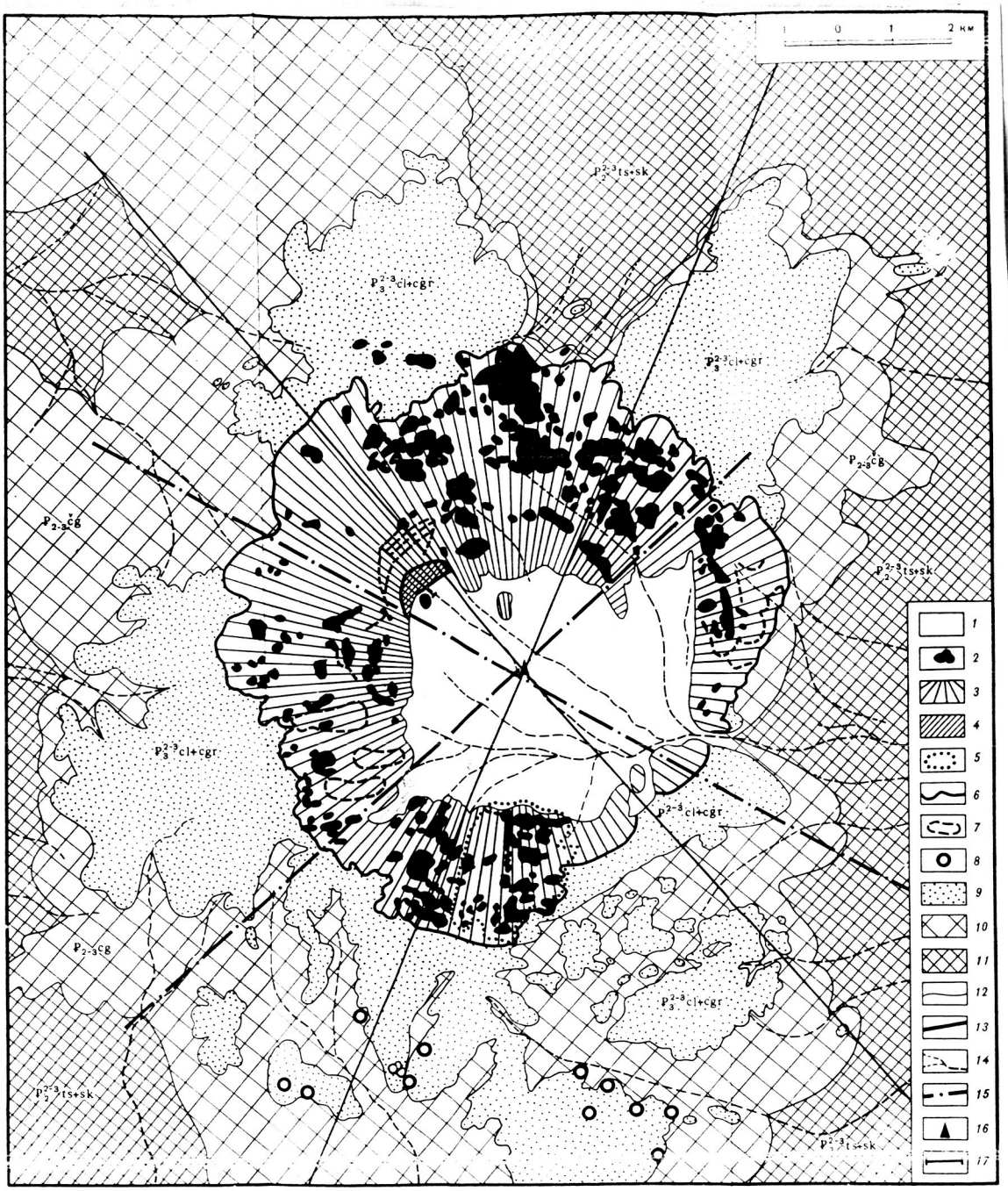

Fig. 5. Geologic map of Zhamanshin crater: 1. Quaternary loesses and lake deposits filling crater; 2. allogenic breccia with Paleozoic rock fragments; 3. allogenic breccia without Paleozoic rock fragments and dislocated Tertiary deposits; 4. block of displaced and dislocated Paleozoic, Cretaceous and Tertiary rocks; 5. boundary inside wall; 6. outer wall boundary; 7. Irgizite occurrence limit; 8. probable small craters; 9. Chagray and Chiliktin series of Oligocene; 10. Chegan series of Eocene and Lower Oligocene; 11. Tasaran and Saksaul series of Eocene; 12. stratigraphic boundaries; 13. faults; 14. intermittent waterways; 15. geophysical profiles; 16. drillhole location; 17. geologic profile location.

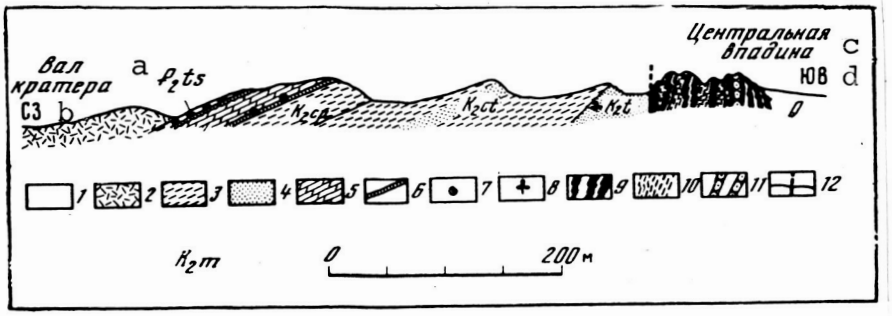

Fig. 6. Cross section through ridge in northwest of natural landmark: 1. in Quaternary loesses and lake deposits of depression; 2. allogenic breccia; 3. clays; 4. sands, sandstones; 5. marls; 6. phosphorites; 7. faunal remains; 8. floral impressions; 9. Premesozoic metamorphic quartzitic schists; 10. rocks crushed to "flour"; 11. quartzites; 12. faults.

Key: a. crater wall; b. NW; c. central depression; d. SE

The upper part of the wall is made up of allogenic breccia. Unconsolidated Tertiary clays ejected from the crater predominate below in it. They are typical allogenic breccias, the preserved thickness of which is approximately 10 m or possibly more. The higher horizons of the allogenic breccia formation were preserved only in isolated, disconnected outcrops (Plate 2a,b), represented by unconsolidated gravel and, together with disintegrated Tertiary clays, they contain up to 10% Paleozoic rock fragments. In isolated outcrops at the base of the upper wall horizon, there is a horizon which is enriched in Cretaceous rock fragments, in which fragments of belemnites, corals and bivalves attract attention.

Thus, the alternation of the rocks is the opposite in the wall interface. The ejected Tertiary clays occur underneath, Cretaceous deposit fragments appear higher and in the upper portion, fragments of the oldest Paleozoic rocks, which were ejected from a depth of more than 200-250 m. The relationships of gravel, sand, clay and irgizites in the upper horizons of the allogenic breccia on the southeast wall, calculated together with V.I. Miklyayev, are presented in Table 1. Such allogenic breccia, which is coarsely bedded strata of mixed and unsorted fragments, Paleozoic and unconsolidated Mesozoic-Cenozoic rock debris, makes up a single formation which now has been preserved in disconnected cone shaped hills which are relics of the wall. It usually forms small fragments (2-5 cm), which is predetermined by the original fracturing of the rock in its bedrock occurrence. Up to 20 cm fragments are frequently encountered however and, on the west and south walls, up to 3 m blocks. The largest ejected block up to 8 m high, made up of Paleozoic porphyrites, is found on the west wall. Clay and sand which make up over half of the breccia are easily washed and blown out of it, and the cone shaped hill surfaces are enriched in and jacketed by Paleozoic rock fragments.

/20

/21

TABLE 1. DISTRIBUTION OF ROCK, IRGIZITE AND GLASS FRAGMENTS ON SOUTHWEST WALL IN ALLOGENIC BRECCIA AND ON ITS SURFACE

Характеристика пробы (площадка 1 м²) a	Масса пробы, кг b	Глина и алевролит (<0,1 мм), % c	Песок (0,1–1 мм), % d	Осколки, дресва (>1 мм), % e	Иргизиты и жаманшиниты f			Иргизиты, % g		
					шт. h	г i	%	капельки j	ажурные k	осколки l
Аллогенная брекчия вала на глубине 1 м, слой мощностью 10 см m	22,3	74,8	7,0	18,1	380	170	0,71	0,07	0,15	0,50
Аллогенная брекчия от поверхности вала до глубины 5 см n	21,0	50,6	6,8	42,5	480	230	1,00	0,09	0,01	0,90
Аллогенная брекчия, поверхностный слой o	6,5	25,8	8,1	65,0	56	24	0,40	Не рассчитано r		
Долина временного потока p	5,5	20,0	3,4	76,0	220	91	1,65	"		
То же q	6,4	13,3	5,4	83,0	310	152	4,20	"		
"	7,0	24,0	13,9	62,0	112	39	0,50	"		

Key:
a. Sample characteristic (1 m^2 area)
b. Sample weight, kg
c. Clay and siltstone (< 0.1 mm),%
d. Sand (0.1-1 mm), %
e. Chips, gravel (> 1 mm),%
f. Irgizites and Zhamanshinites
g. Irgizites, %
h. Pieces
i. g
j. Droplets
k. Skeletons
l. Chips
m. Wall allogenic breccia at 1 m depth, 10 cm thick layer
n. Allogenic breccia from wall surface to 5 cm depth
o. Allogenic breccia, surface layer
p. Intermittent flow valley
q. Same
r. Not calculated

As a result, the cone shaped hills are sometimes assumed to be outcrops of Paleozoic bedrock. In different sections in the upper horizons of the wall, fragments of given varieties of Paleozoic rocks, the distribution of which is symmetrical about a plane oriented to the northwest, predominate. G.A. Kostik and B.V. Piliya described these rocks from the crater petrographically **(86)**. The oldest are quartzitic-chloritic, chlorite-epidote-quartzitic, actinolite-albite-epidote-schists. The dark gray quartzite-like sandstones, sericitic carbonaceous phyllites, siliceous schists and marbles are less metamorphosed. By analogy with the deposits of the Irgiz synclinorium, which contains microfossils, they are classified as Wend-Lower Cambrian and Lower Cambrian respectively.

These rocks are most widespread among the rock fragments in the allogenic breccia and entirely constitute them on the southwest, south and north walls. Their fragments usually are not

over 3-5 cm and rarely reach 10 cm. Fragments of basaltic and andesitic and basaltic porphyrites are found in narrow bands in the south and symmetrically to it on the northeast wall and isolated blocks on the west wall. They are similar in composition and appearance to rocks of the Valerian series of the Turgay depression, the age of which is middle to upper Vise-Namur of the Lower Carboniferous. They form the largest blocks of up to several meters in size. The youngest Mesozoic rocks, red tufagenic polymict siltstones, sandstones and conglomerates, make up the southern and symmetrically to it northeastern parts of the wall. Middle and upper Vise fauna were found in the limestone pebbles /22 contained in the conglomerates. The red rocks are therefore no younger than the Middle Carboniferous. Fragments with 5-20 cm cross sections and sometimes up to 2 m fractured blocks are characteristic of them. Besides, fragments of quartz veins, marbles, granitoids and ultrabasic rocks are found among the allogenic breccia, the presence of which in the crater region is indicated by high positive magnetic anomalies.

Particular attention was given to searching for shatter cones which many investigators classify as one of the most definitive signs of a meteor impact **(141)** (Plate 4b-d). They were found among them the Carboniferous red rocks, where conglomerates are found which contain large (up to 3-10 cm) limestone pebbles of Middle Paleozoic age (Plate 4c). Shatter cones were found in these pebbles. In this case, they can only successfully be seen in the morning and evening, i.e., with indirect illumination. This peculiarity, the finds in the conglomerate pebbles, have been noted for other craters. The "horsetail" type structure of the chips is widespread in massive red volcanogenic-sedimentary rocks (Plate 4b). Single shatter cones and "horsetail" type chips were found in fragments of Cenozoic sandstones and in Paleozoic schists (Plate 4d).

ZHAMANSHINITES AND IRGIZITES

Unique formations which occur in the crater both in the form of individual fragments among the breccia and directly in the Tertiary deposits are rocks which are remelted and calcined to various degrees: clays reddened by calcining; porous scoria; porous and dense glasses which are quite provisionally consolidated in the Zhamanshinites; glassy jets of basic and acid composition, the latter identified with tektites and called Irgizites. All the formations listed differ strongly in appearance, dimensions, chemical composition and zones of occurrence in the crater.

In the east of the crater, several ridges were preserved, which are stretched out in three parallel submeridional rows (Plate 5a). Their western slopes, inclined toward the center of the crater at a 20° angle, are covered with scoria formed of bodies made up of diverse fragments of clays which have been calcined and remelted to various degrees, and are of type of the Zyuvites from

Ries Crater. The largest body of such rocks **(82)** is 1-2 m thick and 10-15 m wide from west to east. This body, now preserved only on the summits of separate hills, probably was part of the scoria cover. All three parallel rows possibly were part of one cover which was later broken by imbricate overthrusts in movement of blocks from the crater and which now form apparent waves. The greenish gray softening Tertiary clays underlying the scoria were reddened and caked at the contact, and they form pumice like porous nonsoftening fragments. Some of them were more thoroughly remelted and became black and less porous. They formed varieties which are transitional to scorias and to dark glasses. A similar body of /23
scoria and melt on the northeast wall flowed into the cracks in the allogenic breccia (Plate 5b). Scoriaceous rocks are most widespread in the crater. Many of them probably were ejected in the semimolten viscous state by the explosion. "Footprints" are sometimes seen on their bottom surfaces, and surfaces are covered with "disintegrating breadcrusts" (Plate 5c). The scoria also forms the largest of the known (up to 1 m) impactite fragments. In chemical composition they are closest to Tertiary clays. In them, silica is at a minimum ($\sim$ 50%) and alumina is at a maximum ($\sim$ 20%).

The glasses are black in lumps, yellow in the porous portions and rarely have blue veinlets. They from partly fused and acute angled fragments which usually are 10-15 cm in cross section and reach 0.5 m, and they are found partically everywhere among the allogenic breccia. There are many of them in some local sections and they cover individual sections, but only isolated fragments are found in others. Paleolithic tools were made from just these glasses. Flow traces are easily noted in the glasses, which is evidence of hardening from a viscous melt. The "disintegrating breadcrust" structure also is visible sometimes on their surfaces (Plate 5c), and impressions of the underlying rock on the bottoms. The glass chips are shiny as a rule, but varieties are found with a dull break, which are decrystallized. The glasses are broken down into two groups of basic and acid composition by petrographic characteristic and chemical composition, which are similar in composition to the corresponding groups of glass jets.

On the northwest wall around the block of Paleozoic rock which contains quartz veins (see Fig. 6, Table 3a-c), unique blocks (up to 0.5 m) of lechatelierite (pure foam silica) were found, which were formed by melting of the quartz from the veins.

Glass droplets, jets, dumbbells, beads and fragments 1-3 cm long and weighing approximately 0.6 g are of special interest. They are widespread on the southeast wall in a total area of 1-2 km^2 where they constitute up to 0.5-1 % of the weight of all the allogenic breccia (see Table 1). To decide from approximate calculations, the number of them reaches 10^7-10^8 and the weight tens of tons.

DRILL HOLE IN CRATER CENTER

As was noted above, the inner depression of Zhamanshin Crater is filled on the surface with loess-like loams. To determine the internal structure of the central depression, drill hole No. 100 was drilled to a depth of 275 m in the center of the natural landmark by the efforts of the Western Kazakhstan Geologic Administration. Initial study of the core sample was conducted by V.P. Yegorov and G.P. Samsonov, as well as by V.I. Miklyayev and A.V. Gur'yanov. The description of the drill hole section made by them is presented below.

0-35.5 m: dark gray horizontally bedded clays with 1-2 cm thick bands of quartz sand and siltstone; the clays in the upper part of the cross section contain gypsum. The rocks are very similar to the Tertiary deposits. However, they differ from them /24 by the specific nature of the bedding. They contain Quaternary age spores and pollen.

35.5-80.0 m: uniform greenish gray lumpy clays with rare bands of sand and siltstone with carbonized plant residues.

80.0-115.7 m: greenish gray clays with slickensides (99.5-115.7 m), with carbonized plant residues, sometimes with fragments of brecciated Paleozoic rock.

115.7-154.5 m: alternation of 10-15 m thick dark gray clays containing plant residues with 3-7 mm thick bluish white very loose clays. At 120-127 m depth in brown clays, numerous slickensides are seen. Between depths of 33.5 and 154.5 m, a mixed complex of spores, pollens and microfauna of Tertiary and Cretaceous ages are distinguished.

154.5-231.5 m: loose, white but brown in places clays, the middle portion of which contains a four meter horizon of brown sandy breccia with Paleozoic rock fragments.

231.5-240.0 m: dark gray clays, banded with slickensides.

240.0-275.0 m: brown, pinkish, very loose easily wetted clays with bands of breccias and acute angled fragments of diverse Paleozoic rocks among which effusives predominate. The clays are crumpled to fine folds and are set "head down" in places.

There is no doubt that the drill hole did not reach the bottom of the crater. Lake clays formed by washing out of the allogenic breccia which constituted the wall probably occur above 115 m (or 154 m). Allogenic breccia therefore occurs below a depth of 154 m. In the initial stage of existence of the crater depression, numerous landslides occurred from the wall, which caused dislocation of the rocks.

ACCOMPANYING SMALL CIRCULAR STRUCTURES

In the fall of a large meteorite, together with the main impact crater, smaller impact craters could have occurred, but their origin can vary. They were formed either by the impact of meteorite fragments split off, or the accompanying craters could have been formed by fragments ejected from the central crater like, for example, the craterlets formed on the moon around Copernicus Crater.

Many circular structures similar to craters in appearance can be distinguished in the Northern Aral region. They occur hundreds of kilometers north of Zhamanshin Crater and they occur closer. A circular system of lakes in the Irgiz (Comintern) region has a 10 km diameter 30 km east of Zhamanshin Crater. Lake Kamys-Kul', 2 km in diameter, is 7 km northeast of the natural landmark. They are of ideally circular shape and have a poorly expressed wall with a flat bottom. There are several similar structures in the area. It should be stipulated however that they can develop in desert and steppe regions by wind erosion of the soil. It therefore requires /25 detailed and special field studies, primarily shallow drilling and pit sampling, to establish the genesis of each of these structures.

On the oldest surface 3 km south of the edge of Zhamanshin Crater, where Chagrak sandstones and gritstones were preserved, a whole series of small, 50-200 m diameter circular structures was found from aerial photographs **(46)**. They were both separate (Plate 6a,b) and grouped by twos and threes (Plate 6a,c). Where they reached the beds of Middle and Late Quaternary intermittent flows, they were eroded. Although these structures are easily seen in aerial photographs, they are very difficult to distinguish on ground courses. In those cases when they have a wall, it is not over 0.5 m high. The bottom is flat, sometimes filled with clays are similar in structre to a takyr. It is not excluded that these small craters were formed by ejecta from the main crater. The finding of single fragments of black impact glass around the small craters is in favor of this.

SOILS AND VEGETATION

The vegetation and soil cover of the crater area was studied by G.V. Zonov (Institute of Soil Science, Kazakhstan SSR Academy of Sciences), who kindly reported some results of his studies. The crater soils are brown, but with traits of steppe soil formation, which is characteristic of the transitional band from light chestnut steppe soils in the north to desert soils. In this case, the complex of plants and soils in the crater area is unique, unusual and moreover carries relict traits. A small grove of heterophyllous Turanga poplar (a species preserved from Quaternary times) and bush Saxaul was even preserved here.

Sections of the wall surface are distinguished against the background of the surrounding territory, which have indications of salinity characteristic of depressions, but which are unusual in a well drained elevated wall and in permeable sandy soils. The vegetation here covers only a third of the surface and is not completely the normal biyurgun-winterfat-meadow grass characteristic of saline places. The following have been located here: prostrate summer cypress, konurbas, meadowgrass, gray wormwood, tyrsa feathergrass, ilyak sedge, pyrethrum, camphor fume, biyurgun saltwort, winterfat, bush spirea, as well as chetyr', ebelek, petrisomonia, Ceratocephalus Moench genus, saliferous goosefoot, yams and other plants. The soil in many sections of the wall has a high gypsum content. Gypsum crystals have been found on the surface, and they form unusual hemispherical nodules 15-25 cm in size similar to cacti. All this is evidence that a substantial amount of salts, particulary sulfates, rises from below and gets into the surface of the wall. It is not excluded that finely dispersed iron sulfides, which fill the Tertiary clays, are broken down in the loose breccia, brown streaks of limonite appear, and sulphur forms the sulfate anion. Under the arid climatic conditions which exist here, moisture is still insufficient to wash out these salts which get into the wall surface in large amounts.

ARCHEOLOGICAL OBSERVATIONS

Impact glasses and tektites have long interested people. They /26
are well known as amulets among the peoples of Southeast Asia and Australia, and the famous Neolithic Willendorf Venus from Central Europe was chiseled from a moldavite tektite. Many such glasses have been used as a raw material for Paleolithic and Neolithic tools. There is therefore special interest in the traces of ancient industry based on Zhamanshinite impactites in Zhamanshin Crater, which were described by colleagues of the Institute of Geological Sciences, Kazakhstan SSR Academy of Sciences V.D. Aubekerov and A.G. Medoyev, who kindly reported the material presented below. The stone tools in the crater are divided into three groups which are distinguished by the composition of the raw material, working technique and age (Plate 7). The oldest, extremely rough chips, flakes and other tools were made of gray and black quite brittle glasses, characteristic of the Late Paleolithic in appearance. Their age varies between 10,000 and 25,000 years.

Practically everywhere in the crater where Zhamanshinites lie, traces of open campsites were found: scattered chips, flakes, nuclei, flat bilateral (bifacial) 5-10 cm long dart tips. Tools of the same type but of different materials are widespread in Kazakhstan and Central Asia, and they are dated Epipaleolithic, 10,000-12,000 years before our era. Third group tools were made of stronger, more malleable flint imported from widespread concretions in Danish age Ural region, Usturt and particularly Mangyshlak limestones. These tools are well worked arrow tips, scrapers, flakes, knife blades, etc., not over 2-5 cm long. They also are

widespread everywhere in extensive surrounding areas, especially in Mangyshlak, and they are classified in the microlith culture of the Neolithic, the age of which is 3,000-4,000 years before our era. Further study of ancient industry from the Zhamanshin Crater impactites may place it in the series of unique archeological objects. There is still another aspect of the participation of archeologists in the study of tektites. Analysis of archeological discards and searches in them for possible tektites and impactites among the tools and amulets are necessary.

Zhamanshin Crater is thus a unique place both geologically and mineralogically, and geograhically and archeologically. This permits it to be hoped that a combined preserve will be created here in time.

CRATER AND IRGIZITE AGES

AGE DETERMINATION BY GEOLOGICAL, GEOMORPHOLOGICAL, PALEOMAGNETIC AND POTASSIUM-ARGON METHODS[1]

In the crater area, the youngest deposits are represented by the Chiliktin series of the Middle Oligocene and the Chagray series of /27
the Upper Oligocene, which are no younger than 25,000,000 years old. They are exposed on the oldest and highest erosion surfaces, which began to form at the end of the Sarmatian stage. The upper age of its formation, according to the data of L.I. Solov'yev (private communication), is the end of the Late Pliocene N^3_2, probably approximately 1,000,000 years. Ejecta from the crater, as well as secondary craters approximately 200 m in diameter lie on precisely this surface. This evidently indicates a lower limit of of the crater age. On the other hand, both the wall and the secondary craters are being eroded. To decide from the nature of the branching of the stream network, their origin occurred in the initial stages of destruction of the peneplain and corresponds to Q_3, which permits an uppper age limit of at least 100,000 years to be spoken of. Drilling data do not contradict these figures. In the cross section of drill hole No. 100, drilled in the center of Zhamanshin Crater by the Western Kazakhstan Geologic Administration, lake deposits with carbonized residues occur down to a depth of 154 m, in which an indefinite, mixed (from Paleozoic to Tertiary) spectrum of pollen and microfauna with admixture of Oligocene and Quaternary forms is found, i.e., filling of the crater occurred in the Quaternary.

1. Age determination by the fission track method was conducted by the author together with V.P. Perelygin, D. Lkhagvasuren and S.G. Stetsenko (Joint Institute of Nuclear Research, Dubna) and paleomagnetically together with M.L. Bazhenov (Institute of Geology, USSR Academy of Sciences) **(46, 48)**.

In age determinations of the glasses by the potassium-argon method in various laboratories, the following data were obtained: 59, 35, 28, 10 and 8 million years **(88);** 8.1 ± 0.9 and 4.8 ± 0.8 million years **(86);** less than 1,000,000 years **(42, 43).** Such discrepencies of the isotope age are explained by the complexity of determinations by the potassium-argon method with low potassium and insignificant argon content in young glasses, and they require refinement and verification.

The paleomagnetic method also was used to get additional information on the age of the crater. Oriented samples were taken from Tertiary clays of unaltered greenish samples, reddened because of calcining at the contact, but softening clays, and samples from ignimbrite-like Zhamanshinites consisting of caked, calcined and remelted scoria-like aggregates (Plate 5a). The magnetism of the Zhamanshinites was destroyed by a 600 Oe alternating magnetic field. The remaining samples passed through thermomagnetic cleaning at 220° C. After cleaning, as a result of measurements by standard procedures, it was established that the magnetism of the Zhamanshinites and the majority of calcined clays is opposite (Fig. 7). The youngest positive reverse polarity epoch, Matsuyama Epoch, began 2,420,000 years ago and ended 690,000 years ago. The normal polarity Jaramillo episode is noted at the end of it (1,000,000-850,000 years). The Brunes Epoch began after 690,000 years ago. It is distinguished by normal polarity which has continued up to the present. It was interrupted by extremely brief (considerably shorter than 10,000 years) reverse polarity episodes. Therefore, with account taken of determination by the geomorphological method, it is most likely that Zhamanshin Crater was formed in the Matsuyama Epoch, but after the Jaramillo episode, i.e., it is older than 690,000, but younger than 850,000 years.

AGE DETERMINATION BY FISSION TRACK METHOD

For determination of the Zhamanshinite and Irgizite ages by the fission track method, the samples were embedded in epoxy resin, ground down to obtain a transparent layer (down to 2 mm for Zhamanshinites and down to 0.5 mm for the darker irgizites), polished and etched with hydrofluoric acid. For selection of the optimum etching conditions and to obtain uniformity of the glasses and the uranium distribution in them, the samples were irradiated perpendicular to their surfaces by accelerated ^{136}Xe ions with 1.09 MeV energy per nucleon, with a 10^6 per cm^2 flux density. It was found that 5-6 μm diameter tracks appear best of all by etching the glasses for 15-25 min in 10% hydrofluoric acid. The resulting preparations were examined under a microscope at 600 power magnification. The xenon ion track dimensions had negligible dispersion for each individual sample. This indicates adequate relative uniformity of composition of the Zhamanshinites and particularly of the tektites.

/28

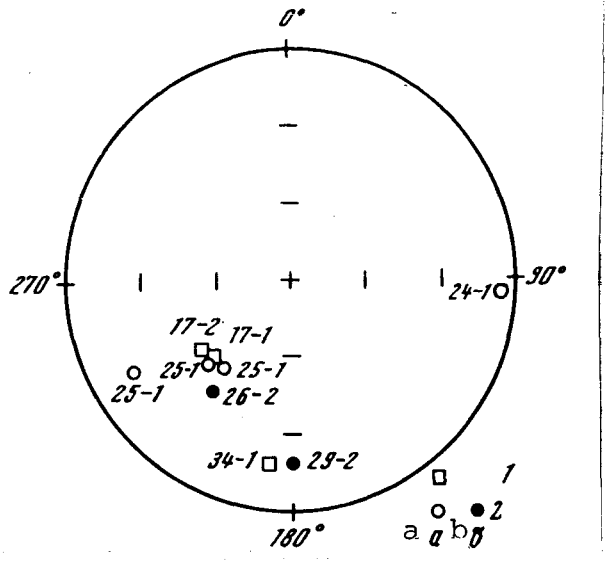

Fig. 7. Stereogram of magnetization vectors of samples from Zhamanshin Crater: 1. ignimbrite-like Zhamanshinites; 2. calcined Tertiary clays (a,b. projections on upper and lower hemispheres respectively); figures are numbers of samples **(48)**.

The efficiency of recording of nuclear fission fragments in a thin, flat preparation is characterized by the solid angle in which fission tracks are recorded within the detector. For determination of the recording efficiency, a thin uniform preparation containing 12.5 μg of uranium per cm^2 is applied to the polished surfaces of the Zhamanshinites and to the irgizites. The same preparation was applied to the reference, a silicate glass with known 42 ± 3% recording efficiency **(108)**. The preparations were then irradiated with a $2 \cdot 10^{11}$ cm thermal neutron flux, after which they were etched with hydrofluoric acid until the appearance of approximately 5 μm tracks of fragments from the neutron induced fission of uranium. By comparison of the density of the tracks developed on the samples with the reference, the recording efficiency of the uranium fission fragments in Zhamanshinites and irgizites was calculated. It is 40 ±8% of the total number of uranium nuclei in the uranium containing preparation applied. /29

Since numerous 1-10 μm diameter microbubbles interfered with counting the tracks in the irgizites and Zhamanshinites, only an upper density limit on the order of 100 tracks per cm^2 could be established for the irgizites. For the Zhamanshinites, by inspection of an object with 192 mm^2 area, 179 uranium fission fragment tracks were found (Plate 8a, b) and, if the area occupied by bubbles and inclusions is excluded, the spontaneous uranium fission track density in Zhamanshinites is 174 tracks per cm^2.

With the passage of time however, especially upon heating even to 50-100 °C, the tracks in the glasses can regress (they are reduced or disappear completely) are are closed up. To check the degree and nature of regression of the tracks in Zhamanshinites, the maximum diameter of 133 tracks of spontaneous uranium fission fragments and 438 tracks formed after irradiation with thermal neutrons was measured (Fig. 8). It turned out that the dimension

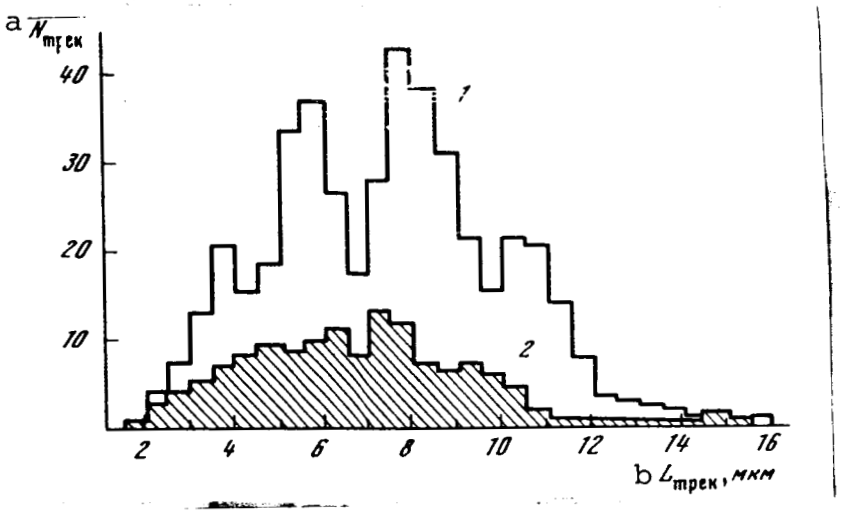

Fig. 8. Diameter distribution of 133 fragment tracks of spontaneous (1) and 438 fragment tracks of thermal neutron induced (2) uranium fission in Zhamanshinite **(48)**.

Key: a. N_{track}; b. L_{track}, μm

distribution of the tracks of spontaneous and induced fission have a similar shape, but the tracks of larger (over 12 μm diameter are confined to local sections with a high etching rate, which evidently differs in composition. The modal diameter of fresh induced fission tracks (approximately 7.41 μm is greater than the diameter of spontaneous fission tracks (6.80 μm (see Fig. 8) preserved in the glasses. This indicates some regression of the spontaneous fission tracks during the time the Zhamanshinite block was in the soil and on the surface, where it was exposed to the atmosphere and the heat of the sun. The established regression can somewhat understate the age determined, although insignificantly. Corrections are therefore introduced in the calculations.

In calculation of the absolute age of rocks by the fission track method, their uranium content must be known. It is determined by two independent methods, in a lump and in a powder. In the first method, a layer of the Soviet equivalent of Dacron was applied to the polished sample and the induced nuclear fission fragments were recorded in it. In the second method, the sample was ground up and placed in a Soviet equivalent of Dacron packet approximately 1 cm^2 in size. For calibration of the integral thermal neutron flux, a prepartion containing 0.13 μg uranium per cm^2 was enclosed in a similar packet. The samples were then simultaneously irradiated with a thermal neutron flux of approximately 10^{16} cm^{-2}. The detector (Soviet equivalent of Dacron) was then etched and examined under a microscope. It was established as a result that the track density in the polished /30

glasses was uniform within the limits of statistical error, except for the bubbly sections and dark inclusions where the tracks were not observed. In several cases, very small (0.01 mm) sections with the track density increased by 2 or 3 order of magnitude were detected in the Dacron detector adjacent to the polished sample (Plate 8c). Similar nonuniformities were found in the irradiated Dacron package containing Zhamanshinite powder. They evidently were formed near relicts of minerals which contained an elevated amount of uranium, zirconium for example. However, the local uranium concentrations described did not appear upon etching the Zhamanshinites and irgizites and, consequently, they could not have made a significant contribution to the total number of tracks found in the glasses. Such sections were therefore excluded from the counts. Uranium content C_U was determined from the ratio of the densities of the tracks in the Dacron detectors of the reference N_1 and the samples investigated N_2 by the equation

$$C_U=\frac{C_1 N_2 e_1}{N_1 R_{eff}},$$

where e_1 is the recording efficiency of a detector placed in contact with the reference, and R_{eff} is the effective thickness of the working layer of the sample, which depends on its chemical composition, sensitivity and recording efficiency of the detector and is determined by the equation

$$R_{eff}=(0.046\Sigma a_i z_i+0.78)^2.$$

Here, a_i is the atomic concentration of the i-th element, z_i is its atomic number, and 0.046 and 0.78 are experimentally obtained constants for external detectors made of Dacron, mica or polycarbonate.

The results of determination of the uranium content by both methods agrees within the limits of experimental error ($\pm$ 15%), and they are summarized in Table 2, from which it follows that the uranium in irgizites and Zhamanshinites is (1.3-2.1) . 10^{-6} g/g, an average of $1.8 \cdot 10^{-6}$ g/g.

Based on what has been reported, as well as on the constant spontaneous fission of ^{238}U, of $7.0 \cdot 10^{-7}$ year, the fission track age of Zhamanshinites and irgizites is $(0.81 \pm 0.16) \cdot 10^6$ years.

Determination of the age of Zhamanshinite and irgizite specimens obtained from the Geological Institute, USSR Academy of Sciences, by the fission track method also was carried out by D. Storzer and G.A. Wagner **(128)**, who obtained a value of (1.07 $\pm$ 0.05) /31

TABLE 2. AVERAGE URANIUM CONTENT OF SAMPLES FROM ZHAMANSHIN NATURAL LANDMARK

Наименование образца [a]	Эффективность регистрации, % [b]	Содержание урана, 10^{-6} г/г [c]
Жаманшинит [d]		
с поверхности [e]	40	1,94
с поверхности [e]	42	1,61
с поверхности [e]	38	1,80
из почвы [f]	40	2,05
большая глыба [g]	40	1,97
Иргизит [h]		
с поверхности [e]	45	1,38
пористый из почвы [i]	40	1,65

Key: a. Sample name
b. Recording efficiency, %
c. Uranium content, 10^{-6}, g/g
d. Zhamanshinite
e. From surface
f. From soil
g. Large block
h. Irgizite
i. Porous from soil

$\cdot 10^6$ years. It is possible that the disagreement of the results is connected with different corrections for partial track regression. While the correction in the present work was determined by comparision of the modal track diameters of spontaneous and induced fission, D. Storzer and G.A. Wagner were based on the gradual track annealing method, when tracks from induced fission were brought to the average diameter of the ancient tracks by heating. It is difficult however in both methods to estimate the contribution of localization with an increased rate of etching, which could differ by uranium content, and the thermal stability of the tracks, which could result in some overstatement of the calculated figure. The accuracy of determination of the fission track age of Zhamanshinites is therefore not over 20%.

DISCUSSION OF RESULTS

The tektites of the entire world are broken down by absolute age into five age groups, which correspond to different regions of their occurence.

1. Indochinites, Philippinites and part of the Australites,

which are widespread over an extensive area from Southeast Asia to Australia inclusive, as well as microtektites of the adjacent water areas of the Indian and Pacific Oceans are 700,000 years old **(39, 128).** Impactites from the approximately 1 km diameter Darwin meteor crater in Tasmania are of the same age **(39, 63).**

2. Ivory Coast tektites and microtektites have an age of 1,300,000 years. Impactites in the Ashan (Bosumtvi) Crater located in Ghana are of the same age **(39, 40).**

3. Part of the Australites which differ by an increased amount of potassium are 4,000,000 years old **(40).**

4. Moldavites are 15,000,000 years old; impactites from Ries meteor crater are of the same age **(39, 40).**

5. The oldest (35,000,000 years) formations are from regions extremely distant from each other: Libyan glass (Libya); bediasites (Texas, USA); tektites from Georgia (USA) and /32 microtektites from the Caribbean Sea **(39, 63, 128).**

The hypothesis that the Manicouagan and Clearwater Lake meteor craters (Canada) are of the same age has not been confirmed; the ages of impactites from them proved to be (208 ± 25) and $(290 \pm 30) \cdot 10^6$ years respectively **(40).**

Thus, in four cases of five, the formation of tektites occurred simultaneously with known impacts of large meteorites and the formation of craters. Determination of the age of the new group of irgizite tektites, which are directly connected with Zhamanshinite Crater, is naturally exremely important.

The series of age determinations of Zhamanshin meteor crater conducted permitted a quite narrow age inverval of the time of impact of the meteorite to be found by successive refinement by various methods. By geologic data it is post-Tertiary (younger than 25,000,000 years), by geomorphological data, it is Early or Middle Quaternary $((1.0-0.5) \cdot 10^6$ years) which does not contradict the most reliable determination by the potassium-argon method (younger than 1,000,000 years). According to paleomagnetic data, the crater was formed in the Matsuyama reverse magnetic field epoch $((0.6-2.42) \cdot 10^6$ years). Comparison of these figures permits the assumption that the meteor impact occurred later than the Jaramillo positive inversion episode $((1-0.85) \cdot 10^6$ years). The $(0.81 \pm 0.16) \cdot 10^6$ year determination by the fission track method falls in this interval $((0.85-0.69) \cdot 10^6$ years), i.e., $(0.97-0.65) \cdot 10^6$ years. Thus, five independent methods permit extremely specific classification of the time of impact of the meteorite and formation of Zhamanshin Crater in the upper portion of the Matsuyma epoch, the Eopleistocene $((0.69-0.85) \cdot 10^6$ years).

The age of the Indochinites, Javaites, Philippinites, Australites and Pacific and Indian Ocean microtektites ($(0.7 \pm 0.2) \cdot 10^6$ years) is within this interval. Therefore, synchronism of the irgizite tektites from Zhamanshin meteor crater with them and possibly synchronism of these events with the inversion of the magnetic field of the earth (glaciation began at this same time) cannot be excluded. However, the hypothesis that Zhamanshin Crater is the source of the Australasian tektite field is improbable **(30, 129, 65)**. Their formation in a local crater is very much more likely **(73, 127)**.

GEOPHYSICAL CHARACTERISTICS OF CRATER

The prerequisite for application of geophysical methods to study of meteor craters and their plutonic structure is sharp differentiation of the physical properties of the rocks subjected to the action of an explosive shock wave: ejection; displacement; melting; formation of a substantial fracture zone (Fig. 9). First and foremost, the rocks are abruptly dispersed. Lenses of shattered breccia differ in density from undisturbed basement rock and from later sedimentary rocks which cover the crater. Thus, for example, for the ancient West Hock Crater, it was established that the density of the sedimentary rock younger than the crater which covered it is 2.60-2.45 g/cm^3, 2.7 g/cm^3, for brecciated rock and the density of the same rock not subjected to shattering is 3.03 g/cm^3, i.e., the effective density is more than 0.3 g/cm^3 **(70)**. For Holleford Crater, the effective density between the shattered material and normal rock is 0.16 g/cm^3 **(8)**. The effective density of the shattered and undisturbed rocks at Popigay is 0.3-0.4 g/cm^3 **(95)**. Even for the small Sikhote-Alin meteor impact craters, a decrease of density of the rock exposed to the meteorite shock compared with rocks not subjected to shock was found to be an average of 4.7% **(107)**. Together with shattering and crushing of rocks, local compaction of rocks is sometimes noted. Thus, at the Puchezh-Katun Crater **(38)**, compaction of argillaceous rocks from 2.04-2.08 to 2.12-2.15 g/cm^3 occurred in argillaceous breccia and compaction of marls from 2.15-2.27 to 2.25-2.35 g/cm^3 occurred in marlaceous breccia, i.e., the effective positive fragmental density (approximately 0.08 g/cm^3) is substantially less than the negative effective density between shattered and undisturbed rocks over the crater as a whole. /33

Anomalies of the terrestrial magnetic field are determined basically by the magnetic susceptability and the magnitude and direction of the remanent magnetism of the rocks. First, impact action demagnetizes the target rocks and reduces their remanent magnetism. This leads to a general decrease in magnetic field intensity in the area. Second, previously established locations of the magnetic domains (regions of magnetism of the same sign) is disturbed in the crust of the earth, and mixing of differently magnetized fragments occurs in the brecciated rock zone. The

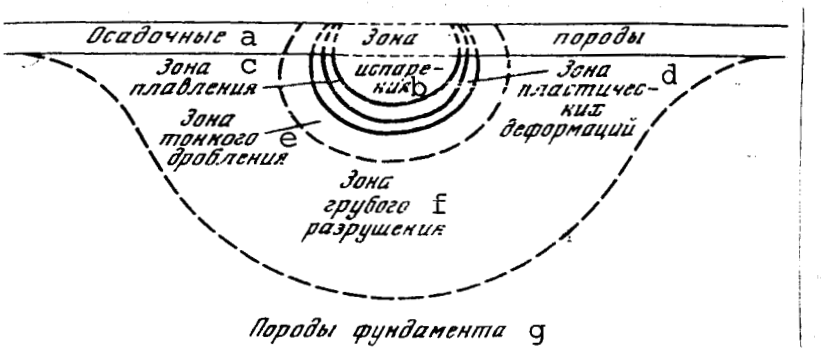

Fig. 9. Shock wave zones of action.

Key:
a. Sedimentary rocks
b. Vaporization zone
c. Melting zone
d. Plastic deformation zone
e. Fine crushing zone
f. Coarse shattering zone
g. Basement rocks

magnetic field of the impact region is broken down into a mosaic of individual anomalies which have randomly oriented extent over the impact area of the crater. Finally, third, the presence of a substantial volume of rock subjected to complete or partial remelting is characteristic of large craters. Upon hardening, the rocks acquire thermal remanent magnetism, and the direction of this magnetism reflects the direction of the magnetic field of the earth at the time of hardening of the remelted rock. This can be a /34 criterion for determination of crater age on the paleomagnetic scale. The intensity of the remanent magnetism of remelted rocks differs considerably from the magnetism of the surrounding rocks. For Ries Crater for example, the intensity of the remanent magnetism of the zyuvites is more than 5 times greater than the magnetism of the crystalline rocks induced by the modern terrestrial magnetic field **(111)**.

Electric geophysical exploration gives important information for the study of meteor craters. The electrical properties of rocks are evaluated by their resistivity. Local sections of reduction of resistance noted in zones where interstitial waters accumulate. It is therefore evident that a hemispherical lens of shattered breccia in the base of a crater, frequently saturated with water solutions, should cause a decrease in electrical resistance.

The internal structure of a crater and different zones of it, due to the formation of boundaries with abrupt and substantial changes of elastic properties of the rocks, makes craters extremely convenient objects for seismic studies.

GRAVIMETRIC STUDIES

A density cross section in the area of Zhamanshin Crater was studied both by direct densitometric measurements in the crater area and by density determinations in the natural bedding. In addition, the density characteristics of the rocks of the Turan plate have been quite well studied in general. The density of the Paleozoic basement rocks, represented basically by schists, quartzites, porphyrites and volcanogenic sedimentary rocks, is 2.7-2.9 g/cm^3. The Upper Mesozoic-Cenozoic part of the cross section is made up of clays (density 2.2 g/cm^3) and sandstones (density 2.4-2.5 g/cm^3). Because of such a sharp difference, the regional gravity field (Fig. 10) reflects the behavior of the basement surface and, to a lesser degree, its internal structure. The rocks formed as a result of melting differ considerably from the basement rock of the two layer target. The density of the impact glass is an average of 2.1 g/cm^3.

The Zhamanshinite scoria has a density of 1.5-1.7 g/cm^3 and /35
sometimes more, decreasing to 1.5 g/cm^3 depending on porosity and the nature and number of inclusions. Pumice-like formations have 1.2 g/cm^3 average density, but is lighter than 1.0 g/cm^3 in some samples and it therefore floats in water (Fig. 11).

For density determination of the rocks of the upper part of the cross section of allogenic breccia in the natural bedding, the Nettleton problem was solved over several profiles in places with a highly broken relief. The problem consisted of calculation of the anomalies in the Bouguer reduction with different intermediate layer densities by the equation

$$\Delta g_B = g_{obs} + (0{,}3086 - 0{,}0419\sigma) H,$$

where Δg is in mGal, σ is in g/cm^3 and H is in m.

With a correctly selected intermediate layer corresponding to the actual density, the calculated anomalies are not correlated with the relief, but should change linearly along the profile. Examples of such determinations are presented in Fig. 12. Solution of the Nettleton problem permitted demonstration of the absence of "roots" in exposed blocks of Paleozoic basement rocks on the /36
northwest wall. It turned out that their density is less than 2.0 g/cm^3, while the density of the Paleozoic basement rock is 2.7-2.9 g/cm^3, and that these hills are, with respect to density, "hollow," "empty" compared with Paleozoic rocks. The ejecta of basement rock fragments proved to be an armoring layer which preserved individual sections from destruction and are now singled out in the form of cone shaped hills.

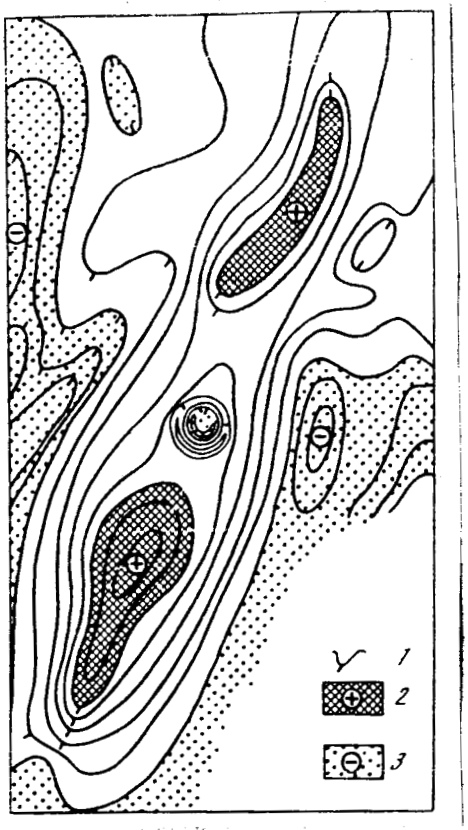

Fig. 10. Diagram of regional gravity field in provisional isolines:
1. provision isolines;
2. positive anomalies;
3. negative anomalies.

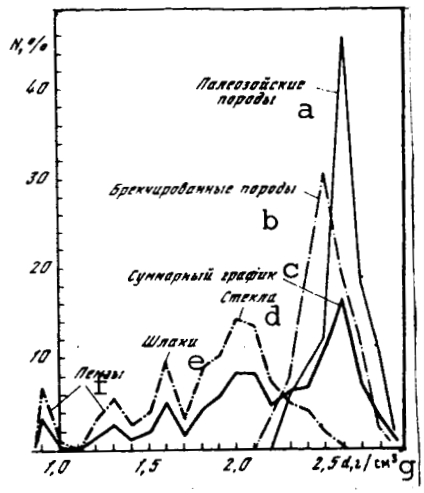

Fig. 11. Density distribution histogram of rocks of Zhamanshin Crater region.

Key: a. Paleozoic rocks
b. Brecciated rock
c. Cumulative curve
d. Glasses
e. Scoria
f. Pumice
g. d, g/cm^3

The local gravity field in Zhamanshin Crater and its vicinity was studied in 1977 by a detailed gravimetric survey along two profiles which intersected in the center of the crater, northeast and southwest. Regionally, the crater is located in a basement uplift zone which extends in the submeridional direction. This 10-15 km wide zone is reflected in the gravity field in the form of a linear positive anomaly (see Figs. 3 and 10). In the Zhamanshin uplift region itself, the regional gravity field is reduced by 3-4 kGal, which is caused by submergence of the basement by 250-300 m with 0.3 g/cm^3 excess density of the sedimentary rocks and basement. The 14 mGal sublatitudinal change of amplitude of the anomaly with a 40 Oe gradient is connected with both sinking of the basement and with the fracture zone which separates blocks of Paleozoic rocks of different densities. /37

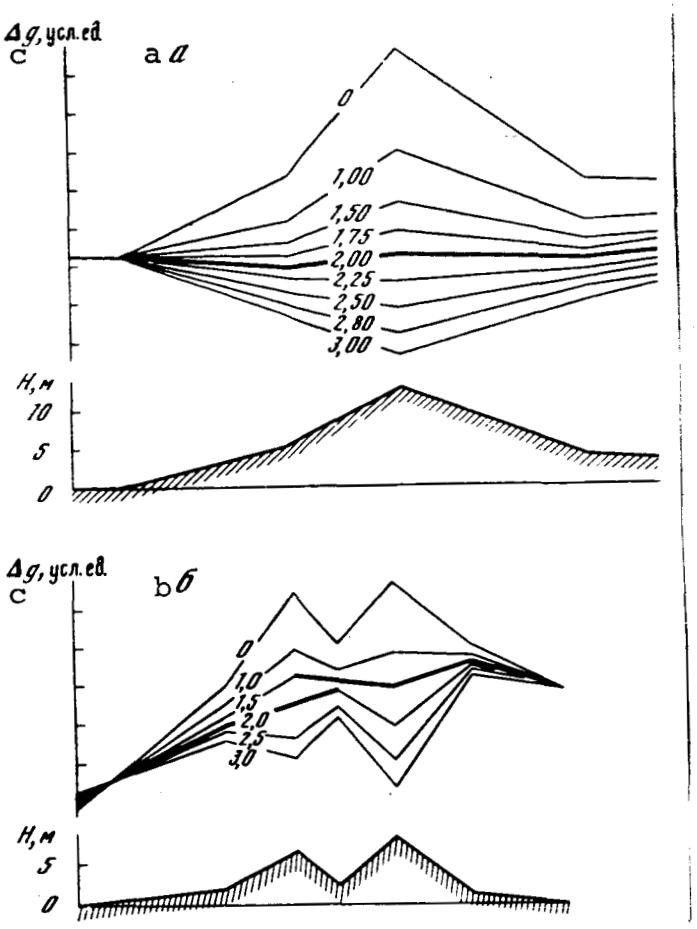

Fig. 12. Density determination by Nettleton method: a. on southern part of wall in allogenic breccia containing Paleozoic rock fragments; b. above Paleozoic rock body (see Fig. 6 , Plate 3a); figures on curves are density values.

Key: c. Δg, arbitrary units

The size of Zhamanshin Crater is commensurable with the dimensions of the basement blocks which produce intense gravity anomalies. Its center is confined to the axis of the analogous uplift. As a result, the crater corresponds directly to a negative gravity anomaly in the Bouguer reduction with approximately 6 mGal (Fig. 13). The shape of the anomaly in both profiles is very similar. This is evidence that the bodies which form them are isometric. The anomaly is circular in plan, similar to those established at the Gosse's Bluff, Carswell and other meteor craters (Fig. 14). The anomaly contours again permitted determination of the crater diameter as 5.5 km. The circular maximum along the edges of the structure reflects the uplift of the basement connected with the general uplift of the basement in the

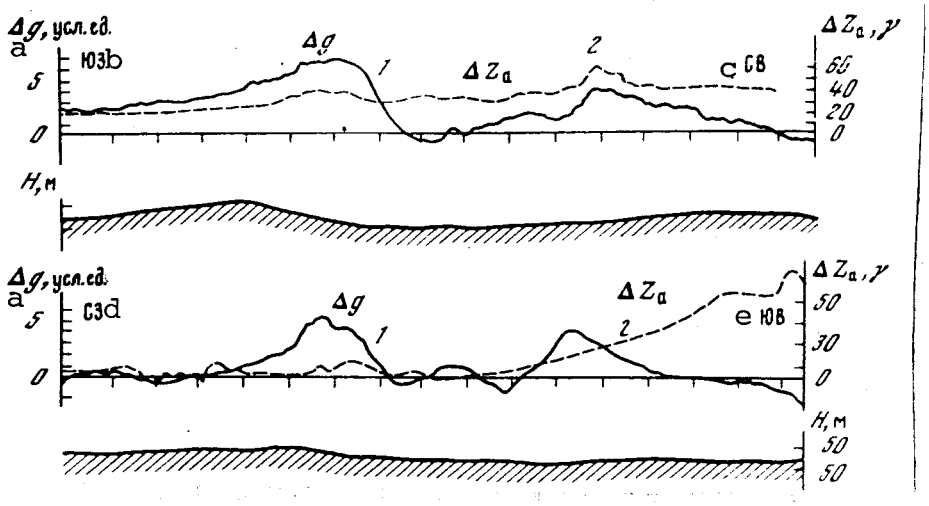

Fig. 13. Gravity anomaly curves in arbitrary units in Bouguer reduction (1) and magnetic anomalies (2) above Zhamanshin Crater.

Key: a. Δg, arbitrary units; b. southwest; c. northeast; d. northwest; e. southeast

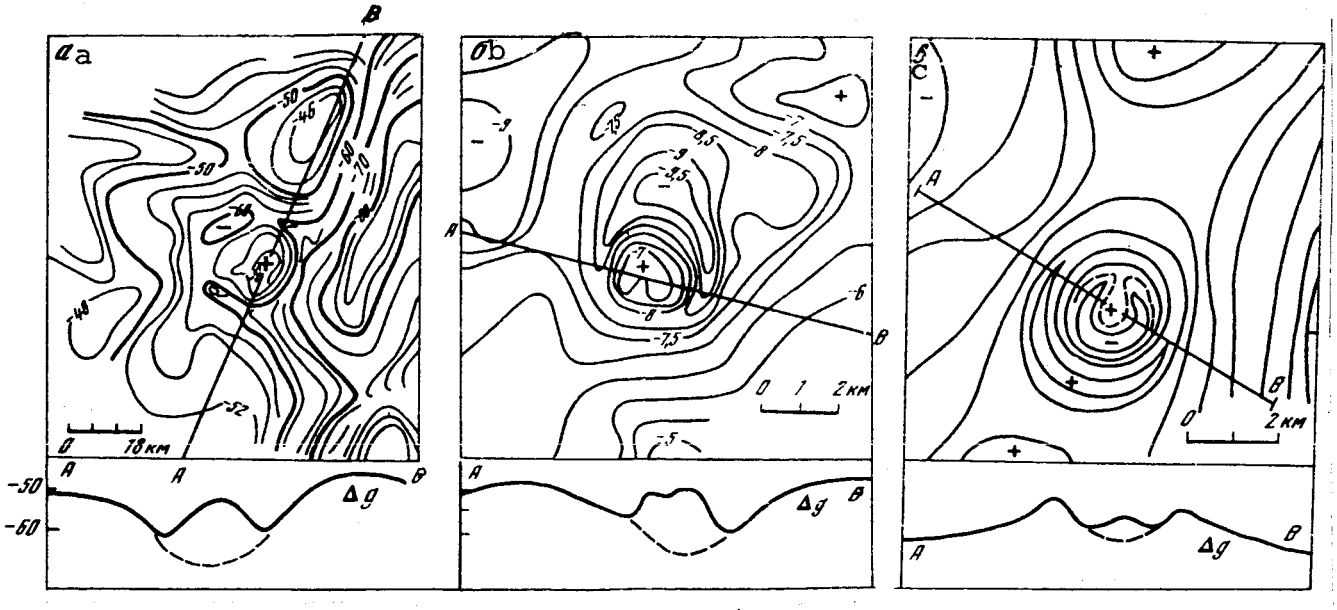

Fig. 14. Negative gravity anomalies above Carswell (a), Gosse's Bluff **(18)** (b) and Zhamanshin (c) Craters complicated by positive anomalies in center.

region of the Zhamanshin structure. A positive 1.5 mGal anomaly was established in the central part of the crater. It corresponds to either the central uplift or a small lens of denser rock, melted impactites for example. The amplitude of the central uplift or the thickness of the rock lens of increased density can be estimated at 100-200 m from the magnitude of this anomaly.

The observations made indicate considerable correspondence of the gravimetric characteristics of Zhamanshin Crater to the correlations made by analysis of a large number of structures. A negative anomaly (Fig. 15), connected with a large volume of /38
dispersed rock of breccia formed by explosion, corresponds to small meteor craters (Deep Bay, Holleford, West Hock, Clearwater West and East in Canada; Ries, FRG; Kaluga, Yanisjarvi, Boltysh, Shunak and others in the USSR). The lens thickness and dimensions determine the amplitude of the gravity anomaly. Thus for example, the negative gravity anomaly above 2.5 km diameter Holleford Crater is 1.8-2.0 mGal and is 16 mGal above Deep Bay Crater (11 km). The connection of the structure dimensions and the magnitude of the negative gravity anomaly is regular (Fig. 16), and it permits important conclusions to be drawn.

1. The nature of the relationship changes greatly and becomes complicated in the transition from small craters to craters of large dimensions.

2. Craters less than 1 km in diameter are weakly represented in the gravity field.

3. For craters from 1 to 50 km in diameter, a distinct relationship of the negative gravity anomaly to crater diameter is observed: the larger the crater, the greater the amplitude of the anomaly.

4. For structures over 50 km in diameter, this relationship is weakened (the curve tends toward the asymptote). The value of the negative anomalies of large structures depends little on their diameters. The increase observed here in scatter of the anomaly values with increase in structure dimensions is connected with the complexity of the structure, the high degree of disturbance and the isostatic dynamics of the structure itself during the subsequent substantial geologic time following the impact, as well as with the specific block structure of the region, etc.

Point (2) related to salt domes, the Salt Pan cryptovolcano (UAR) **(58)**, Kuttuyaro Caldera (Japan) **(147)** and the ancient paleovolcano Aragats in Armenia are indicated for comparison in /39
Fig. 16. They all lie outside zones which characterize the relationships of a structure of impact origin. For salt domes, it is practically impossible to plot a curve of gravity anomaly amplitude vs. dimensions. For the 20 kilometer Kuttuyaro volcanic caldera in Hokkaido, the gravity anomaly is 46 mGal, in which the

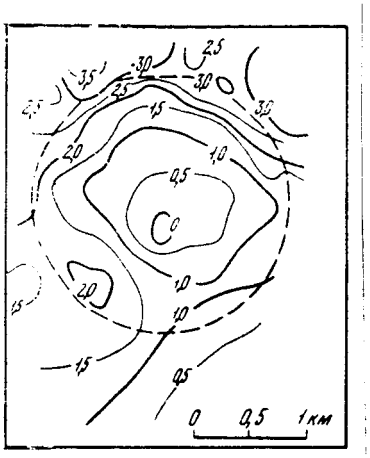

Fig. 15. Typical negative gravity anomaly above Holleford meteor crater. (76).

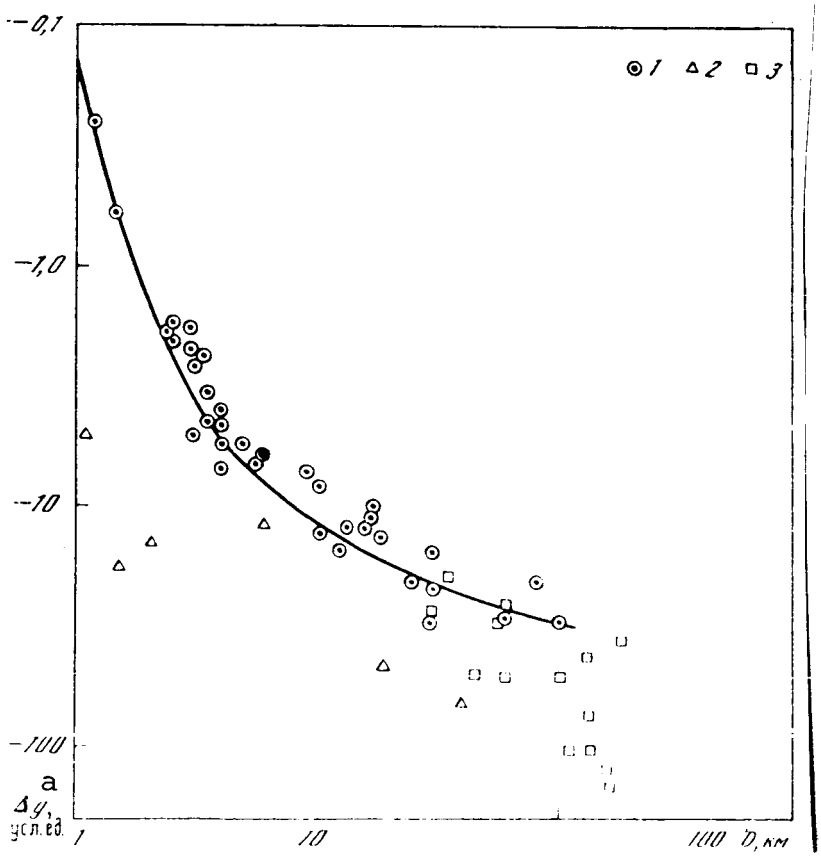

Fig. 16. Gravity anomaly amplitude vs. structure dimensions (here and subsequently, Zhamanshin Crater is noted by a solid circle): 1. meteorite; 2. non-meteorite; 3. lunar craters.

Key: a. Δg, arbitrary units

center of the negative gravity anomaly does not coincide with the center of the caldera. According to Yokoyama **(147)**, this anomaly is caused by "loose material" which occurs at a depth of several kilometers on sunken blocks of volcanic rock, but there may be both loose products of collapse and light magma of acid composition under the calderas which together causes such an intense negative anomaly. The relative amplitude of the negative anomaly for the 40-45 km diameter ancient Aragats Volcano is 64 mGal. There are no gravity anomalies in Fuji and Asama Volcanos in Japan **(139)** but, for the Mihara caldera on the other hand, a positive gravity anomaly of approximately 15 mGal is found in the central portion. Above the Koolau caldera on the island of Oahu (Hawaii), which is similar to a meteor crater in outward appearance, the large positive gravity anomaly reaches a value of 116 mGal **(91)**, and it is interpreted as a vertical stock of mantle material introduced from subcrustal depths. Positive gravity anomalies also are characteristic of the Karym, Avachin, Ksudach, Krasheninnikov **(151)** and Malyy Semyachik **(67)** volcanos of Kamchatka. Both positive and negative anomalies can thus correspond to volcanic structures. Their amplitudes, as well as the parameters which determine them (mass deficiency, depth to center of gravity and others), do not correspond to values characteristic of meteor craters.

The next stage of interpretation is quantitative **/41** interpretation of the gravity anomaly, in which the depth of occurrence, shape, dimensions and mass of the body causing this anomaly are determined. Quantitative characteristics of meteor craters and astroblems are compared and data are presented on structures of various dimensions, including Zhamanshin Crater, in Table 3. Because of the ambiguity of the general solution of the inverse problem, some a priori premises on the physical and geological properties of the crater must be assigned for the conduct of quantitative calculations. Since premises are nearly always assigned with specific errors, the results of interpretation of geophysical data are one of the possible models. Calculations to determine the excess mass, depth of its center of gravity, as well as the limiting surfaces and excess densities were conducted.

Meteor craters and astroblems are characterized by intense negative gravity anomalies, the amplitudes of which depend on the dimensions of these structures. Anomalies of the same amplitude can however be from sources of disturbance of varied mass. The mass deficiency of the structure, calculated from the gravity anomaly is more representative than amplitude of the source of the gravity anomaly, since it carries integral information in itself. The anomalous mass for meteor craters is due to the amount of rock ejected and the formation of lenses of dispersed and shattered breccias near the surface. For cryptovolcanic and diapiric structures, explosion pipes and volcanic calderas, for structures of endogenous origin, the distribution of the mass anomaly will be different in connection with the presence of roots in these

TABLE 3. QUANTITATIVE PARAMETERS OF METEOR STRUCTURES

Наименование структур a	Диаметр структуры, км b	Амплитуда аномалии силы тяжести, мГал c	Дефектная масса, 10^9 т d	Глубина центра тяжести, км e	Отношение глубины центра тяжести к диаметру f	Отношение значений дефектной массы к площади, 10^9 г/см^3 g	Предельная избыточная плотность, г/см^3 h	Приблизительная масса метеорита, образовавшего кратер, т i
Аризона (США) j	1,2	-0,6	0,017	0,16	0,13	0,16		$n(10^3-10^4)$
Холлефорд (Канада) k	2,5	-1,8-2	0,07 (0,34) *	0,6	0,24	0,016 (0,08) *	0,066	10^4
Брент (Канада) l	3,6	-4,5	0,92 (0,92) *	0,75	0,21	0,09	0,06	10^5
Уэст Хок (Канада) m	5,0	-6,6	0,8	0,8	0,16	0,041	0,026	10^5-10^6
Жаманшин (СССР) n	5,5	-6,0	1,06	1,4	0,25	0,15	0,08	$(1,2-2)\cdot10^6$
Уанапитей (Канада) o	9,6	-13	17,0	2,1	0,22	0,234	0,05	10^6
Дип Бэй (Канада) p	11-12	-16	21,0 (21,0) *	1,5	0,14	0,181	0,06	10^6
Калужская (СССР) q	16	-12	43,6	2,4	0,15	0,208	0,043	10^6-10^7
Восточный Клируотер (Канада) r	18	-13	37,7	2,2	0,12	0,149	0,034	10^7
Рис (ФРГ) s	20-24	-20	62,1 (74) **	2,1	0,10	0,164 (0,195) **	0,046	10^7
Янис-Ярви (СССР) t	20-23	-12	51,5	2,6	0,11	0,164	0,031	10^7
Болтышская (СССР) u	26	-30	312,0	4,2	0,16	0,44	0,05	10^7
Западный Клируотер (Канада) v	28-30	-16	48,1	3,1	0,11	0,078	0,013	10^7-10^8

* (76)
** (79)

Key: a. Structure name; b. Structure diameter, m; c. gravity anomaly amplitude, mGal; d. Mass deficiency, 10^9 tons; e. Center of gravity depth, km; f. Center of gravity depth to diameter ratio; g. Mass deficiency to area ratio, 10^9 g/cm^3; h. Maximum excess density, g/cm^3; i. Approximate mass of crater forming meteorite, tons; j. Arizona (USA); k. Holleford (Canada); l. Brent (Canada); m. West Hock (Canada); n. Zhamanshin (USSR); o. Wanapitei (Canada); p. Deep Bay (Canada); q. Kaluga (USSR); r. Clearwater East (Canada); s. Ries (FRG); t. Yanisjarvi (USSR); u. Boltysh (USSR); v. Clearwater West (Canada)

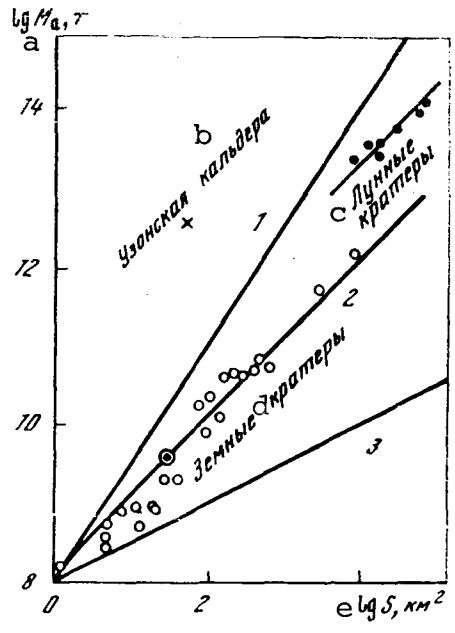

Fig. 17. Deficient mass of terrestrial and lunar craters vs. $S^{3/2}$ (1), S^2 and $S^{1/2}$ (3).

Key: a. log Ma, t; b. Uzon Caldera; c. Lunar craters; d. terrestrial craters; e. log s, km2

structures, although the amplitude may be the same in some cases as for meteor craters.

The expression for calculation of anomalous mass Ma from the gravity anomaly can be derived from the Gauss theorem. The power flow through a closed surface determines the magnitude of its source,

$$\int_S \Delta g_a \, dS = 4\pi f M_a.$$

For an infinite plane lying above a perturbation source, the magnitude of the field of force is half as much in the direction toward the anomalous mass. Because of the fact that the OZ axis is directed down, the expression for calculation of this mass will have the form /42

$$M_a = \frac{1}{2\pi f} \int \Delta g_a dS,$$

where the integral is taken over all of area S of gravity anomaly Δg_a, f is the gravitational constant equal to $6.67 \cdot 10^{-8}$ $cm^3/(g \cdot s^2)$. In rectangular coordinates,

$$M_a \approx \frac{1}{2\pi f} \sum_i \left(\sum_j \Delta g_{ij} \Delta x_i \right) \Delta y_j,$$

where Δx_i and Δy_j is the step (distance) between points of initial values of gravity Δg_a. This expression was used practically in calculation of the deficient mass of the craters.

The deficient mass for Zhamanshin Crater, calculated from the gravimetric survey results, is approximately $1.06 \cdot 10^9$ tons, and it corresponds to the previously derived **[20]** dependence of its dimensions for terrestrial meteor craters.

For a number of meteor craters and astroblems of varied size where gravimetric surveys have been conducted, the deficient masses have been calculated. The results of these calculations are represented in Fig. 17, where Ma vs structure area S is shown. /43 With increase in size of meteor craters, the deficient mass increases in direct proportion to structure area S and not diameter D or volume V. In Fig. 17, together with observed Ma vs S, straight lines also are drawn which correspond to functions $S^{1/2}$, S, $S^{3/2}$, which are proportional to crater diameter, area and volume respectively. They show graphically that empirical relationship Ma

=c(f) most closely (correlation coefficient Ø.9975) approximates the straight line M_a=cS. This fact deserves attention, since apparently topographic expression, the volume of rock changed by impact metamorphism and other diagnostic indicators like anomalous mass are proportional to the area of the meteor structures. The fact is that quite large craters exist as two dimensional and not three dimensional objects. They do not have deep roots commensurable with their diameter, and this determines processes of gradual destruction of the craters, since the lifetimes of two dimensional geologic objects is significantly shorter than the lifetimes of 3 dimensional objects **[37]**.

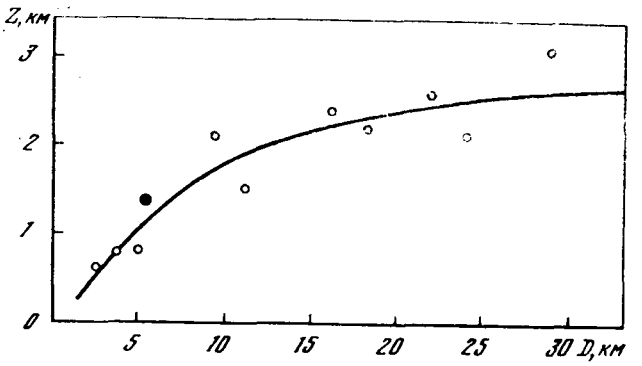

Fig. 18. Center of gravity depth Z vs. structure dimensions D.

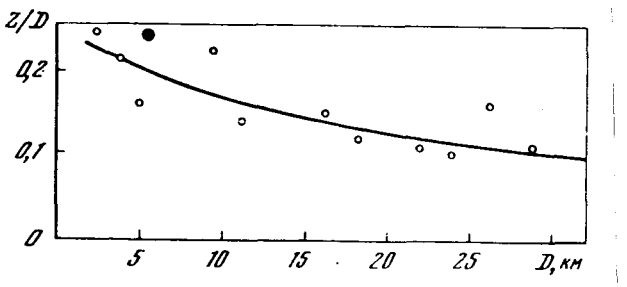

Fig. 19. Curve of ratio of center of gravity depth Z to structure diameter D vs structure diameter.

The calculated anomalous mass undoubtedly is somewhat understated compared with the initial mass, since the crater is eroded and filled with sediments or is even relaxing (recovering) over time. As a result of removal of the load because of ejection of a large amount of material from a limited area, a reduced pressure zone is formed and an inflow of plutonic matter of increased density to it occurs, partly compensating the anomalous mass deficiency. This is particularly characteristic of large structures /44 **[24]**. Finally however, while this phenomenon strongly affects the amplitude of the anomaly, it has substantially less effect on the value of the deficient mass. Deficient masses of volcanogenic structures are two orders of magnitude greater than those of meteor craters of the same dimensions. Their values are, for example, $1.5 \cdot 10^{11}$ tons for the Pauzhet Caldera and $(2.0-2.5) \cdot 10^{12}$ tons for the Bol'she-Semyachinsk and Uzon Calderas **[151]**. Another characteristic of the object is the location of its center of gravity. Since meteor craters are lenses of dispersed rocks which occur near or on the surface itself, their centers of gravity are shallow, no deeper than a few kilometers (Fig. 18). This depth increases insignificantly with increase in dimensions of the structure **[22]**. It is 1.4 km for Zhamanshin Crater, and it fits into the general dimensional relationship for meteor craters. The center of gravity of volcanic structures is

considerably deeper. The depth of the center of gravity of the anomaly forming objects for the Pauzhet and Bol'she-Semyachinsk Calderas is 10-15 km and 10 km respectively. The depth of the center of gravity of the Uzon Caldera is 14-18 km **[151]**.

The ratios of the center of gravity depth and dimensions of the structures (Fig. 19) of the Brent, Kaluga and Ries Craters are 0.25, 0.15 and 0.10 respectively. These values are very small and they decrease with increase in dimensions of the structure. This indicates relative closeness of the deficient masses to the surface and "flushing out" of the depression (a decrease in relative thickness of the breccia with increase in dimensions), i.e., it indicates a limited depth of penetration of the explosions. This is evident in Fig. 19, and it also has been demonstrated theoretically and experimentally in the craters formed by nuclear explosions **[141]**. The same picture is observed for the ratio of crater depth to dimensions of the structure **[5]**.

Since meteor crater structures are near the surface and lack roots, rapid loss of amplitude of the gravity anomaly occurs in conversion to the height **[22]**. It is therefore of interest to calculate the deficient surface density, which reflects the amount of matter removed and the amount of shattered mass per unit area of the crater. It is obtained by as though "spreading" the anomalous mass over the entire area of the crater, and it is calculated by the equation $\mu = M_a/\pi R^2$. For terrestrial meteor craters and astroblems, the value of μ varies stably from 0.5 to $0.2 \cdot 10^5$ g/cm^2. This means that, despite the increase in total energy, with increase of mass of the incident space body per unit area, the specific density of that part of the energy which works to eject and shatter remains approximately constant (μ =const$\approx$120 t/m^2). The resulting figures can be interpreted differently, by considering that, in the impact and explosion of large meteorites accompanied by the formation of large craters (more than one km), at least 120 $\pm$ 50 t of rock is removed per m^2 on the average. These figures are consistent with actual data. Thus for example, approximately 300 t was removed per m^2 in the central part of the Arizona Crater, and the average over the entire area of the crater /45
was approximately 60 t/m^2. For small craters (less than one km), this value is substantially smaller, but it varies for small craters of different dimensions. This is connected with the fact that the gravity of the earth still does not play a large part in the formation of small impact craters. For example, approximately 30-35 t/m^2 was removed from the central part of the Main Kaali Crater, but only approximately 10 tons from the largest Sikhote-Alin crater. The value of μ for Zhamanshin Crater is approximately 150 ton/m^2. A V shaped body with 3.2 km maximum depth, 1.5 km center of gravity and excess density $\Delta\sigma$=-0.08 g/cm^3 was successfully calculated by the trial and error method. It corresponded to anomaly Δg_a observed above Zhamanshin Crater. These parameters are consistent with data on crater structure obtained from geological observations. The 0.08g/cm^3 density deficit is somewhat higher than the average density deficit for other meteor craters,

which is approximately 0.04-0.06g/cm^3 [22].

The figures obtained can be compared with data on lunar craters, which are represented similarly in the gravity field, and points which correspond to the anomaly amplitude and excess mass of lunar craters lie on the same curve as the terrestrial craters, as if they were a continuation of them (see Fig. 16, 17). Analysis of data on the gravity field of the visible side of the moon shows [124] that the majority of circular structures less than the /46
majority of circular structures less than 200 km in size give a negative gravity anomaly (although some of the most ancient of them like, for example, Landsberg, Reiner, Petavius and Fracastorius Craters, are not represented in the gravity field), and the amplitude of the anomaly has a tendency to increase with increase in size of the structure [20]. The deficient masses were calculated for a number of lunar craters [124], based on the gravity field with respect to the mass of the moon. They are from -0.32 to 1.5·10^{-6} M (M, the mass of the moon is 7.35·10^{25}g). The deficient masses of the lunar craters of different sizes are within the limits of (0.23-1.0)·10^{14} t. On the curve (see Fig. 17) of lunar crater mass vs their areas, the mass values for lunar craters continue the relationship for terrestrial craters with a parallel shift toward larger masses, which reflects the general nature of the genesis of terrestrial astroblems and lunar craters. The break in the curve upon change from terrestrial to lunar craters is explained by the lack of information on the gravity field of lunar craters less than 100 km in diameter.

The surface density of lunar craters is (1.5-3.0)·10^5 g/cm^3, which is an order of magnitude greater than that of terrestrial meteor craters. The reason for the presence of such a large deficient mass and surface density in lunar craters compared with the same parameters of terrestrial craters is that first, on the moon, because of lower gravity (1.6 vs. 9.8 m/s^2 on the earth) with the same explosion energy, considerably more material should be ejected from the crater (1900 $\pm$ 500 t/m^2) than on the earth. This difference increases with increase in dimensions, when the factor of the effect of the difference in gravity shows up particularly strongly [23]. Second, lunar craters are obliterated, filled, and destroyed over time immeasurably more slowly than terrestrial craters [37]. Third, isostatic processes on the moon occur incommensurably more slowly. There is therefore on the moon a truer, and therefore larger deficient mass than in terrestrial craters.

The results obtained permit doubt of the Baldwin curve [5], which describes a common relationship of depth to dimension for lunar craters, terrestrial artificial craters and meteor craters. This cannot be, even if because different amounts of material are ejected from terrestrial and lunar craters of the same size. Further, terrestrial astroblems most often are eroded, their original morphology has changed to a considerable extent and is difficult to restore, and upon reconstruction, their initial

appearance usually is based upon the Baldwin relationship, with the use of which for terrestrial structures corrections are necessary.

MAGNETOMETRIC STUDIES

The majority of the rocks in the Zhamanshin Crater region are slightly magnetic. The basement rocks have $\kappa = 0\text{-}200 \cdot 10^{-6}$ CGS units. The red rocks of the Lower Carboniferous are practically nonmagnetic ($\kappa = 0\text{-}20 \cdot 10^{-6}$ CGS units). Some shales with $\kappa = 1500 \cdot 10^{-6}$ proved to be the most magnetic.

E. S. Gorshkov (Leningrad Section, Institute of Terrestrial Magnetism, the Ionosphere and Radiowave Propagation, USSR Academy of Sciences) determined specific magnetic susceptibility κ of 266 Irgizites. With quite broad limits of change (from 4 to $50 \cdot 10^{-6}$ /47

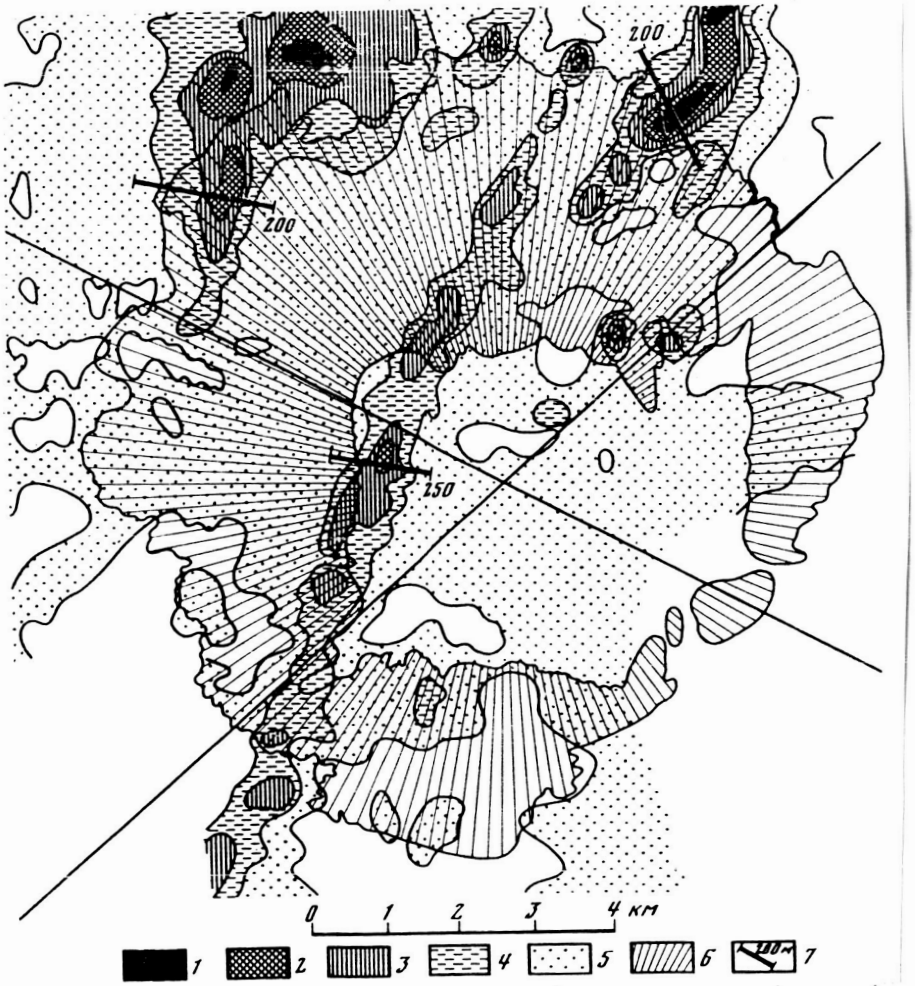

Fig. 20. Map of magnetic anomalies in Zhamanshin Crater region: 1. intense positive anomalies; 2. positive anomalies; 3. slightly negative field; 4. negative field; 5. intense negative field; 6. allogenic breccia of wall; 7. depth of magnetically perturbed masses; profile locations indicated by lines.

CGS units), the maximum of the distribution histogram corresponds to values of (10-12)·10^{-6} CGS units The magnetic susceptibility of tektites from other dispersions is somewhat lower and usually varies within (2-8)·10^{-6} CGS units **[130]**. The magnetic susceptibility of Zhamanshinites is considerably higher: an order of magnitude in the dark glasses (κ=100·10^{-6} CGS units); two orders of magnitude in the basaltoid rocks (κ=1500·10^{-6} CGS units). The natural remanent magnetization of the basaltoid rocks, according to the type of the curves of demagnetization by an alternating magnetic field, is of a thermal remanent nature. A. de Gasparis obtained similar results **[57]**.

In addition, the specific magnetic susceptibility of tectites and impactites from other regions of the world was determined. We present modal figures (the number of samples measured x is in parentheses): moldavites (38), 3·10^{-6} CGS units; indochinites (3), 7·10^{-6} CGS units; bediasites (8), 5.5 CGS units; australites (1), 6·10^{-6} CGS units; regolith (1), 10.6·10^{-6} CGS units; Darwin glass (9), 6·10^{-6} CGS units; Auellul Crater impactite (9), 6·10^{-6} CGS units; impactite from Henbury Crater (1), 470·10^{-6} CGS units.

The anomalous magnetic field of the Zhamanshin Crater vicinity (Fig. 20) is defined by zones of occurrence of various folded basement rocks extended to the north-northeast. In the western part of the crater, a narrow, linearly extended positive anomaly with values up to 100 γ extends, which is connected with a fault and probably is caused by a body of ancient ultrabasic rocks. Their course coincides with the general north-northeast strike of structures in the Northern Aral region. Other northeastern anomalies are distinguished in the magnetic field picture, which reflect zones of uplift of the basement and alternation of Upper and Lower Paleozoic rocks in it, which are distinguished by different magnetic properties.

In the immediate region of the crater, from analysis of the map and of four detailed profiles which cross the crater, it follows that the connection of the magnetic field and the structure of the crater itself is extremely weak. Magnetic field Δz_a is mild in the crater region with reduced values (-100-150γ). Nearly isometric, relatively positive anomalies are confined to the outer part of the structure, "cutoff" of the anomalies is noted in the north of the structure along the outer boundary of the crater, and the anomalies form a ring. Estimation of the depth of occurrence of the basement by the characteristic points method gave a value on the order of 200 m within the inner slope of the crater at the location of the anomaly.

The interpretive possibilities of the anomalous magnetic field also are limited because of insignificant differentiation of the magnetic properties of the rocks which make up the region.

Comparison of the gravity and magnetic fields and their combined interpretation provides useful information. It should be

noted first and foremost that regional gravity anomalies (see Fig. 14c) and magnetic anomalies (see Fig. 20) have the same north-northeast strike. The basement uplift zone has the same strike, /48 i.e. anomalies Δg and anomalies Δz_a are connected with the rocks of the basement and its internal structure. It is evident from curves of a detailed magnetic and gravity survey (see Fig. 10) that there is a close correlation between anomalies Δg and Δz along the SW-NE profile in the crater area. This permits the conclusion to be drawn that the source of both anomaly Δg and anomaly Δz is one and the same. The correlation is weaker along the NW-SE profile, but it also occurs.

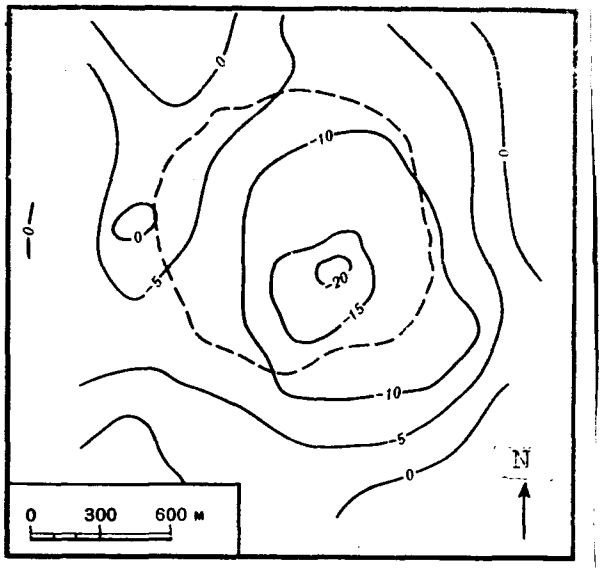

Fig. 21. Magnetic anomaly above Arizona Crater **[114]**.

In comparing the resulting pattern for Zhamanshin Crater with information on other structures, it should be noted that the general decrease of magnetic field strength within a /49 crater and its variegation are a characteristic feature of astroblems. Thus for example, for Brent Crater (Canada), the field intensity within the crater is 160 γ lower than its vicinity, 20 γ lower for the Arizona Crater (1.2 km dimension) (Fig. 21) **[114]** and, for Mishinogorsk (diameter 3-4 km), Yanisjarvi, Karsk, Puchezh-Katun, Shunak, El' tgygytgyn and other craters (USSR) as well as Carswell, Clearwater West and East and other craters (Canada) and Ries Crater (FRG), the magnetic field strength is less than the field of the regions surrounding the structure.

The volume of remelted rock for small craters is relatively small, and they practically do not produce any noticeable central anomaly. In explosive meteor structures more than 5 km in diameter, reduced and variegated fields with sharply expressed anomalies in the central part of the structure are observed, which are due to the mass of rock melted by the explosion and magnetized by the magnetic field of the earth upon hardening. The magnitude of the observable central magnetic anomalies of large craters depends particularly on the volume of melted rock, and the direction of its remanent magnetism (and consequently the sign of the anomaly) reflect the direction of the magnetic field vector of the earth of the site at the time of the meteorite impact. In principle, this makes it possible to determine the crater age on the paleomagnetic scale and inversely, to refine the paleomagnetic scale from the structures studied. Thus for example, in the center of Ries Crater (Fig. 22), there are several negative magnetic anomalies with values up to -300 γ, which are bounded on the north

by an arc of positive anomalies. A positive anomaly of up to +150 γ lies southwest of Ries, and extended slightly positive anomalies /50
are to the south. Intense negative anomalies appear generally as though they were encompassed by a collar of positive anomalies. The negative magnetic anomalies are due to zyuvite impactites which occur within the crater. Zyuvites have an inversely directed remanent magnetization vector, which corresponds to the direction of the magnetic field of the earth at the time of formation of Ries Crater ($15 \cdot 10^{-6}$ years ago). The intensity of magnetization of the Zyuvites reaches values which cause negative magnetic anomalies **[111]**.

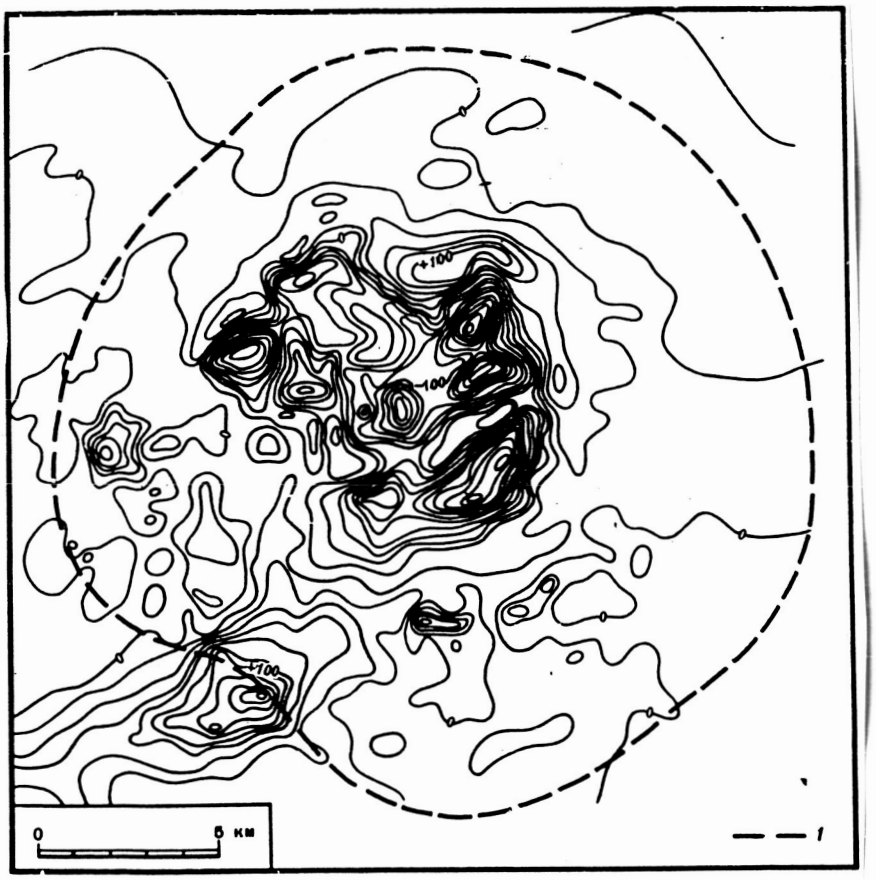

Fig. 22. Anomalies of total magnetic field strength vector above Ries Crater **[111]**, 10^{-5} Oe cross section: 1. 450 m isoline.

The magnetic field of very large craters (over 50 km in diameter), just like the gravity field **[22]**, is still more complicated, in which the effect of the tectonic blocks of the target predominate, and its initial heterogeneity shows up. This is evident in the magnetic field of the 80 kilometer Puchezh-Katun meteor crater. Some meteor structures are almost completely not reflected in the magnetic field, like the Kaluga or Boltysh Craters /51

for example, since they are buried under thick strata of nonmagnetic sedimentary rocks, or they are reflected slightly in the form of anomalous deviations of the regional field, like the Brent Crater, for example. Part of the structures is singled out by a ring of local positive and negative magnetic anomalies gravitating toward the crater edges, the Gagarin structure for example **[21]**. The complex picture of the magnetic properties of the rocks in the areas of some craters frequently leads to specific difficulties in the interpretation of magnetic anomalies, although they undoubtedly bear substantial information.

The magnetic fields of volcanos and calderas are of a completely different nature. Small in area but intense anomalies, positive or negative depending on the time and conditions of their formation, are characteristic of them. They are connected either with volcanic pipes or with intrusions (Tolbachek, Karym, Koryak, Avacha, Talov, Koolau and others).

ELECTRIC GEOPHYSICAL EXPLORATION

Electric geophysical exploration was applied to study of Zhamanshin Crater. The geoelectric cross-section beyond its limits is stable and quite simple. Mesozoic-Cenozoic clays with apparent resistance in the order of 3-5 Ohm·m are replaced by Cretaceous sands and sandstones with 30-200 Ohm·m resistance. Metamorphic and igneous basement rocks with 100-900 Ohm·m resistance occur lower. A weathering crust with 5-25 Ohm·m resistance is distinguished its roof. The great thickness of the Tertiary clays with their quite low resistance (only 5-10 Ohm·m) is an obstacle to the use of electric geophysical exploration in this region. Electric geophysical exploration was used in the VEZ (vertical electric logging) modification for the purpose of separating the crater cross-section vertically and to search for a reference horizon. Two layer and three layer type H and four layer type HA curves were obtained as a result of the observation (Fig. 23). They were interpreted with the aid of theoretical patterns, as a result of which the layer thicknesses and their resistances were determined and two geoelectric cross-sections were plotted (Fig. 24). A reference geoelectric horizon was established in the vicinity of the crater at 100-150 m depths by means of vertical electric logging. The apparent resistance of the Tertiary clays, which occur above this horizon, is 5-10 Ohm· m, and Cretaceous rocks with 20-80 Ohm·m average apparent resistance lie lower.

Within the crater, after a break, a new but intermittent horizon appears. This is connected with the nature of the crater filling deposit. A new geoelectric horizon was detected at 70-90 m depth in the central part of the crater, which perhaps reflects the central uplift. The separations found in different parts of the profile correspond to genetically different geological boundaries. Outside the crater, this is a Campanian and Santonian marl roof, perhaps the foot of the allogenic breccia in the area of the crater wall and horizons within the crater in the rocks filling it.

The boundary of the intermediate geoelectric horizon generally /52
duplicates the behavior of the gravity anomaly. This boundary in all likelihood inherited the shape of the surface (excavation) of the crater connected with the basement. A correlation curve was plotted between the values of Δg and the geoelectric horizon depth (Fig. 25). It is noted that the value of Δg decreases with increase in depth of the reference geoelectric horizon. The excess density calculated from these values is 0.25 g/cm^3. Such a density corresponds to the density difference of the sedimentary rocks and the basement. It can be concluded from this that a significant part of the gravity effect is connected with the boundary of the basement and sedimentary rocks.

Of the examples of the use of inductive methods of electric geophysical exploration, we present two. High frequency electric geophysical exploration in Kentland Crater in the USA **[112]** /53
revealed the true dimensions of the disturbed rock zone from the positive field strength anomaly. Data on damping of induced fields in the Wanapitei Crater region **[115]** is evidence of the presence of a crater wall in its western and eastern portions in the form of a semicircular sunken wall. The results of dipole electromagnetic profiling (DEMP) in the Gagarin structure **[21]** indicates a substantial decrease in electrical resistance of the rock in the central part of the structure, in which the structure is not distinguished on the dipole electromagnetic profiling graphs at high frequencies (512/Hz) but appears only at low frequencies (32/Hz). The effective resistance in the central part is approximately 35-40 Ohm·m and 50-90 Ohm·m outside the structure.

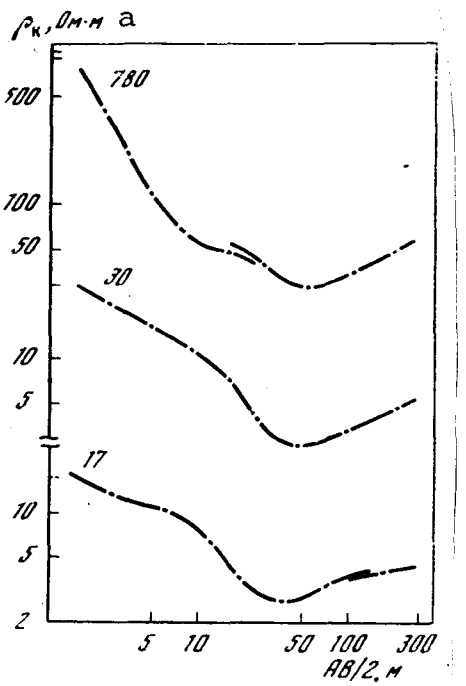

Fig. 23. Typical vertical electric logging curves of Zhamanshin Crater; Figures on curves are values of ρ.

Key: a: ρ_k, Ohm·m

Electric geophysical exploration by the direct current method was carried out for the first time in Holleford Crater in Canada in 1955 **[4]**. The vertical electrical logging curves in the center, on the edge and outside the structure are different. In the central part of the cross-section, 130-200 m thick limestones with 1000-3000 Ohm·m electrical resistance, 600-1000 m thick sands and breccias with 30-100 Ohm·m resistance and the undisturbed /54
Precambrian base with 2000-3000 Ohm·m resistance occur. On the electrical profiling curves, the edge of the structure with abrupt reduction of apparent resistance is clearly measured

out with small separations AB/2 of the electrodes. With large separations, a stepped curve characterizes the sedimentary rocks of high resistance within the crater and rocks with reduced resistance on the edge of the structure.

Electrical geophysical exploration by the direct current method was conducted in the main Kaali Crater [2] (Fig. 26), where it turned out to be most effective.

Despite the fact that the electric profiling curves have a jump type of change of ρ_k, the boundary between the fragmentation

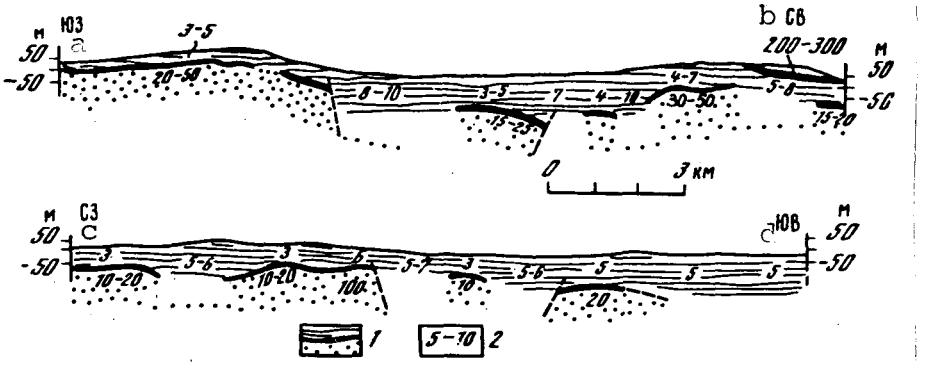

Fig. 24. Geoelectric cross sections of upper part of Zhamanshin Crater: 1. reference geoelectric horizon; 2. apparent resistance values, Ohm • m.

Key: a. SW, b. NE, c. NW, d. SE

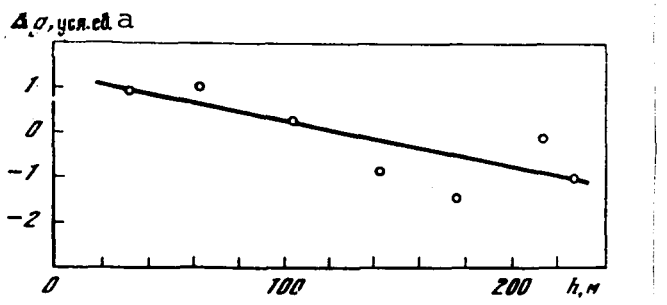

Fig. 25. Reference electric horizon depth vs. force of gravity.

Key: a. Δg, arbitrary units.

zone and the undisturbed rocks is drawn quite confidently, since the average value of ρ_k increases sharply above rocks which occur undisturbed. The resistance of the silts at the bottom of the crater lake is 23-27 Ohm•m, the apparent resistance of highly shattered dolomites is 130-150 Ohm•m, approximately 250 Ohm•m for less shattered, and more than 300-400 Ohm•m for slightly disturbed and undisturbed dolomites. The electric profiling results permitted mapping of the shattering zone. It turned out that, while the crater diameter is 110m, the diameter of the shattering zone is slightly less than 250m, where the projection of the shattering zone on the surface is not a circle, but has more complex bilateral

outlines, which apparently reflects the direction of the meteorite impact. Vertical electric logging was carried out in order to determine the depth of the shattering zone, which is indicated by the change in resistance with change in depth.

The electrical resistance of the breccia in Ries Crater is approximately 20 Ohm·m, and the undisturbed basement rock has resistance of 150-300 Ohm·m. The internal underground wall of the Ries structure stands out clearly in the electric geophysical exploration results **[36]**.

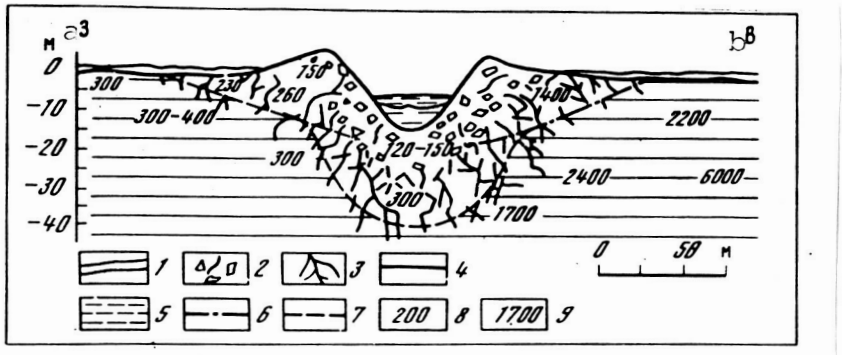

Fig. 26. Cross section of main Kaali Crater: 1. loose Quarterny deposits; 2. breccia; 3. fractured basement rock; 4. unaffected basement rock; 5. lake silts; 6. outer zone boundary; 7. inner zone boundary; 8. apparent resistance values; 9. seismic wave velocity.

Key: a. W; b. E

In Shunak Crater in Kazakhstan, the behavior of the bottom of the lake deposits with 3-5 Ohm·m apparent resistance filling the crater depression was successively traced from electric geophysical exploration data. Thinning out of the allogenic breccia with approximately 30 Ohm·m resistance was found on the edges of the structure. The resistance of the authigenic breccia is hundreds of Ohm·m. The inner structure of the crater bottom is complex, and it has the appearance of enclosed craters of different diameters. A similar structure has been found in many craters, such as the Arizona, Gosse's Bluff, Ries, Brent, Odessa and other craters **[19]**. It was proposed to call such a crater structure (a crater enclosed in the base of a flat saucer shaped depression) a "dish" **[19]**.

SEISMIC PROSPECTING

As a result of the impact and explosion of a meteorite, the development of a system of cracks occurs in the rocks as a result of the shock wave, which leads to disturbance of the monolithic nature of the rock and degrades the contacts between particles. This leads to a change in elastic properties of the rock, and to a decrease in the velocity of passage of seismic waves in them. /55 Analysis of seismic materials on craters gives a clear demonstration of the presence of an underlying low velocity lens. The velocity decrease in it is due to the development of secondary fracturing. Analysis of the seismic data on several craters (Deep Bay, Gosse's Bluff, Ries, Arizona, Kaali, and others) makes it possible to note the seismic characteristics of meteor structures. A typical example is seismic studies in Ries Crater **[111]**, carried out by reflected and refracted wave methods. A number of features characteristic of craters was found as a result of these studies: a complex wave pattern, especially on the boundaries of the crater; disturbance of the horizontal interfaces existing before the meteorite impact in the crater zone; a sharp decrease in strata and boundary velocities toward the center of the crater in both the crater filling rocks and in the underlying rocks, and a number of other features.

For study of the plutonic structure of Zhamanshin Crater and its vicinity, a seismic party of the Kustanay geological and geophysical expedition of the Northern Kazakhstan Territorial Geologic Administration made two intersecting KMPV profiles (refracted wave correlation method) through the crater (Fig. 27). They were carried out with the Poisk-1-48-MOV-OV seismic station by the standard total correlation system of observation of an explosion from four points.

The seismic profile was plotted by A.M. Yesenalinov, V.G. Korotovskiy and G.P. Navasardyan, who kindly presented it for publication.

Outside the crater, the roof of the Paleozoic basement corresponds to seismic velocities between 4.Ø and 6.8 km/s, which probably reflects nonuniformity of composition and structure of its constituent rocks. The basement roof gently slopes from 35m deep on the north to 250-300 m in the south. The basement lies 150-200 m from the surface in the vicinity of the crater, which is close to zero in absolute markers. In the cross-section of the overlying undisturbed Cretaceous and Tertiary deposits, a refraction boundary was found with a 3.5 km/s velocity, which possibly is confined to the roof of the Tasaran series or to the roof of the Maastrichian marls. This boundary comes out on the surface in the north of the region, where these deposits are exposed. The seismic velocity above this boundary is 1200 m/s, but it increases to 1500 m/s below it. It is important that the seismic boundaries in the strata of the Cretaceous and Tertiary deposits disappear at a distance of 1-3 km from the edge of the crater. The static bedding of the rocks

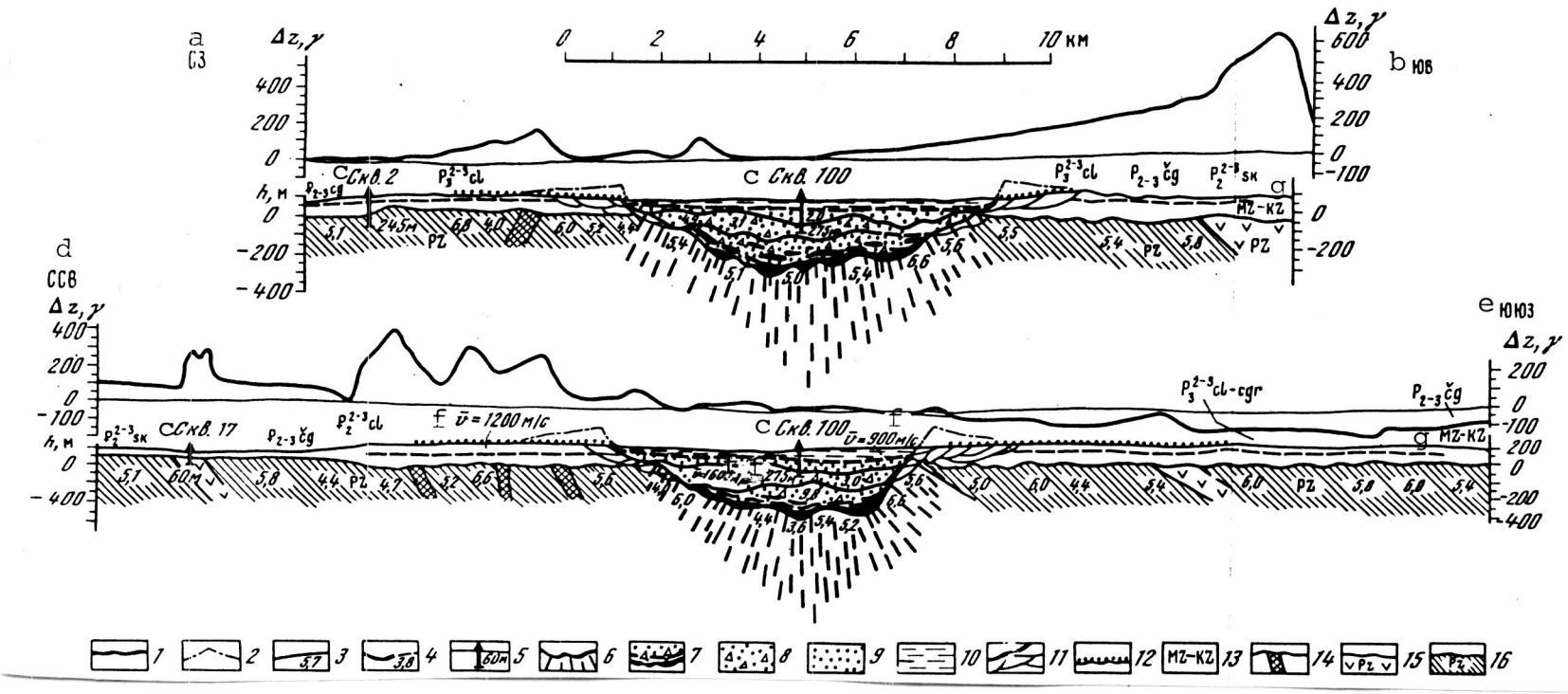

Fig. 27. Refracted wave correlation method seismic profiles (from materials of V. G. Korotovskiy, A. M. Yesenalinov, V. I. Makarov); See Fig. 3 for profile locations; 1. modern relief; 2. wall relief reconstruction; 3. seismic boundaries (authentic and hypothetical) in undisturbed sections and boundary velocities in km/s; 4. seismic boundaries (authentic and hypothetical) in crater and boundary velocities in km/s; 5. drill holes, their numbers and depths; 6. authigenic breccia (fractures arbitrary); 7. allogenic breccia which has fallen back into crater still in incandescent state, black section is hypothetical melt body; 8. allogenic breccia, large fragmental slid into crater from wall; 9. small fragmental breccia slid into crater from wall; 10. clay-siltstone rocks of crater lake; 11. hypothetical plates of rock displaced from crater; 12. exposed allogenic breccia; 13. undisturbed Mesozoic and Cenozoic deposits; 14. ultrabasic rocks; 15. Upper Paleozoic volconogenic-sedimentary rocks; 16. Lower Paleozoic schists.

Key: a. NW; b. SE; c. Drill hole 2,17,100; d. N-NE; e. S-SW; f. $\bar{v}$=900,1200,1600,m/s; g. Mesozoic-Cenzoic

probably was disturbed here, and they form a series of slivers "pushed out" of the crater.

The seismic pattern acquires a specific nature within the crater. The boundary which corresponds to the basement roof is submerged to 775 m in the center of the crater. The diameter of the crater is 6.3 km (NW-SE) and 5.5 km (NNE-SSW). The boundary velocity is somewhat reduced, 3.6-6.6 km/s, which reflects the fractured nature of the rock. However, the diversity of seismic velocities in the basement roof in the crater and outside it does not permit unambiguous interpretation of them.

Only within the crater above the basement roof, at a depth of 300-475 m, is a seismic boundary distinguished with boundary velocities of 2.0-4.0 km/s, which duplicates the structure of the basement surface in smoothed form. It is most likely that this boundary is the roof of the allogenic breccia which fell into the crater immediately after the explosion in the incandescent state, and is therefore caked and compacted. There may be a body of molten rock in the breccia cross section and a melt "lake" in the base, the thickness of which by analogy with other craters of like size may reach 10 m. The high seismic velocity within the breccia lens is evidence of the latter. /56

Higher, at a depth of 100-300 m, also only within the crater, still another seismic boundary is found with a boundary velocity of 3.0-3.5 km/s in the center of the crater, and 4.0 -4.2 km/s along the edges. This layer evidently also is formed of allogenic breccia, but its rocks initially formed the crater wall and later slid down the slope. Since the inner slopes of the crater wall are very steep, and the allogenic breccia containing much loose clay is dense, sliding of the wall and its reaching of an equilibrium profile probably occurred soon after the explosion. This horizon was found by the drill hole in the center of the crater at a depth of 230 m.

In the uppermost part of the deposits filling the crater at a depth of 50-100 m, still another layer was found with a 900-1200 m/s seismic velocity. To decide from the cross-section of drill hole 100 in the center of the crater, where its bottom is passed at 95 m depth, it corresponds to the bottom of small fractural lake deposits which contain carbonized plant residues. Lower, besides clays similar to the overlying rocks, there are many lenses of allogenic breccia, which also probably slid from the wall. The seismic velocity here reaches 1600 m/s.

CRATER RECONSTRUCTION

All large meteor craters on the earth are presently eroded to some extent, or even buried under a mantle of younger sediments. However, their original dimensions and the shape of their plutonic structure must be reconstructed. This is done on the basis of extrapolation of the results of study of the preserved smaller /57

craters, comparison with lunar craters and the use of a number of artificial craters.

An attempt is made in the present section to reconstruct the original structure of Zhamanshin Crater and to estimate the energy indicators of the explosion and the volume and mass of the volatilized, remelted, ejected and brecciated target matter.

The diameter of the flat bottom of the Zhamanshin depression is 5.5 km. The diameter to the watershed ridge is 9-10 km. However, the present day dimensions and shape of the structure are highly transformed by erosion, particularly intensively because of the fact that the crater wall, made up basically of loose clays of the allogenic breccia, has almost completely slid and washed back into the crater. Its original shape and dimensions were reconstructed on the basis of geomorphological analysis, analysis of geophysical data, and interpretation of aerospace photographic materials.

The depth of the crater, without allowance for a possible central peak, was determined from calculation of the depth of occurrence of magnetically perturbing masses (200-250 m). A body of ultrabasic rock extending to the north-northeast and connected with a basement fault corresponds to it. These rocks are traced under the crater on the slope of its west side. Crater excavation depth z was obtained by its approximation by a paraboloid of rotation:

$$x^2 + y^2 = 2pz.$$

With the known crater diameter (5.5 km), the distance from the edge and the depth of the magnetically perturbing mass mentioned, the maximum depth of the crater from the surface can be calculated (0.60-0.75 km). The volume of this depression is 7 km^3. The matter filling this crater has almost entirely slid from the wall. The outer boundary of the wall can be reconstructed by extrapolation of the modern relief, and the inner boundary above the zero level, based on extrapolation of the calculated paraboloid of rotation.

Based on this reconstruction, the wall height will be approximately 0.3 km. The volume of the wall made up of allogenic breccia should be approximately 7 km^3. In this reconstruction, the crater diameter to the highest edge of the wall was 6.5 km, and the total depth of it relative to this edge was 0.9 km.

Reconstruction of the processes which occur in the formation of meteor craters, based on crater formation theory and their present day structures was carried out quantitatively for the /58
Arizona Crater **[122]** and qualitatively for the Popigay Crater **[98]**. Since artificial explosions with previously known energy causing the formation of more than 0.5 km craters have not occurred, estimates of the energies of explosions causing the formation of large craters are only quantitative to within an order of

magnitude. Therefore, the calculation of such parameters as the mass and volume of a meteorite forming a crater, the volume of melt, dimensions of the shattering zone and other parameters, the calculation of which is based on knowledge of the explosion energy, are determined only approximately within an order of magnitude.

Based on the reconstructed dimensions of Zhamanshin crater from the edge of the wall (6.5 km), explosion energy W was approximately $1.1 \cdot 10^{25}$ ergs **[122, 27]**. The meteorite could have fallen to the earth with velocity V=10-40 km/s. Its mass M (tons) is determined by the equation:

$$M=2W/V^2=(1.25-20) \cdot 10^6.$$

The size of the meteorite, assuming it to be of spherical shape, is estimated at 50-160 m if it is an iron meteorite, which is more likely, or 90-220 m if it is a stony meteorite. It follows from other calculations **[126]** that the radius of the crater is approximately 45 times the radius of a stony meteorite striking at a velocity of 15 km/s. The diameter of the meteorite will then be approximately 140 m. It is considered that, upon impact, the meteorite is buried to a depth of 2-3 diameters, which with 0.60-0.75 km crater depth constitutes similar figures. Converging results of the conjectural dimensions of the meteorite were thus obtained by three independent calculations.

It is known that the mass of the crater forming meteorite is 10^2-10^4 times less than the mass of matter removed from the crater. The amount of matter removed by the explosion from Zhamanshin Crater is estimated at approximately 10^9 tons.

If it assumed **[7]** that 5% of the total energy of the explosion goes to melting of the rock, the melt volume in Zhamanshin Crater was more than 0.07 km^3 and its mass was $\sim 1.75 \cdot 10^8$ tons. Part of the melt was ejected from the crater. If it is assumed, however, that half of it remained in the crater, it should form a lens approximately 2 km in radius and 2-3 m thick. The mass of vaporized matter exceeds the mass of the meteorite by an order of magnitude **[126]**, and it can therefore exceed 10^7-10^8 tons.

From the point of energy release where a growing cavity is formed, a powerful shock wave propagates, and as a result of the instantaneous shock compression, the rocks are heated and are melted after unloading. The pressure in the shock front decreases with increase in distance from the center of the explosion, and the minerals experience phase transformations, but the rocks are only shattered when this energy decreases to 10^{12} erg/g. The limiting energy of shattering is very much less than the energy of fusion, and particularly vaporization. The mass of shattered matter is therefore many times greater than the mass of vaporized and melted matter **[148]**.

Following the shock wave, the rarefaction wave leads to /59

explosive ejection. The target material therefore, after it has undergone impact metamorphism, is scattered from the center of the explosion, partly falling back into the crater and partly forming a wall and extracrater ejecta. The latter has not yet been found around Zhamanshin Crater. It should be sought at distances of up to several crater diameters. Radial ejection of material consisting of grits of the melt and incandescent gases forms a fireball. In a high speed 15-20 km/s impact, the temperature in the fireball rapidly decreased to 3,000-5,000°, i.e., it did not exceed the vaporization temperature of silicates. Partly as a result of vapor condensation and partly aeorsol accretion, Irgizite tektites formed from this fireball.

A substantial portion of the material was displaced in the form of blocks from the explosion site, sliding in a mass of fragments and forming slivers. Since the speed of the slivers was tremendous and the masses and pressure on the displacement planes were high, melting and the formation of melt horizons in the form of such interlayers occurred near the displacement surfaces. The depth of the brecciation boundary is calculated **[122]** by the equation

$$R = 1.7\ W^{1/3},$$

where R is the radius of the brecciation zone, m, and W is the total energy of the explosion in tons of TNT equivalent. The lower boundary of the brecciation is therefore found deeper than 1 km, which does not contradict the geophysical model.

Because of relief after the explosion, a central uplift sometimes forms, which is reflected in an anomalous gravity field. If it is assumed that the excavated crater was half filled with material which fell back immediately after the explosion **[135]**, the apparent depth of Zhamanshin Crater reached 400 m. The remaining part of the depression was later filled with rocks which slid from the wall into the crater and still later by lake sediments, as a result of which the presently visible crater differs significantly from the original.

EVOLUTIONARY PLACE OF ZHAMANSHIN CRATER

Analysis of crater distribution as a function of their absolute age and diameter permitted the determination of the evolutionary positions of the craters.

In the diagram (Fig. 28) of crater distribution as a function of their dimensions and age, a region proves to be "populated" in which the inequality

$$0.1 \leq \sqrt{T/D} \leq 10$$

is observed. This inequality has a probabilistic meaning. The probability of finding a crater outside the region specified is very small.

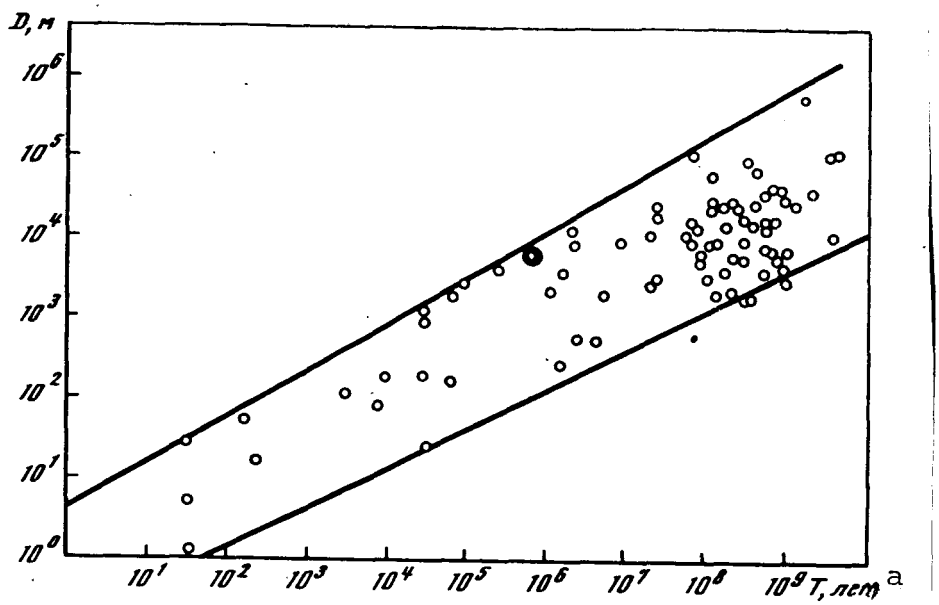

Fig. 28. Diagram of meteor crater distribution by age T and dimensions D; time is counted from the present to the past **[37]**.

Key: a. T, years

It is evident that the lower boundary of the region on the D-T diagram determines the lifetime of meteor craters on the surface of the earth as a function of their dimensions. It is /60 evident in Fig. 28 that this time is determined by the formula $T \sim (45\text{-}50)\ D^2$.

We note that this value differs from estimates obtained by another method **[71]**. The greatest possible age of postmare craters on the moon is: 1 km diameter, age $6.25 \cdot 10^8$ years; 10 km, $1.09 \cdot 10^9$ years; 100 km, $1.63 \cdot 10^9$ years. The upper limit in Fig. 28 separates the region of low probability of appearance of large crater forming meteorites and determines the start of existence of a crater as a geological object. While more than 30 craters more than 10 km in diameter formed in 10^9 years, not a single such crater is known for the last 10^6, and only one crater younger than 10^7 years is known. Zhamanshin Crater is located closer to the upper limit. It can therefore be considered relatively young among craters of similar size.

Part of the craters on the surface of the earth disappear over time because of various geologic factors which depend on a set of specific circumstances **[24]**. A specific fraction of the craters always disappears in a certain time interval. The crater "extinction" process is similar to radioactive decay, and it can be

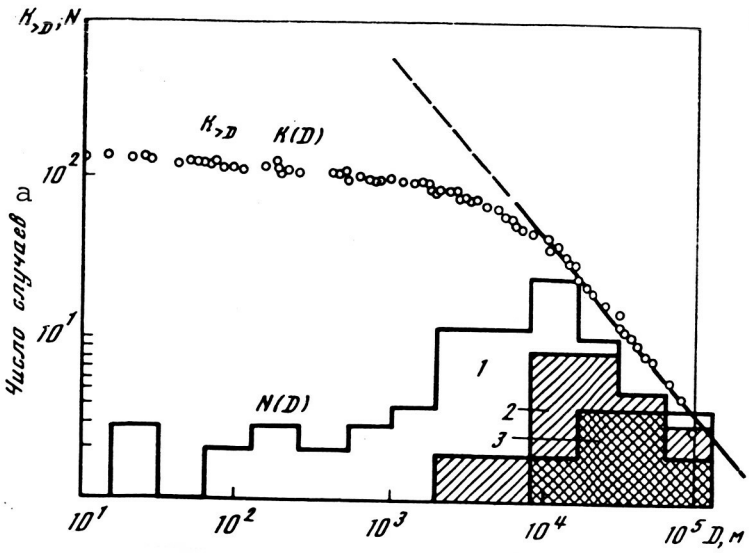

Fig. 29. Integral and differential size distribution of number of craters; 1. all craters; 2. craters with central uplift; 3. same with circular uplift.

Key: a. Number of cases.

described as $e^{-T/D^2\theta}$. Quantity $D^2\theta$ is the relaxation time of the surface or the characteristic crater lifetime which is assumed to be proportional to the crater area. This representation is based on the nature of the lower limit of the crater existence region in the Fig. 28 diagram. In order of magnitude, $\theta = 10-100$ year/m^2.

The size and age /62
distribution of the craters is connected with the selectivity of the methods of their discovery. All else being equal, small craters are lost more rapidly than large ones, and young ones also are found more easily than old ones. It can evidently be considered that the probability of discovery of a meteor crater is proportional to its area and inversely proportional to age. Craters do not have deep roots and practically exist as two dimensional geologic objects **[22, 150]**. On the other hand, a diagnostic indicator of eroded structures is the presence of rocks carrying indications of shock metamorphism, the amount of which also depends on the dimensions of the exposed part of the crater. Over time, the amount of shock altered matter, expressed either by a geophysical anomaly or by the volume of breccia and impactites, decreases and is eroded. One of the most common mechanisms in nature of smoothing out any perturbation is diffusion or cooling. If this mechanism is adopted as an analog, a characteristic indicator of perturbation within a crater, formally analogous to temperature or concentration, in the case of two dimensional diffusion decreases in proportion to time, i.e., T^{-1}. It can therefore be concluded that the region of existence of real terrestrial craters is limited by size and age, and that the limits of this region are determined by the relationships of accumulation and disappearance of craters.

Available factual material on meteor crater dimensions and ages can be interpreted based on the following assumptions:

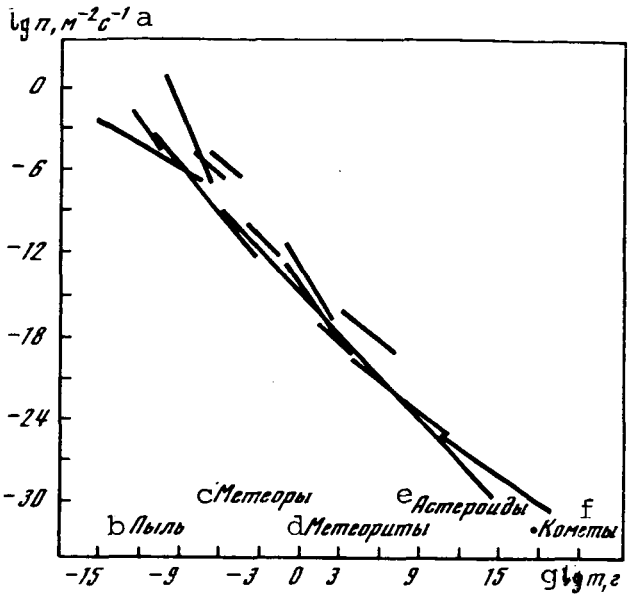

Fig 30. Distribution of fragmental bodies in solar system ([144] with additions by I. T. Zotkin).

Key: a. log n, $m^{-2} \cdot s^{-1}$; b. dust; c. meteors; d. meteorites; e. asteroids; f. comets; g. log m,g

1. crater size distribution is gradual (Fig. 29); this gradual relationship reflects the general principle of distribution of fragmental bodies in the solar system, which is traced over a tremendous mass interval (approximately 30 orders of magnitude) and covers microparticles, meteors, meteorites, and asteroids (Fig. 30); for terrestrial craters, the exponent is 2.15 [37] but, for lunar craters, it is approximately 2 [49] or 2.0-2.4 [72];

2. obliteration of the crater population on the earth occurs exponentially over time;

3. the characteristic lifetime of a crater or of its relaxation is determined by its area;

4. the probability of discovery of a crater is proportional to its area and inversely proportional to its geologic age;

5. the order of magnitude of the crater forming meteorite flux intensity has changed little in the last billion years; the absolute value of the fraction of the flux which is crater forming meteorites and its variation over time can be determined when a large region on the surface of the earth is studied exhaustively in meteor craters.

PETROGRAPHIC CHARACTERISTICS OF BRECCIA, ZHAMANSHINITES AND IRGIZITES

Existing petrographic methods have been developed for rocks of igneous, sedimentary and metamorphic origin, and their application to impactite formations somewhat erases the fundamental difference of the latter, the more so that in the fundamental genetic specifics of their explosion transformed rocks, there are many features which outwardly connect them with igneous and metamorphic rocks. Nevertheless, microscopic study of more than 1,000 polished sections of Zhamanshin Crater rocks, supported by delicate mineralogical, microchemical and petrographic studies, permitted some specific traits to be found. /63

BRECCIAS

Rocks shattered to various degrees, but still not started to melt are classified as breccias. The pressure on them evidently did not exceed 1500 kbar. They are extremely widespread in the crater. Strictly speaking, nearly the entire amount of allogenic breccia which forms wall is classified in this group and was described above. The petrographic characteristics of breccias formed by shattering in basically Paleozoic rocks carrying traces of shattering and phase transitions are given in this section.

Paleozoic rock breccias are quite numerous in the form of individual blocks and lumps up to 0.5 m long, which consist of acute angled fragments from 1-2 mm to 5-10 mm, sometimes up to 5 cm in size, cemented with secondary carbonate gypsum and sometimes limonite cement. A series can be distinguished in rocks shattered to various degrees, from fractured lumps to nearly maskelynitized samples containing diaplectic glasses. While the particles fit against each other in tectonic breccias, impact breccias are loose and porous, and the fragments are separated. Several types of breccias can be distinguished by fragment composition, among which breccias made up of quartz, limestones, rarely shales, effusives, and red rocks are common. This reflects the composition of the basement rock subjected to shattering, as well as rocks completely converted to flour.

Macrocrystalline calcite from marbles (Plate 3d) were subjected to brecciation and acquired a number of unusual traits. Upon weathering, its surface is similar to the edge of a book because of the jointing found. It therefore breaks down into thin plates. Under the microscope, such calcite is still more similar to mica because of the distinctly visible, extremely complete cleavage. More than that, crystals of such calcite are sometimes curved and have a fibrous and wavy end. Less altered calcite contains numerous twin systems.

Quartz subjected to shock has been studied well **[123 et al]**. /64
Its breccia is frequently found near quartz veins (Plate 3d) and among the rocks of the wall. The quartz acquires a brecciated structure and wavy and nebulous ends, it is broken down into microblocks, and planar elements appear in it systematically (Plate 4a) in the form of crack systems, the locations of which correspond to the directions of least strength of the quartz crystal lattice, primarily $\omega(0133)$ and others. A diagram of planar element distribution is presented in Fig. 31, which was plotted from two samples from Zhamanshin Crater by N. Short (NASA, Maryland, USA). In still more reworked sections, the quartz has been made isotropic, its index of refraction has decreased since the lattice has been disturbed, and it changes to diaplectic glass without melting.

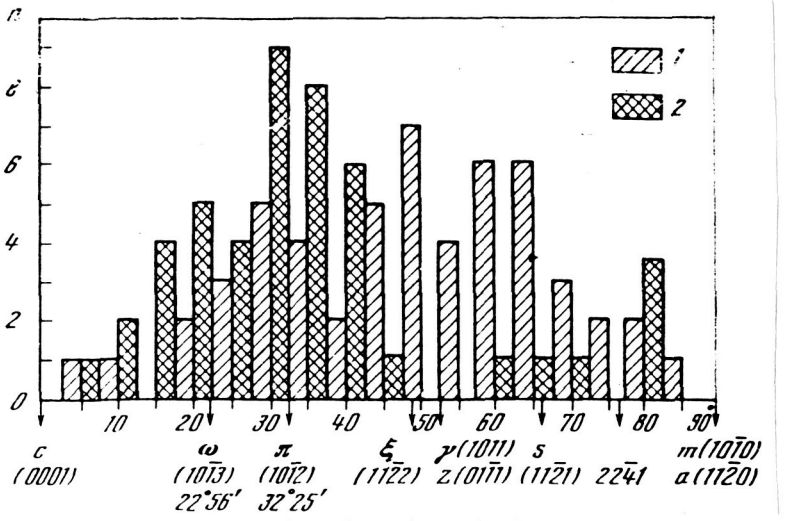

Fig. 31. Frequency histograms of planar Systems (ordinate) with different angles between normal to these systems and optical axis of quartz (abscissa): 1,2. samples 76-11 and 76-17 respectively.

Profoundly disturbed maskelynitized samples have been found in brecciated schists, quartzites and effusives, in one of which Yu.P. Dikov found high pressure phases of silica (coesite and stishovite) in a residue insoluble in hydrofluoric acid. Coesite was found later in Zhamanshinites **[137]**. Stishovite was found in nature in the USSR a second time. It was first discovered in Popigay Crater. It should be noted that these minerals form a paragenesis with high pressure phases of carbon in Ries Crater **[97]**. A sample of maskeylnitized rock containing these minerals was studied by X-ray spectral analysis(see below), which permitted it to be established that many of its minerals have been broken down to the elementary oxides. For example, feldspar and mica were transformed to phases containing pure Al_2O_3. The rocks were broken down to flour, which easily changes to kaolinite-like varieties.

ZHAMANSHINITES

Impactites and tektites have been quite comprehensively described petrographically **[130, 141, 9 , 135, 113 et al]**. In study of them however, one of the same difficulties arises as is connected with the fact that they are made up of isotropic glass, in which there are almost no separate particles. /65

Scoria is the most widespread impactite in the crater, and there was especially much of it on the eastern part of the wall. A complex texture is seen in it without an analyser. It consists of fragments and fibers of gray or brownish and yellowish glass, colorless lechatelierite, and opaque ore minerals. The gas inclusions are irregular, rarely round, 0.01-1mm in cross-section, and they sometimes constitute up to 30% of the rock. The index of refraction of the glass in the scoria is 1.554. The scoria is almost entirely isotropic with the analyzer. Only in isolated sections of it is the glass slightly birefringent in gray tones, and plagioclase microliths up to 0.02 mm long are sometimes distinguished. In chemical composition, the scoria is closest to Tertiary clays, and it is characterized by minimum silica (~50%)

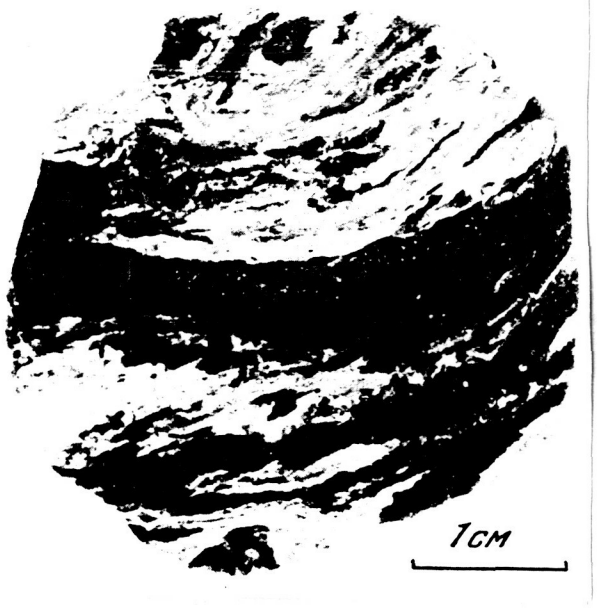

Fig. 32. Folded together flow texture Zhamanshinites formed by alternation of dense black and porous yellow zones deformed by viscous flow.

and maximum alumina (20%) content.

Zhamanshinites are glasses of a basic black composition and yellow in porous sections. The black and the yellow sections are interstratified and mixed, forming a flow texture with fantastically curved, frequently folded and smashed together layers from 2-5 cm to 1-2 mm thick, which indicates mixing of a viscous melt before hardening (Fig. 32). Bubbles are usually 0.1-2 mm, but sometimes up to 1 cm in size, and up to 5 cm cavities are found. There are no porous yellow interlayers in some samples and others are almost wholly porous yellow. Zhamanshinites are quite diverse petrographically, and they form two groups by chemical composition: acid varieties similar to Irgizites, containing 75% silica; basic, containing 50-60% silica. The former never contain microliths, but the latter contain them and are sometimes almost entirely decrystallized.

The acid composition glasses are not decrystallized and are very similar to the Irgizites described below. In transmitted light, they are yellow and colorless and nonuniformly saturated with bubbles. Striations and bands of different colors are saturated with bubbles to different degrees and are fantastically interwoven or are inversely drawn out in parallel and the glass then seems to be laminated. Lechatelierite fibers are present in the rocks. They differ by a low index of refraction (Plate 8d). The bubbles constitute up to half the volume in individual interlayers, usually 0.1-3 mm in size, but they are up to 3-5 mm. Opaque particles of a gray ore mineral and sulfides are found in the glasses. V.P. Florenskiy found tektites and impactites among just these varieties in 1977, which are blue in reflected and and dirty brown color in transmitted light. V.N. Krupko, V.L. Fedorov and O.M. Shipilov found blue impactites in the same year, but in the eastern part of the wall. As Yu.P. Dikov showed, this color is connected here with the presence of titanium reduced from the /66
normal tetravalent to the trivalent form. He detected chromium in these same sections, reduced from the normal trivalent to the divalent form.

The basic composition glasses are yellow and brown in transmitted light, and fibrous similar to that described above, but there are plagioclase microliths in them, which are slightly birefringent in gray shades and which saturate individual zones. These zones sometimes form interlayers and sometimes sections, and the plagioclases in them are randomly oriented, they sometimes form radially radiating rosettes and are usually surrounded by a darker brown aureole. There frequently are lechatelierite fibers with a low index of refraction in the glasses. At the same time, individual sections and fibers of glass have a higher index of refraction, probably at the points of melting of some minerals. Isolated devitrified sections evidently are connected with mineral relicts and are distinguished by a crystalline aggregate structure and slight birefringence. Relicts of uranium containing accessory minerals were noted in study of fission tracks. There are round, elongated and irregular 0.02-2 mm size bubbles in the glasses. This type of glass generally contains quite a lot of foreign inclusions. In observations under a scanning electron microscope, numerous porous pumice-like inclusions of up to 1-2 mm cross-section and up to 0.01 mm sulfide inclusions are successfully seen. In one glass sample with microliths, quite a number of up to 0.5 mm sulfides of two types were found, spherical and acute angled fragments.

Zyuvites, glasses with rock inclusions, are found quite rarely. The basic mass of such rock, of which there usually is much in meteor craters, probably remained in the depths of the /67
crater and only isolated pieces of them were ejected to the rim of the wall. In the brown glasses with microliths described above, quite many pumice-like particles, as well as acute angled and partly fused grains of quartz, feldspar and ore minerals were found. Difficult to define fragments of aggregate cryptocrystalline structures which are birefringent in gray tones also are found.

A heavy black basalt-like rock, which is dull on fractures, is made up of 20-30% translucent glass with a relatively high index of refraction (1.561). It contains up to 50-70% randomly oriented plagioclase microliths. The up to 0.05 mm long plagioclase microliths saturate the rock irregularly. They constitute it almost entirely in some sections and only 20-30% of it in others. Although the mircoliths are randomly oriented, the rock is similar to basalt (Plate 8e). They most often form radially radiating concretions and, intersecting at nearly right angles, they differ strongly from igneous rocks. Moreover, small (up to 0.02 mm) crystal particles are seen, which have a high index of refraction interfering in the yellowish tones. They probably are monoclinic pyroxenes.

The lechatelierite is found only in the northwest on the inner slope of the wall, around quartzitic shists, quartzites and quartz veins which form a block of Lower Paleozoic rocks (see Fig. 8, Plate 3a). This is a white sugar-like rock, which is lighter than

water because of numerous Ø.1-Ø.5 mm size bubbles which make up more than 7Ø% of it. Without the analyzer, this is a grayish rock with an extremely low index of refraction (1.46Ø). The majority of the bubbles are clean and without inclusions. Some of the cavities are filled with powder, however. With the analyzer, the rock is isotropic, only sometimes powder and inclusions with high refraction are distinguished with a slight birefringence. In observations in the scanning electron microscope, various types of new growths contained in the rocks are found. The majority of the pores have clean, smooth walls. However, needle-shape crystal particles are found in some pores, which possibly are cristobalite, and thin twisted leaflets are found in others. It is not excluded that part of the similar new growth developed in isolated pores by condensation.

The porous, pumice-like yellowish pieces are outwardly similar to the variety described. Although they contain much lechatelierite, their glass is mixed with other varieties with a higher index of refraction and a yellowish color. Slightly birefringent sections are seen in places in them. While pure lechatelierite is formed by melting and foaming of a quartz vein, this variety was formed by reworking of sedimentary argillaceous sandy rocks.

IRGIZITES

Irgizites are glass droplets of acid composition, they are transparent and brown in transmitted light (Plate 9), and the index of refraction is 1.5Ø9. Their internal structure is irregularly fibrous and fluid: brown fibers alternate with colorless ones made /68
up of lechatelierite (index of refraction 1.46Ø). Round up to Ø.Ø1 mm transparent and opaque inclusions are present, as are round bubbles and those elongated parallel to the fibers, which emphasize the flow structure. In a whole series of polished sections, the aggregate structure of Irgizites is easily seen. They consist of many globules up to Ø.1-2 mm in size which have adhered, sometimes melted and mixed and sometimes (along the edges) having preserved their shape and boundaries. Separating segments of welded cracks are seen along the edges, but they are noticeable because of their dark color. They probably developed by cracking during the hardening process. With the analyzer, the Irgizites are isotropic, and anisotropic sections connected with stressed zones in the glass are seen only very rarely. Anisotropic inclusions are extremely rare in Irgizites.

Special attention was given to the morphological features of Irgizites and their comparison with other impact glasses. The name of tektites, given to them by Franz Zeuss carries the characteristic of their shape (τηκτοη, molten, Greek). Their specific aerodynamic shape is therefore a decisive indicator. They frequently are rounded or in the shape of a button, sometimes with a cracked crust, because of which they are similar to lapilli and volcanic bombs. Traces of blowing off of the melt are seen on

their surfaces, which makes them similar to the surfaces of meteorites. In addition, tektites frequently undergo partial disso ing from the surface, which reveals their unusual structure still more. Actually, tektites and Irgizites in particular have extremely unusual shapes and surfaces, which indicate their hardening while falling and formation from a viscous melt (Plates 10-12).

In the work, we adopted the approach developed in detailed studies of regolith particles **[116]**, to some of which the surfaces of Irgizites are very similar.

TABLE 4. DISTRIBUTION OF IRGIZITES AND ZHAMANSHINITE FRAGMENTS BY TYPE

a Морфология частиц	b Средняя длина, мм	c Средняя ширина, мм	Отношение длины к ширине d	e Средняя масса, г	Количество экземпляров, % f	g Суммарная масса, %
h Поверхность гладкая блестящая						
Капли, гантели, шарики, иногда закрученные, с прилипшими шариками i	12	4	1,0 ÷ 4,5	0,3	13	10
Капли и обломки плоские с волокнистой поверхностью и прилипшими шариками j	15	8	1,5 ÷ 3,5	0,5	26	29
Обломки вытянутые и плоские с волокнистой и струйчатой поверхностью k	16	8	2,0 ÷ 3,5	0,5	12	14
Обломки крупных капель и волокна гладкие l	28	7	3,5 ÷ 4,5	1,7	1	2
Частицы ажурные, состоящие из слипшихся волокон и шариков m	10	8	1,0 ÷ 2,0	0,4	11	9
n Поверхность матовая						
Обломки капель закрученные, согнутые, с волокном и прилипшими шариками o	15	5	3,0 ÷ 4,0	0,4	9	8
Осколки со струйчатой поверхностью p	11	7	1,0 ÷ 2,0	1,0	2	4
Осколки с неровными краями, пористые, иногда окатанные, возможно, что много осколков жаманшинитов q	11	7	1,0 ÷ 1,5	0,5	26	24
Среднее r	14	7	1,0 ÷ 4,5	0,6		
Сумма s					100	100

Key: a. particle morphology; b. average length, mm; c. average width, mm; d. length to width ratio; e. average mass, g; f. number of samples, %; g. total weight, %; h. smooth shiny surface; i. drops, dumbbells, globules, sometimes rounded, with adherent globules; j. drops and fragments, flat with fibrous surfaces and adherent globules; k. elongated, flat fragments with fibrous and striated surfaces; l. fragments of large drops and smooth fibers; m. openwork particles consisting of adhered fibers and globules; n. dull surface; o. rounded, curved drop fragments with fiber and adhered globules; p. fragments with striated surfaces; q. fragments with uneven edges, porous, sometimes rounded, many fragments possibly are Zhamanshinites; r. average; s. total

Description and observation of the morphological characteristics were carried on two levels: macroscopically, by mass measurements and development of a visual classification of

particle shapes; microscopically by detailed observation of the surfaces of selected particles in a scanning electron microscope. Approximately 3,000 Irgizite samples, which constituted a little less than 1.5 kg, were selectively collected in an area of approximately 30 m^2 on the southwest part of the wall. T.M. Gayeva divided this material into three groups which combine a number of types (Table 4): 1. particles with shiny conserved surfaces, which constitute more than two thirds of the material (Plates 10-12); 2. particles with weathered surfaces, considerably more than 10%; 3. small fragments which sometimes make up one fourth and sometimes the entire sample. Fragments of both Irgizites and Zhamanshinite impactites were classified in this group. The fragments here are therefore most of all of basic composition. Only the most significant specimens of the first two groups are presented in Plates 10-12. Detailed study of Irgizite surfaces was carried out with the aid of JSM-50A scanning electron microscope of the JEOL Company (Japan) jointly with R.A. Bochko and V.A. Kuz'min.

Before scanning, the specimens were washed in alcohol, then /70
cemented to the object holder with electrically conducting cement on a silver base and, for removal of the charge from the surface of the object, which develops upon passage of the electron beam through it, a thin silver film (100Å) was sputtered in a JEE-4C vacuum sputtering unit.

The sample size was not over 1 cm. Scanning and photography of the preparations were carried out in secondary electrons with a 25 kV accelerating voltage over a wide range of magnifications from 50 to 50,000.

As has been pointed out, the surfaces of unweathered Irgizites are smooth and shiny, which is evident at low magnification. The structural formations which complicate their surfaces carry traces of the features of individual stages of their formation and existence. They can be divided into positive and negative. The former are the result of growth and formation of Irgizites, and the second are formed in their destruction.

POSITIVE STRUCTURES

The surfaces of a substantial portion of Irgizites are complicated by numerous glass globules which have adhered or been captured previously, and now very slightly project and are from 1 mm to 1 μm in diameter. In some sections, the entire surface therefore becomes uneven. Openwork Irgizites consist to a substantial degree of such particles (Plate 13). Smaller globules (0.001 mm or less) frequently sit on relatively large globules (0.5 mm) (Plate 13a-c). In other cases, the globules adhere to threadlike sprays (Plate 13d-f). Probably the adhesion of some globules occurred in the liquid state and of others in the viscous state at the start of hardening, when a hard film is formed initially. This is indicated by the formation of exfoliation zones at the point of contact of particles (Plate 13d,f), but they are

absent in other places. To decide from the uniform nature of the reflection, the composition of the globules is practically independent of their size and corresponds to Irgizite composition. Besides the globules, threadlike sprays and striations are seen in many Irgizites, which are evidence of the hardening of glasses from a very fluid state.

Thus, the nature of the positive structures of Irgizites is evidence that, in their formation, active adhesion of minute silicate sprays occurred. Captured "drops" frequently only crop out on the surfaces of Irgizites (Plate 14a-c), which was seen in polished sections and in specimens (Plates 9, 10, etc.).

NEGATIVE SURFACE FORMS

They are represented by shear craters upon quenching and holes and craters formed by the opening of cavities, which disclose a particular similarity with structures observed in glasses from the regolith.

A specific type of hole is spallation holes (Plate 14d-f). They are quite normal for the surfaces of Irgizites, and their dimensions are from a micron to a few millimeters. They are found in other tektites, particularly bediasites, where they reach 5 mm. There is no doubt of their formation as a result of the development of stresses upon cooling in the surface layer. These stresses later cause spallation. Spallation holes sometimes are very similar to impact microcraters in particles from the regolith.

The holes are small round or irregular depressions with /71
smoothed outlines from 1 to 20 μm in size. They are sometimes surrounded by a low wall. The craters are deep circular depressions with steep walls. Their depth is greater than the diameter. There are transition forms between holes and craters, undoubtedly syngenetic Irgizites formed upon separation of bubbles from a silicate melt before hardening of the glass. In cases when the holes formed, the bubbles were located next to the surface, and if the bubbles were deep, craters formed and gas escaped from the "depths" of the silicate mass (Plate 15). The presence of cavities and bubbles is evidence of the formation of Irgizites by the adhesion of several particles or directly from the melt.

Cavities are openings with irregular, notched edges without noticeable traces of melting (Plate 15a,b,d,e). They form as a result of the opening of cavities, when a particle has already acquired at least a hard crust. The edges of the cavities have characteristic conchoidal chips (Plate 15e), and they are filled on the inside with glass flakes which have peeled off (Plate 15c,f).

As a result of dissolving, separate structural formations are made on the surfaces of Irgizites which permit their characteristics to be precisely defined (Plate 16a). The entire surface of a weathered Irgizite consists of fibers and cavities (Plate 16a-c), globules and particles captured by the Irgizites

during their formation (Plate 16d,e). It is evident that a cavity apparently separates the fibers which bend around it. At high magnifications, the cavity surfaces are uneven. Irgizites apparently contain a certain amount of foreign inclusions, some of which (Plate 16a,d,e) have angular edges and, and at their contacts with the surrounding glass (Plate 16e), compressed fragments of flaked off glass are seen.

A mircogranular structure also has been established on the surfaces of moldavites (Ločenice deposits), which indicate the adhesion of particles in the process of formation of the moldavites.

Thus, petrographically and mineralogically, the breccias and glasses from Zhamanshin Crater are highly specific objects. Crushed calcite of unusual form, quartz with planar and isotropic elements, as well as its high pressure phases coesite and

TABLE 5. CHEMICAL COMPOSITION OF SOME ROCKS ENCLOSING CRATER

a Окисел элемент	b Кварцито-сланцы	c Порфирит	d Глина		
			e красная обожженная		f слабообож-женная
SiO_2	98,40	53,20	56,00	54,00	45,7
TiO_2	0,02	0,64	1,12	1,06	1,58
Al_2O_3	0,40	20,60	21,20	24,20	16,75
Fe_2O_3	0,07	7,14	9,70	9,00	12,70
FeO	0,30	0,59	g Не опр.	g Не опр.	1,87
MnO	0,01	0,11	0,17	0,21	0,13
MgO	0,37	2,35	1,43	1,85	3,39
CaO	0,26	6,79	5,65	5,48	6,96
Na_2O	0,10	4,80	4,05	4,03	2,78
K_2O	0,06	0,68	0,67	0,84	1,38
S	0,02	0,20	g Не опр.	g Не опр.	g Не опр.
CO_2	0,10	2,01	"	"	2,83
H_2O^+	0,30	1,24	"	"	3,01
Сумма h	100,41	100,35	99,99	100,67	99,08
a	0,4	12,6	10,2	11,6	9,2
c	0,1	8,8	7,1	6,8	8,2
b	1,0	11,8	16,1	18,6	22,3
s	98,5	66,8	66,1	63,0	60,3
a'	–	61,4	30,0	40,5	–
f'	27,0	36,7	54,2	42,5	64,8
m'	50,0	1,9	15,7	17,0	28,7
c'	22,2	91,7	–	–	6,7
n	66,7	55,7	91,0	77,0	75,3
φ	5,6	0,9	g Не опр.	g Не опр.	54,9
t	–	1,4	1,5	1,6	2,5
Q	96,1	0,4	5,7	–3,6	–6,0
a/c	4,0	1,4	1,5	1,9	1,1

Key: a. element oxide; b. quartzitic shists; c. porphyrite; d. clay; e. red calcined; f. slightly calcined; g. not determined; h. total.

stishovite found in the breccias. Zhamanshinites, which are a facies of more thorough impact metamorphism, are partly or completely melted rocks, sometimes partly recrystallized. Particularly interesting information was obtained in study of Irgizites under the scanning electron microscope at various magnifications. This permitted the finding of traces of processes of Irgizite formation by adhesion of particles in the molten state, probably still in the fireball.

TABLE 6. CHEMICAL COMPOSITION OF IMPACTITES FROM ZHAMANSHIN CRATER (from 40 analyses)

a Окисел	b Лешательерит	c Импактиты стекловатые						d Шлаки и обожженные глины	
	3*	2	7	5	6	3	4	5	5
SiO_2	98,02	88,09	77,56	75,07	72,73	66,83	62,88	50,12	54,37
TiO_2	–	0,23	0,54	0,68	0,74	1,04	1,10	0,80	0,79
Al_2O_3	0,10	4,80	10,89	12,62	13,97	18,56	21,15	21,10	20,01
Fe_2O_3	0,31	0,60	0,77	0,80	0,78	3,83	6,44	7,27	7,31
FeO	0,28	1,44	3,58	4,06	4,54	4,60	1,03	2,72	2,60
MnO	0,01	–	0,09	0,09	0,28	0,12	0,44	0,09	0,17
MgO	0,20	0,34	0,73	0,87	0,99	1,16	1,10	2,01	3,01
CaO	0,30	0,77	0,69	0,79	1,00	2,01	2,16	5,33	7,54
Na_2O	0,09	0,57	1,84	1,69	1,60	1,25	1,46	2,62	3,74
K_2O	0,06	0,10	3,07	2,92	2,84	1,77	1,99	1,70	1,46
P_2O_5	–	–	0,08	0,12	0,12	0,07	–	0,16	0,20
e Сумма	99,37	96,94	99,84	99,71	99,59	101,18	99,75	93,92	101,2
a	0,2	2,0	7,8	7,4	7,2	5,7	5,9	6,3	10,6
c	0,4	2,0	0,8	0,8	1,4	2,3	2,7	5,4	8,3
b	0,8	3,0	9,1	12,1	14,2	20,4	21,9	23,3	15,4
s	98,6	93,0	82,3	79,5	77,4	71,6	69,4	65,2	65,5
a'	–	18,0	40,1	53,2	54,2	59,7	61,2	54,9	14,1
f'	35,6	55,0	42,4	35,6	34,6	30,8	30,8	33,3	50,5
m'	23,2	27,0	12,8	8,8	10,9	9,9	8,5	13,8	34,9
c'	37,2	–	–	–	–	–	–	–	–
n	50,0	68,0	47,5	46,5	45,1	56,7	53,2	52,7	54,1
φ	–	18,0	6,5	6,7	4,6	10,9	31,2	64,4	27,7
t	0,0	0,2	0,6	0,7	0,8	1,0	1,3	1,1	1,5
Q	97,0	80,0	48,8	43,3	38,2	29,5	27,7	8,9	0,5
a/c	0,2	1,0	10,2	9,7	6,6	2,9	4,4	1,2	1,2

*figures are number of analyses averaged

key: a. oxide; b. lechatelierite; c. glassy impactites; d. scoria and calcined clays; e. total

CHEMICAL COMPOSITION OF ZHAMANSHINITES AND IRGIZITES

One basic criterion which distinguishes tektites, and to a lesser degree impactites, from conventional igneous rock is the relationship of the chemical elements in them. They differ from /72

igneous rocks of acid composition by the almost total absence of water, the prevalence of bivalent over trivalent iron, a severe deficiency of potassium and sodium and, on the other hand, large amounts of calcium and magnesium, as well as increased amounts of nickel and cobalt and an unusual content of other elements. After

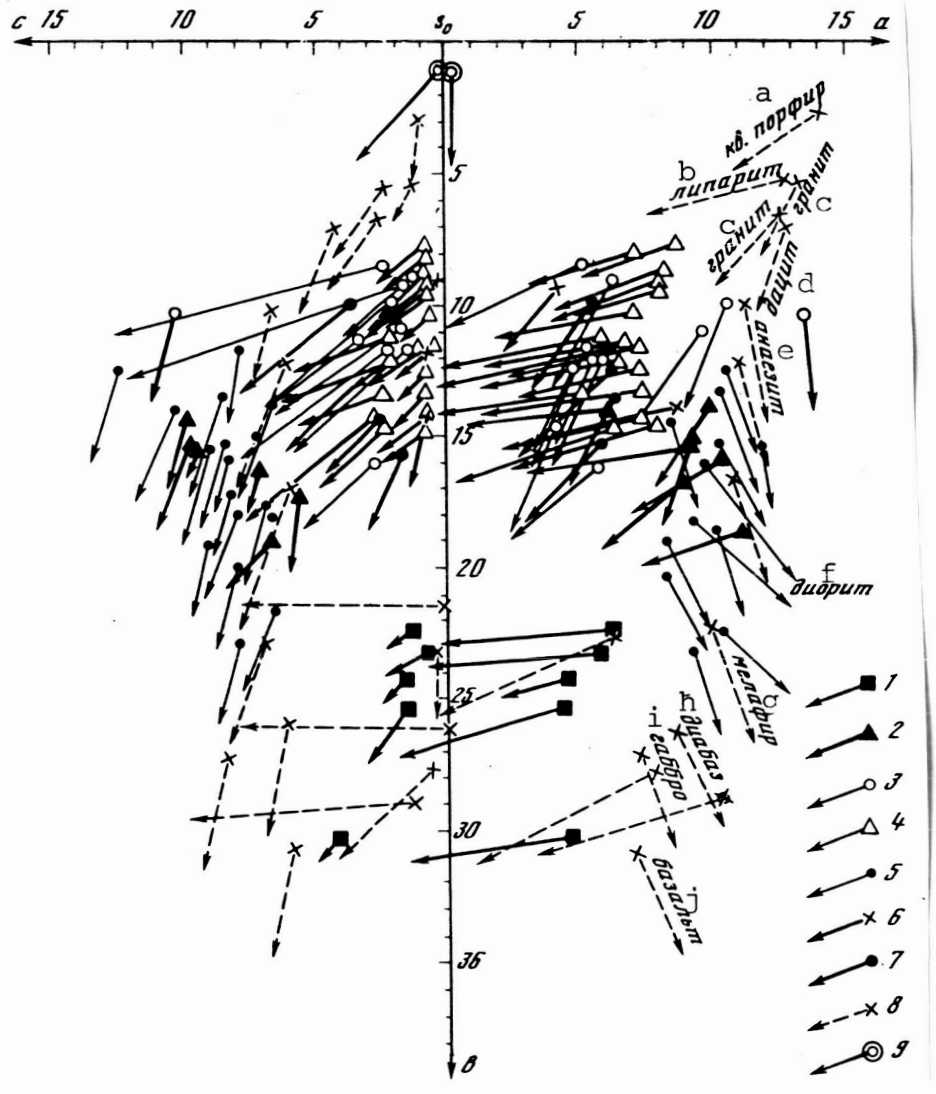

Fig. 33. Vector diagram of A.N. Zavaritskiy (compiled together with I.L. Dmitrenko and T.B. Khakhayeva): 1. black, dense glasses; 2. scoria and calcined clays; 3. Irgizite tektites of acid composition; 4. Zhamanshinite glasses; 5. Irgizite tektites of basic composition; 6. tektites; 7. impactites; 8. igneous and sedimentary rocks; 9. lechatelierites.

Key: a. quartzitic porphyry; b. rhyolite; c. granite; d. dacite; e. andesite; f. diorite; g. melaphyre; h. diabase; i. gabbro; j. basalt.

publication of the first silicate analyses of glasses from the Zhamanshin natural landmark **[82, 86, 88, 42, 43]**, the anomalous composition of the glasses became indisputable, which gave grounds for identifying Irgizites with tektites by chemical composition, as well as for distinguishing groups of basic and acid composition among the glasses, which were classified as impactites. Since that time, silicate, X-ray and radioactivation analyses have repeatedly been done both here and abroad. As a result, approximately 150 analyses of different samples made in different laboratories and by different methods have been correlated in the present work **[50-53, 33, 57, 129]**. In processing, all the analyses were recalculated by the method of A.N. Zavaritskiy, which is reduced to calculation of provisional coefficients which characterize the distribution of the minerals in idealized completely crystalline rock of the same composition. The results of the recalculations and analyses are presented in the form of a vector diagram (Fig. 33). Tables 5-8 present average figures which characterize varieties of similar composition. The average compositions of tektites from different regions are presented in addition (Table 9). On the A.N. Zavaritskiy diagram, besides those listed, the results of chemical analyses of various tektites **[120]**, some impactites **[13, 84]** and typical igneous rocks are plotted for comparison. /73 /74

TABLE 7. COMPOSITION OF BASIC COMPOSITION SPRAYS (from 15 analyses)

a Окисел	b Число анализов					
	3	2	1	3	3	3
SiO_2	54,22	55,84	53,79	54,79	54,10	53,56
TiO_2	0,98	0,83	0,79	0,79	0,94	0,84
Al_2O_3	19,21	19,76	20,07	21,24	20,64	20,59
FeO	7,78	6,93	7,68	7,53	7,95	7,88
MnO	c He опр.	c He опр.	c He опр.	0,19	c He опр.	c He опр.
MgO	2,69	3,00	2,74	2,62	2,67	2,71
CuO	8,98	8,01	8,91	8,38	8,83	8,59
Na_2O	3,72	3,74	3,48	4,12	3,99	3,86
K_2O	1,37	1,68	1,42	1,33	1,31	1,33
P_2O_5	0,24	0,25	c He опр.	0,22	0,25	0,14
Сумма d	99,19	100,04	99,88	101,21	100,68	99,50
a	10,2	11,0	10,3	10,9	10,8	11,7
c	7,6	8,2	9,2	9,1	8,9	8,6
b	14,4	14,1	15,1	14,5	15,2	15,1
s	66,3	66,7	65,4	65,3	65,1	64,6
f'	49,3	48,6	53,2	53,2	51,5	52,3
m'	30,2	37,5	37,6	37,6	31,4	31,8
c'	20,5	13,8	9,2	9,2	17,1	15,9
n	81,0	77,5	78,2	78,2	79,4	82,5
t	1,4	1,1	0,9	0,9	1,1	1,2
Q	7,2	3,2	0,1	−0,1	−0,3	−2,8
a/c	1,3	1,3	1,2	1,2	1,2	1,4

Key: a. oxide; b. number of analyses; c. not determined; d. total

The A.N. Zavaritskiy method was developed for recalculation /75
of the composition of crystalline rocks, but tektites and impactites are almost completely made up of glass, an amorphous substance. Therefore recalculations based on the idea of crystallization of a melt are artificial. A certain model of the rock is created mentally which, having the chemical composition of tektite, would have a crystal structure.

By morphological geochemical and petrographic characteristics, rocks melted in a meteorite impact form relatively isolated groups connected by transitional differences which, by occupying different fields, are easily noted in the A.N. Zavaritskiy diagram (see Fig. 33).

The main thing which is seen in the diagram is the sharp difference of Zhamanshinites and Irgizites from igneous rocks and their similarity to tektites and impactites. Zhamanshinites and Irgizites therefore form a regular series by chemical composition, which has its fundamentally important traits indicating their connection with each other and their difference from igneous rock. Some parameters of A.N. Zavaritskiy which characterize these features can be examined, as was done in a general comparison of

TABLE 8. IRGIZITE COMPOSITION (from 32 analyses)

a Окисел	b Число анализов									
	1	4	5	4	5	4	4	1	1	3
SiO_2	77,14	74,39	74,42	74,32	74,35	74,01	73,00	73,32	72,03	74,40
TiO_2	0,82	0,86	0,82	0,76	0,80	0,85	0,79	0,72	0,85	0,80
Al_2O_3	9,45	10,00	10,00	10,09	10,22	10,35	9,82	9,99	10,13	10,35
FeO	4,24	5,62	5,43	5,36	5,48	5,46	6,06	6,49	6,50	5,64
MnO	c Не опр.	0,11	c Не опр.	c Не опр.	c Не опр.	c Не опр.	c Не опр.	c Не опр.	c Не опр.	0,10
MgO	2,16	2,70	2,68	2,68	2,79	2,70	3,20	3,69	3,75	2,78
CaO	1,75	2,50	2,41	2,44	2,50	2,58	2,68	2,43	2,58	2,46
Na_2O	1,04	1,06	1,10	1,09	1,11	1,10	1,06	0,85	1,00	1,12
K_2O	2,10	1,94	1,98	2,03	2,01	2,08	1,83	1,74	1,58	2,13
P_2O_5	0,04	0,02	0,03	0,02	0,02	0,05	0,02	Не опр.c	0,04	0,01
Сумма d	98,74	99,20	98,87	98,79	99,28	99,18	98,46	99,23	98,46	99,79
a	5,8	4,8	5,0	5,1	5,0	5,2	4,5	4,1	4,0	5,6
c	2,0	2,9	2,8	2,8	2,8	3,0	3,1	2,7	3,0	2,8
b	9,3	10,8	11,0	11,3	11,7	11,4	12,9	14,6	14,5	12,6
s	82,9	81,5	81,2	80,8	80,5	80,4	79,5	78,6	78,5	79,3
a'	22,1	20,5	19,0	18,5	18,5	18,3	12,8	20,2	18,3	22,0
f'	40,7	43,9	43,6	43,4	43,0	43,9	44,4	39,4	40,2	40,2
m'	37,2	35,6	37,4	38,1	38,5	37,8	42,8	40,4	41,5	38,5
n	25,3	47,3	45,7	45,9	46,7	45,5	48,5	43,8	51,6	45,0
t	0,8	0,8	0,8	0,8	0,7	0,8	0,8	0,7	0,8	0,8
Q	52,2	50,3	49,2	48,6	47,9	47,4	46,6	46,3	45,9	44,7
a/c	2,9	1,6	1,8	1,8	1,8	1,7	1,5	1,5	1,3	1,9

Key: a. oxide; b. number of analyses; c. not determined; d. total

tektites and igneous rock compositions **[89]**.

The potassium and sodium content and, from them, the orthoclase and albite content, indicate parameter a. While it equals 12-15 In igneous rocks, it is 1/2-1/3 as much in Zhamanshinites and tektites, and this is reflected in the diagram by displacement of the points to the left toward the vertical axis. Actually, a deficiency of sodium and potassium compared with conventional igneous rocks is a characteristic trait of tektites. /76

The amount of calcium basically included in the composition of the anorthite molecule (parameter c) is constant of both one igneous rock body and even for one type of them. Parameter c of Zhamanshinites varies within wide limits from Ø.6 to 11.Ø. In particular, a high value of parameter c is characteristic of Zhamanshinites probably formed by the reworking of marls and calcareous clays.

TABLE 9. CHEMICAL COMPOSITION OF TEKTITES OF DIFFERENT GROUPS **[12Ø]**

a Окисел	b Молдавиты (14) *	c Бедиазиты (6)	d Австралиты (32)	Тектиты Берега Слоно-е вой Кости (3)	f Индошиниты (36)	g Филиппиниты (21)	h Биллитониты и Явайты (13)
SiO_2	79,01	78,59	73,06	71,05	73,09	70,87	71,29
TiO_2	0,69	0,64	0,68	0,73	0,87	0,83	0,79
Al_2O_3	11,09	12,57	12,23	14,60	12,60	13,48	12,37
Fe_2O_3	0,30	0,44	0,60	0,18	0,34	0,79	0,78
FeO	2,15	3,01	4,14	5,51	4,78	4,30	5,08
MnO	0,08	0,03	0,12	0,08	0,12	0,09	0,14
MgO	1,49	0,63	2,04	3,29	2,16	2,67	3,16
CaO	2,08	0,57	3,38	1,67	2,31	3,14	2,95
Na_2O	0,52	1,34	1,27	1,71	1,45	1,41	1,57
K_2O	3,04	2,13	2,20	1,53	2,40	2,31	2,20
Сумма[i]	100,45	99,95	99,72	100,35	100,12	99,89	100,33
a	5,2	6,1	5,7	5,5	6,1	6,1	6,2
c	2,4	0,6	3,9	1,9	2,6	3,7	3,4
b	8,4	11,7	9,8	15,1	14,1	12,7	13,2
s	84,0	81,6	80,6	77,5	77,2	77,6	77,2
a'	48,0	67,7	22,8	32,9	30,8	29,2	16,7
f'	28,0	24,4	43,7	33,1	45,5	37,0	45,1
m'	24,0	7,9	33,5	34,0	23,7	33,8	38,2
n	20,7	48,5	47,2	62,0	49,9	49,0	52,5
φ	3,2	3,2	4,0	3,7	1,8	4,6	4,3
t	0,5	0,6	0,7	0,7	0,8	0,8	0,9
Q	55,2	50,4	45,9	42,1	39,6	39,1	38,6
a/c	3,5	10,1	1,4	2,9	2,3	1,6	1,8

*In parentheses, the number of analyses averaged.

Key: a. oxide; b. moldavites, c. bediasites; d. australites; e. Ivory Coast tektites; f. Indochinites; g. Phillippinites; h. Billitonites and Javaites; i. total

If there is more aluminum than is necessary for the formation of feldspars, it is included in the composition of dark colored minerals, and parameter a' is introduced into the rock characteristics. There are few such rocks on the earth. For tektites, many impactites and all Zhamanshinites, however, high supersaturation with alumina is characteristic (a' is present and is 30-50, reaching 72). This is expressed on the diagram by a vector directed to the left, while the vector of the majority of igneous rocks is directed to the right.

As a rule, Zhamanshinites are highly supersaturated with silica. Some samples consist almost entirely of it but, in others formed by calcining clays on the other hand, a deficiency of it is observed. Zhamanshinites therefore differ substantially from each other in silica content. /77

The apparent discrepancy of composition of the assumed initial rocks and the glass melted from them can be explained by selective vaporization of more volatile compounds at the extremely high temperatures caused by the impact of the incident meteorite. The possibility of such a process is confirmed by experiments with the melting of rocks in vacuum **[145, 106]**. If it is assumed that the entire excess of alumina and part of the excess of silica was included in the initial rocks in the composition of clay minerals and feldspars, in order to compensate this excess it has to be assumed that the material lost at least a third to half the alkali elements in the melting out of the glasses. The compositions of such assumed initial rocks is highly similar to the composition of the surrounding deposits of different ages.

TABLE 10. CHEMICAL COMPOSITION OF FIVE IRGIZITE AND ZHAMANSHINITE SAMPLES **[129]**

a Окисел	b Кислого состава			c Основного состава	
	d жаманшинит	e иргизиты		f брызги	жаманшинит d
	1	2	3	4	5
SiO_2	72,01	74,28	73,32	53,79	55,34
TiO_2	0,78	0,78	0,78	0,79	0,69
Al_2O_3	15,55	10,16	9,99	20,07	22,16
FeO	5,50	5,60	6,49	7,68	4,68
MgO	1,11	2,93	3,69	2,74	3,23
CaO	0,55	2,36	2,43	8,91	6,68
Na_2O	1,10	0,97	0,85	3,48	4,55
K_2O	2,83	2,00	1,97	1,42	1,85
Сумма g	99,43	99,04	99,23	99,88	99,18
Na/K	0,38	0,49	0,42	2,45	2,47

Key: a. oxide; b. acid composition; c. basic composition; d. Zhamanshinite; e. Irgizites; f. sprays; g. total

TABLE 11. CONTENT OF MINOR AND TRACE ELEMENTS IN FIVE ZHAMANSHINITE AND IRGIZITE SAMPLES [129]

a Название	Номера кривой (рис. 34) b	Cs	Tl	Ba	Pb	Th	U	Zr	Hf	Nb	Sn	Mo
Жаманшинит c	1	7,8*	0,43	374	26	10,3	2,97	272	6,3	16,8	3,1	0,73
Иргизит кислый d	2	2,6	x**	527	2,9	5,98	1,02	351	8,66	12,5	0,75	0,40
	3	1,9	x	508	2,0	5,58	0,83	370	8,4	10,9	0,78	0,23
Брызги основные	4	6,6	x	665	10,9	2,35	0,78	71	1,76	3,2	0,75	0,37
Жаманшинит c	5	3,6	0,08	470	7,2	2,10	1,37	81	1,76	2,8	0,92	0,45

f Таблица 11 (окончание)

a Название	Номера кривой (рис. 34) b	Bi	W	Gr	V	Sc	Ni	Co	Cu	$N_{/Co}$	$Cr_{/Ni}$	$Th_{/U}$
Жаманшинит c	1	0,12	0,73	92	117	15	40	16	36	2,5	2,3	3,45
Иргизит кислый d	2	0,04	0,17	170	46	8,8	1200	73	24	16	0,14	5,87
	3	x	0,13	200	38	9,4	1370	102	19	13,4	0,15	6,75
Брызги основн. e	4	0,09	0,18	g Не опр.	g Не опр.	g Не опр.	g Не опр	g Не опр.	g Не опр.	g Не опр.	g Не опр.	3,0
Жаманшинит c	5	0,02	0,19	22	260	17	12,5	19	17	0,66	1,8	1,53

*All in million g/g; **beyond limits of accuracy of determination.

Key: a. name; b. curve number (Fig. 34); c. Zhamanshinite; d. acid Irgizite; e. basic sprays; f. table 11 (concluded); g. not determined

TABLE 12. CONTENT OF RARE EARTH ELEMENTS IN FIVE ZHAMANSHINITE AND IRGIZITE SAMPLES [129].

a Название	b Номера кривой (рис. 34)	La	Ce	Pr	Nd	Sm	Eu	Gd
Жаманшинит c	1	33,9	83,6	8,98	34,1	6,95	1,56	6,47
Иргизит кислый d	2	19,7	44,2	4,53	18,7	3,78	0,80	3,46
	3	19,7	44,7	4,59	17,3	3,22	0,68	3,01
Брызги основн. e	4	13,1	27,7	3,62	15,7	3,51	1,01	3,00
Жаманшинит c	5	12,4	28,0	3,39	14,5	3,42	1,12	3,23

f Таблица 12 (окончание)

a Название	b Номера кривой (рис. 34)	Tb	Dy	Ho	Er	Yb	g Сумма редкоземельных элементов	Y	h $\frac{Eu_{образец}}{Eu_{хондрит}}$
Жаманшинит c	1	0,97	5,63	1,12	3,29	3,40	192,3	33,8	0,72
Иргизит кислый d	2	0,60	3,45	0,67	1,89	1,90	105,1	17,5	0,68
	3	0,53	2,99	0,58	1,73	1,82	102,2	15,4	0,69
Брызги основн. e	4	0,52	3,04	0,61	1,68	1,51	75,9	17,5	0,96
Жаманшинит c	5	0,53	3,26	0,62	1,74	1,67	74,8	24,0	1,00

Key: a. name; b. curve number (Fig. 34); c. Zhamanshinite; d. acid Irgizite; e. basic sprays; f. table 11 (concluded); g. total rare earth elements; h. $Eu_{sample}/Eu_{chondrite}$

In their morphological, petrographic and geochemical characteristics, the Zhamanshin Crater formations melted out by the meteorite impact formed characteristic groups relatively isolated from each other but connected by transitional differences. On the one hand, these differences depend on the features of the hardening processes of high temperature silicate melts in which their eutectoid equilibria can develop. On the other hand, their composition is determined by the composition of the original rocks. However, in connection with the fact that they are interbedded in their basement bedding and were mixed still more in the explosion, given Zhamanshinites can only provisionally be compared with any original rocks. Nevertheless, a number of common features of the composition of the original rock of the Zhamanshinites and the conditions of their occurrence permit correlation of isolated groups with given differences of the initial rocks: 1. lechatelierite, pure SiO_2, was formed by reworking of the vein quartz near which it was found; a relict pattern of fractures characteristic of vein quartz in the basement bedding is even seen in places in it; 2. dense, dark and light glasses containing 73-70% SiO_2 probably were melted out from the Lower Paleozoic quartzitic schists, which are chemically similar and connected with them in space; 3. black glasses and scoriaceous formations containing 55-65% SiO_2 are most characteristic of Zhamanshin Crater; they likely could have melted out of different rocks, including loose Tertiary clays; similar formations are known from other impact structures; 4. basalt-like varieties containing only 55% SiO_2, but more than 10% Fe^{2+} were possibly melted out of volcanogenic Upper Paleozoic rocks with which they are connected in space; 5. calcined transitions to unaltered Tertiary clays; 6. Irgizite tektites, which constitute a special group and differ by an excess of SiO_2 and Al_2O_3 and a deficiency of alkalis; this product is the most thoroughly differentiated (Table 10). /78 /79

Nickel and cobalt are validly considered to be those elements from which, assuming known composition of the meteorite (iron or stony), the relative amount of matter scattered in a given rock can be decided. Increased nickel content was found in some impactite samples from Popigay Crater **[98]** and from tektites (up to 0.3%) in philippinites and javaites **[13]**. Determination of nickel in Irgizites, done for the first time by Yu.F. Pogrebnyak in 1971, showed anomalously high content of it, up to 0.1%, while the nickel content of of Zhamanshinites is within the Clarke limits of less than 0.01%. These determinations were later confirmed **[33, 129]**. Meteorite or terrestrial origin of the nickel in the rock usually is decided from its ratio to cobalt. Terrestrial rocks contain them in similar quantities, and the Ni/Co ratio is 1.5-2.5. This ratio is higher in stony meteorites, and it reaches 18 in octahedrites. This ratio in acid and basic composition Zhamanshinites and basic composition Irgizites corresponds to the terrestrial ratio, but it is unusually high in acid Irgizite tektites and reaches 13-16. This permits the thought that at least 90% of the nickel in Irgizites is of meteorite origin.

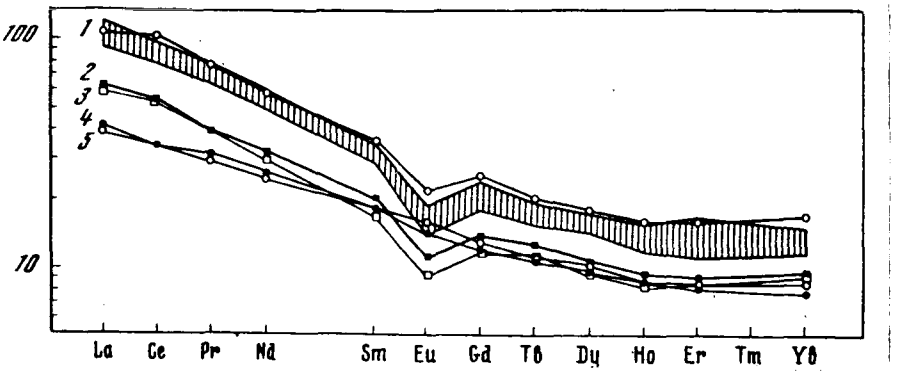

Fig. 34. Distribution of rare earth elements in Australasian tektites (cross hatched), Irgizites and Zhamanshinites, which are normalized with respect to rare earth element content of chondrites **[129]**: 1-5. see tables 10-12.

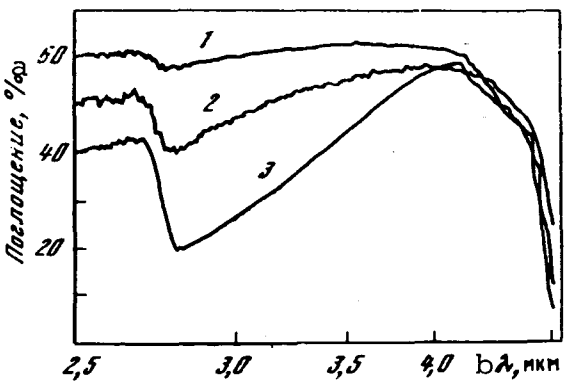

Fig. 35. Infrared absorption spectrum of moldavite (1), Irgizite (2) and obsidian (3); water content of moldavite 0.0092%, Irgizite 0.051%, obsidian 0.156%.

Key: a. absorption, %, b. λ, μm

Volatile and chalcophilic trace elements (Cs, Tl, Pb, Sn, Mo, Bi, W, Cu) (Table 11) are contained in Irgizites in quantities close to their content in other tektites, where there usually is 1.5-2.5 times less of them than in sedimentary rocks. Irgizites are depleted in exactly these same elements, compared with Zhamanshinites. There is no doubt that this is connected with selective vaporization of the more mobile elements at the high temperatures of tektite formation.

Acid Irgizites and Zhamanshanites contain minor elements (Ba, Th, U, Zr, Hf, Nb, Cr, V, Sc) (see Table 11), except for chromium, in the same quantities as in the majority of tektites, i.e., close to the Clarke abundance. The high Th/U ratio of more than five attracts attention. It is characteristic of sedimentary rocks, whereas this ratio is less than three in basic composition rocks, which is characteristic of basalts for example. /82

Rare earth elements(La, Ce, Pr, Nd, Sm, Eu, Gd, Tb, Dy, Ho, Er, Yb) (Table 12, Fig. 34) were determined independently in three laboratories, and their results are similar: V. Boushkaya at Charles University, Czechoslovakian SSR; W.D. Ehmann at NASA, USA

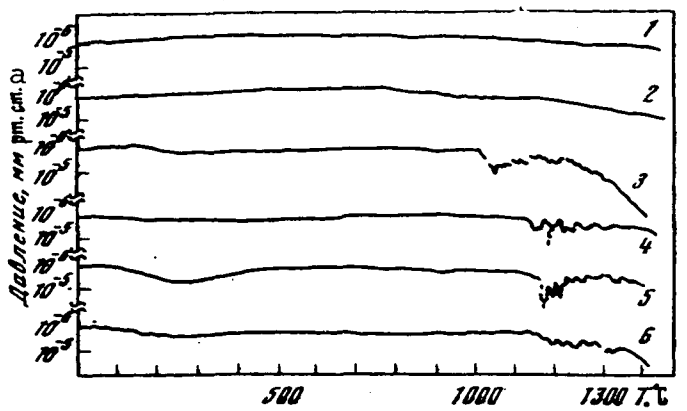

Fig. 36. Pressure drop in proportion to heating of tektites during their outgassing in chamber in vacuum: 1. pressure control (in heating to 1500°C without sample, pressure rose only from $2 \cdot 10^{-6}$ to $8 \cdot 10^{-4}$ mm Hg; 2. Indochinite; 3. basic composition Zhamanshinite; 4-5. Irgizite tektites; 6. tektite composition glass synthesized by F. Heide **[74]**.

Key: a. pressure, mm Hg

[33]; S.R. Taylor and S.M. McLennan at the Australian National University, Canberra **[129]**. They were determined in the greatest detail at the Australian National University and were compared with simultaneously made determinations on tektites of the Australasian scattering field, and impactites from Henbury Crater. The absolute rare earth element content of all tektites and the average /83 content of sedimentary rocks are very similar. It is known here that, if the rare earth element content is normalized to their content in chondrites, the resulting ratios form a stable, uniformly decreasing series for igneous rocks, but a sharp deficiency of europium is observed in sedimentary rocks. Just such an "europium depletion" was established for all tektites in general and Irgizites in particular. It is absent however in Zhamanshinites. Thus, the distribution of rare earth elements indicates a fundamental difference of Irgizites from other glasses of the Zhamanshin natural landmark.

For determination of the amount of water in Irgizites, E.A. King **[80]** took adsorption spectra of moldavite, Irgizite and, for comparison, obsidian (Fig. 35). It turned out that, while obsidian contains 0.156% water and moldavite only 0.0092%, there is unusually much of it for tektites in Irgizite, 0.051%.

It is customarily considered that gas inclusions in tektites contain gas of similar composition to the atmospheric composition, but at extremely low pressure **[130]**. The first analyses from Irgizites gave similar results (L.V. Firsov, Institute of Geology and Geophysics, Siberian Section, USSR Academy of Sciences). Repeated studies were conducted by K. Heide and H.-G. Schmidt **[74]** by fusing tektites up to 1500°C in $8 \cdot 10^{-6}$ mm Hg vacuum. It was established that outgassing and consequently softening of the basic composition glasses was observed at 950-1180°C, and at 1050-1260°C in Irgizite tektites. The pressure in the chamber increased little here, which indicates a rarefied state of the gas in the inclusions (Fig. 36). The composition of the gas in the basic glasses was close to that in effusives. CO_2, H_2O, H_2, H_2S, HCl, CO_2, HF (?) were found, but only H_2, CO_2, H_2O, HF and H_2S were

found in acid glasses. Neither O_2 nor N_2 were found, which unambiguously indicated atmospheric origin of the gases, which is therefore specific for Irgizites.

The thermograms taken by B.S. Sorin (Institute of Steel and Alloys, Moscow) give similar softening temperatures. A diffuse exothermic maximum is seen in them in the 580°C region, which is connected with reorientation of the SiO_2 tetrahedra from α-quartz (bond angle 142°) to β-quartz (bond angle 180°). The initial softening and viscous melting temperature of basic composition glasses is somewhat lower than that of acid glasses, but it is within the limits indicated in both cases.

STRUCTURAL AND CHEMICAL CHARACTERISTICS OF IRGIZITES AND ZHAMANSHINITES

The macrosculpture of tektites, traces of hardening from the viscous state and sometimes subsequent dissolving, can theoretically be formed in glasses of volcanic and artificial origin. The features of the chemical composition of tektites indicates their specific nature more definitely, but they do not provide unambiguous conclusions on genesis and do not permit definite separation of tektites from other formations. The structural features of the glasses which form them on the molecular and atomic levels indicate their uniqueness unambiguously. These features permit establishment of the fundamental difference of tektites from all known terrestrial glasses. The present section reports the results of study of the behavior of silicon, aluminum and calcium ions and indirect estimation of the behavior of potassium and sodium by X-ray spectroscopy, conducted together with Yu.P. Dikov **[47, 54]**, as well as the behavior of iron ions, studied together with T.S. Gendler **[62]** by nuclear gamma resonance (Mossbauer) spectroscopy. /84

PRINCIPLES OF X-RAY SPECTROSCOPY

The following problems are solved by X-ray spectroscopy methods, which are presented in the monograph of Yu.P. Dikov et al **[31]**:

1. Determination of the energy, width and yield of the fluorescence of the internal states of ionized atoms;
2. Estimation of the symmetry of the valence bonds and the coordination number of the absorbing atoms;
3. Study of the polarization of the electron shells of anions in the ionic crystal;
4. Study of the potential field distribution in the crystal lattice;
5. Measurement of the charge of ions in compounds;
6. Study of the energy distribution of halogen and free electron states;
7. Comparison of the total energy systems of electron states of crystal matter, as well as a number of other questions concerning the nature of chemical bonds and solid state physics

[31, 32].

The method is connected with study of free electrons or bound photons with electrons. When electrons or X-ray quanta strike a substance, the electrons of the latter are knocked out and the atoms change to an excited state but, after a certain interval of time, they return to normal. The interaction of matter indicated /85
with X-ray quanta and electrons occurs differently depending on the states of the atoms:

a. the case when a vacancy occurring at a deep level is filled with an electron shifted from a less bound shell, including the valence band; such a transition is accompanied by the emission of an X-ray quantum, the energy distribution of which is studied by X-ray emission spectroscopy;

b. the case when an excited electron does not leave the substance, but only changes to one of the open levels of the conduction band, which is accompanied by the absorption of X-ray quanta; this phenomenon is studied by X-ray absorption spectroscopy (absorption spectra);

c. the case when the absorption of X-ray quanta is accompanied by knocking of photoelectrons out of the substance, i.e., the energy of the quanta is consumed in the energy of the atoms (this case is coupled with the radiation transition described in subparagraph a.);

d. the case of radiationless filling of vacancies; in this case, one only electron from the same or a higher shell is knocked out of the substance and the atom itself remains doubly ionized for some time; electrons knocked out in this manner are called Auger electrons; photoelectrons and Auger electrons are studied by X-ray photoelectron spectroscopy; we have not studied these spectra.

X-ray emission spectroscopy permits a decision on occupied states (emission spectra), and absorption spectroscopy permits a decision on the vacant states (absorption spectra) in a substance.

The energy of a quantum of X-ray radiation of a substance ($h\nu 2$), generated by the excitation of a primary quantum ($h\nu 1$) or an electron beam corresponds to the energy difference of the two levels between which the radiation transfer occurred.

The following designations of electron levels in an atom have been adopted in X-ray spectroscopy:

STATE	$1s$	$2s$	$2p$	$3s$	$3p$	$3d$	$4s$
DESIGNATION	K	L_{I}	$L_{II,III}$	M_{I}	$M_{II,III}$	$M_{IV,V}$	N_{I}

The double subscript corresponds to spin doublet splitting of the corresponding level. The lines of the X-ray spectrum are designated by the level in which the vacancy arose which provided the radiation transition. The transition of an electron from LII, III to the K level is accompanied by the emission of the characteristic spectrum from MII to K-$K\beta_3$, from MIII to K-Kpl, etc.

X-ray transitions obey the dipole selection rules, by which a transition is possible between levels of different parity. X-ray spectroscopy therefore permits study of the density of states of different symmetry, which is particularly important in analysis of the valence band. Since the width of an emission line reflects the sum of the widths of the levels involved in the transitions and the valence band is wider than the inner levels, the resulting spectrum is primarily a spectrum of the valence states. Therefore, by exciting different series of the X-ray spectrum, practically all /86
the electron states of the valence band can be studied. Thus for example, for the electrons of elements of the third period which together with oxygen are the main silicate forming elements, an idea of the distribution of the 3p valence states can be obtained by means of the K spectrum, and the $L_{II, III}$ spectrum gives a picture of the distribution of the 3s states and the 3d valence states.

The intensity and shape of the X-ray lines and bands are determined by the distribution of densities of external electrons by state N(E), as well as the probability of transition P(E), and they can be represented in the form

$$J(E) \sim N(E)P(E).$$

The energy positions proper of the maxima correlate with the charge parameters of the atoms. Strictly speaking, the complex dependence of P(E) on the characteristics of the electrons in a crystal does not permit direct connection of the X-ray band intensities with the density of states. But, at the same time, the characteristics of the X-ray bands correspond to the energy positions of singular points of the N(E) curve, and the probability of X-ray transitions can therefore be taken into account by combined analysis of the X-ray bands of different series.

ABSORPTION

The characteristics of the initial absorption band are connected with the density of vacant states and the probability of a transition. The most informative characteristic is the absorption fringe, since this position corresponds to the energy necessary for transfer of an electron to the first unoccupied level from one of the inner levels of the atom. Upon irradiation of an atom with a quantum, an electron of one of its inner shells can be knocked out to an outer shell where, although there are no electrons, the action of the field of the nucleus still shows up, and there is a set of permitted quantum levels above the normal orbitals, these levels are converging and compacted and they change to a continuum with distance from the nucleus, i.e., with distance from the nucleus, the electrons are displaced by shells practically without being quantized. The presence of electrons in these shells reflects the excited state of the atom. By returning the their initial levels, the electrons emit quanta, the energies

of which correspond to the energies which characterize the absorption fringes of the electrons of the nuclear field of the atom.

To obtain absorption spectra in the 1-7Å region does not cause experimental difficulties. Study of the absorption spectra in the ultrasoft X-ray region (7-800Å) requires the application of thin ($\sim$100Å) uniform films of absorbers. Therefore, information on the absorption spectra in this region is obtained by means of the quantum yield spectra of the X-ray photoelectric effect of the study substance. The basis of this method is that upon irradiation with a X-ray braking spectrum of the substance, the amount of photoelectrons and Auger electrons escaping from it with energies of the incident radiation close to the energies of the absorption fringes of the sample under study will increase sharply, similar to the way this is observed in absorption spectra.

Thus, in study of the occupied states of an atom, emission spectra are used, but vacant states are studied by means of absorption spectra or quantum yield spectra. They were used for /87 study of samples from Zhamanshin Crater, as well as tektites from other locations.

X-ray emission and quantum yield spectra were taken in a RSM-500 X-ray spectrometric chromatograph. The reference lines used were $M_{II, III}$ and $M_{IV, \bar{V}}$ lines of Fe and Cu. The exposure conditions were 5mA current and 10 kV voltage. X-ray photoelectron spectra were taken in a Varian Company JEE-15 spectrometer. The photoelctrons were excited by means of the $K_{\alpha 1,2}$ line of magnesium, the transmission energy of the photoelectrons was 100eV, and the vacuum in the spectrometer chamber was $3 \cdot 10^{-7}$ mm Hg. The spectra were calibrated by the 1s line of carbon spectra, for which a binding energy of 285.0 eV was adopted. The accuracy of determination of the binding energy was $\pm$ 0.1 eV, and the resolution was at least 1.2 eV.

PRINCIPLES OF NUCLEAR (MÖSSBAUER) SPECTROSCOPY

One of the most widespread elements in nature, iron in the di- and trivalent and occasionally metallic form, is part of many minerals and rocks and is highly convenient as an indicator of their formation. The iron ion as part of various compounds is being studied in special detail by nuclear γ resonance spectroscopy (Mossbauer effect) on the isotope ^{57}Fe [25, 92]. The spectrum is the intensity of the resonance γ quanta passing through the substance analyzed (absorber) vs. the rate of displacement relative to this absorber of the source of γ quanta containing the same isotope, but in the excited state. The spectrum is a single line of Lorentz form with specific halfwidth $\Gamma_{1/2}$ only for para- and diamagnetic compounds with strictly cubic symmetry of the immediate vicinity of the iron nucleus. Deviation of the symmetry from cubic leads to the formation of a doublet spectrum by quadrupole splitting of the nuclear levels of ^{57}Fe by the crystal field. The

TABLE 13. MOSSBAUER SPECTRUM PARAMETERS OF SERIES OF IRON CONTAINING COMPOUNDS.

a Вещество	b δE, мм/с		c ΔE, мм/с		d $\Gamma_{1/2}$, мм/с	e $H_{эф}$, кЭ
	M_1	M_2	M_1	M_2		
f Гематит	0,14		0,20		0,35	515
g Магнетит	0,21	0,53	0,0	0,10	−0,35	505–460
h Металлическое железо	0,02		0,0		0,34	333
i Лимонит	–		–			380–300
j Ильменит	1,13		0,50		0,35	–
k Пирит	0,22		0,62		−0,35	–
l Оливины	1,12–1,10		2,89–3,00		0,40	–
m Амфиболы	1,10	0,99	2,80	1,55	0,35	–
n Пироксены						
o синтезированные	0,95	0,94	2,55	2,0	0,35	–
p земные Fe^{2+}	0,99	0,96	2,53	2,0	0,35	–
Fe^{3+}	0,20		0,69		0,35	–
q из метеоритов	0,99	0,96	2,60	2,15	0,35	–
r Лунный реголит	0,99 –0,96		2,10 – 2,02		0,6–0,8	–
s Стекла						
t железосиликатные	0,99		2,11		0,6–0,8	–
u щелочные						
v пироксеновые	0,81		2,03		0,6–0,8	–
w Тектиты	0,88 –0,92		1,84–1,92		0,8–0,9	–
x Образования из кратера Жаманшин						
y обожженные глины						
f гематит	0,14		0,20		0,35	515
z силикаты Fe^{2+}	0,90 –0,94		2,50	1,60	0,35	–
Fe^{3+}	0,17		0,96		0,40	–
aa шлаки Fe^{2+}	0,88		2,50	1,80	0,40	–
Fe^{3+}	0,10		0,85		0,60	–
bb жаманшиниты						
Fe^{2+}	0,80	0,90	2,40	1,78	0,40	–
Fe^{3+}	0,90		2,09		0,9–1,2	–
cc тектиты-иргизиты	0,71–0,79		1,80		1,20	–

Note. δE relative to ^{57}Co. Average values of δE and ΔE change somewhat corresponding to iron content and formation conditions.

Key: a. substance; b. δE, mm/s; c. ΔE, mm/s d. $\Gamma 1/2$, mm/s; e. Heff, kOe; f. Hematite; g. Magnetite; h. Metallic iron; i. Limonite; j. Ilmenite; k. Pyrite; l. Olivines; m. Amphiboles; n. Pyroxenes; o. synthesized; p. terrestrial; q. from meteorites; r. Lunar regolith; s. Glasses; t. iron silicate; u. alkaline; v. pyroxene; w. Tektites; x. Formations from Zhamanshin Crater; y. calcined clays; z. silicates; aa. scoria; bb. Zhamanshinites; cc. Irgizite tektites

spectrum becomes a six component spectrum in magnetic substances, in accordance with the six possible transitions between nuclear half levels in the presence of a magnetic field. All gamma resonance spectra are described by a set of parameters: isomeric chemical shift δE, the position of the center of gravity of the spectrum, characterizes the features of the chemical environment of the ^{57}Fe nucleus; the region of values of δE are sharply different for the ions of di- and trivalent iron as well as in oxygen and silicate compounds; quadrupole splitting ΔE, the distance between the peaks in the doublet spectrum, reflects the deviation of symmetry from cubic, and it also is different for high spin compounds of di- and trivalent iron; effective internal magnetic field H_{eff} acting on the ^{57}Fe nucleus in magnetic compounds is proportional to the distance between the extreme peaks of the spectrum and is connected with the magnetic moment of the iron ion in its structural position in the lattice. The characteristics listed reflect the properties of the immediate vicinity of the ^{57}Fe nucleus. Therefore, if there are several types of immediate /88 vicinity of the nucleus of the substance studied or, all the more if the iron has different valence or coordination, the spectrum becomes complicated and reflects the overall picture. Quite a large amount of experimental material has been accumulated on study of iron containing minerals. This permits reliable identification of them or rocks of different origin by the nature of the spectrum **[25, 92, 93]**. Characteristic parameters of the Mossbauer spectra of widespread minerals are presented in Table 13, where the results /89 of study of other tektites, synthesized glasses, meteorites, lunar soil (regolith) and the results of studies of formations from Zhamanshin Crater **[62]** also are presented.

Samples (150-200 mg) pulverized to powder were analyzed in an electrodynamic type nuclear gamma resonance spectrometer with a R-4000 multichannel analyzer. ^{57}Co in a Pd matrix was the γ quantum source and the detector was a scintilation counter with a Tl activated NaI crystal.

SILICON, ALUMINUM AND CALCIUM IN MASKELYNITIZED BRECCIAS

Impact metamorphism on the periphery of the explosion resulted in the complete destruction of the crystal lattices of the minerals, formation of diaplectic glasses and a change in structure of the electron shells of the atoms and the ions. The magnitude of the pressure in this case was $3 \cdot 10^2$ kilobars. The pressure towards the center of the explosion was still greater and caused melting of the rocks. For the study, a sample of breccia was selected with isotropized quartz and maskelynitized feldspars, in which the coesite and stishovite described above were found. To decide on the nature of the immediate surroundings of silicon, its $L_{II, III}$ emission spectrum was studied. It is characterized by a marked double peaked configuration in the high energy part, and it is similar to the configuration of the crystalline quartz spectrum. It differs from it, however, by a reduced (4.8 eV) degree of splitting of basic maxima A and B compared compared with that of

quartz (5.5 eV). This occurs because of a Ø.3 eV increase in the transition energy of the maximum (i.e., some destabilization of the multicenter σ-binding molecular orbital found by the 3s states and the 3p states of oxygen occurs, and maximum A is displaced Ø.4 eV in the direction of lower transition energies (i.e., an increase occurs in the binding role of the π orbitals found by the 2p atomic orbitals of oxygen). All this is evidence of an increase of the ionic nature of the Si-O bond and is characteristic of coesite. The approach of maxima a and c to 1.4 eV is still more definitive evidence of the increase of the role of ionic bonds. This value is inversely proportional to the Si-O distance which, in this case, has the value $R_{SiO} \simeq 1.7$ Å, which is characteristic of coesite (this distance is less than 1.65 Å in conventional silicates).

Besides, the core levels of a number of elements were taken, for which the binding energies proved to be: 2p Al (75.4 eV); 2p Si (1Ø3.3 eV); $2p_{1/2}$ Ca (352.3 eV); $2p_{3/2}$ Ca (348.5 eV); 1s O (531.7 eV).

To decide from these determinations, the binding energy of the 2p electrons of silicon is Ø.5 eV less than in α quartz. This also confirms the increase in the role of the ionic nature of the Si-O bond. The binding energy of the 2p electrons of aluminum is 75.4 eV. This is considerably higher than in alumosilicates, and it corresponds to the binding energy in aluminum oxide Al_2O_3. This compound apparently is formed in the impact collapse of feldspars to maskelynite.

The spectrum of the 2p electrons of calcium is unusual /9Ø because of the high value of spin doublet splitting $2p_{1/2}$-$2p_{3/2}$, which is 3.8 eV compared with that of conventional silicates (3.3-3.6 eV). In addition, a strong reduction of the line of the $2p_{1/2}$ electron is characteristic of this spectrum. Such a spectrum is evidence that the Ca-O bond is distinguished by substantial ionicity and that the distance from the calcium to the nearest neighbors is variable and extremely diverse. A similar increase of spin doublet splitting is known only in compounds with an increase of the ionic nature of the Ca ligand bond (for example, in the chalcogenides (CaF_2, $CaCl_2$), and a decrease in intensity of the $2p_{1/2}$ electron line occurs where the calcium-oxygen polyhedron is highly distorted, in a situation of high alkalinity for example, which does not occur in this case. Therefore, the behavioral features of the calcium atoms are explained exclusively by the effect of high pressure.

Thus, for minerals subjected to impact transformation which still have not been fused, an increase in the role of ionic nature of the bonds and the formation of the densest packing are characteristic.

SILICON AND ALUMINUM IN SCORIA, ZHAMANSHINITES AND IRGIZITES

In the inner zone of the explosion, where the temperature reaches several thousand degrees and the pressure reaches megabars; impact melting of practicably all minerals occurs. These glasses were studied by X-ray spectroscopy. The K spectra and L spectra of the emission of the quantum yield of silicon and aluminum (Fig. 37) and the $L_{II, III}$ spectra of the silicon emissions of Irgizites, as well as of other tektites and natural and artificial glasses (Fig. 38) were taken. Quartz and albite glasses were used as comparison references. It was establishedthatthe vacant p states of both silicon and aluminum, reflected in the K spectrum of the quantum yield, underwent the greatest rearrangement. The energy position and width of the basic maximum in the initial absorption band of the K_β spectrum is connected with the measure of geometric distortion of the $[SiO_4]^{4-}$ and $[AlO_4]^{5-}$ tetrahedra. The smaller the scatter of the individual Si-O(Al-O) distances and the more symmetrical the tetrahedra themselves, the less is the width of the spectrum maximum and the higher its energy position. The maximum is narrowed down in the absence of perturbing effects on the part of the second coordination sphere, which also results in idealization of the tetrahedra. Narrowing of the maximum of the quantum yield K spectra of silicon and alumina compared with that of albite glass by 10-15% and remarkable constancy of the position of the maxima for silicon (1848.8 eV) and for aluminum (1566.9 eV) are characteristic of various tektites. This indicates idealization and a roughly statistical distribution of the tetrahedra, i.e., of the absence of crystallization effects in tektites. Therefore, to decide from the quantum yield spectra, tektites are characterized by an extremely high degree of vitrification and minimum interaction of different structural units. This is characteristic of a high temperature melt and could have been preserved in very rapid cooling and hardening.

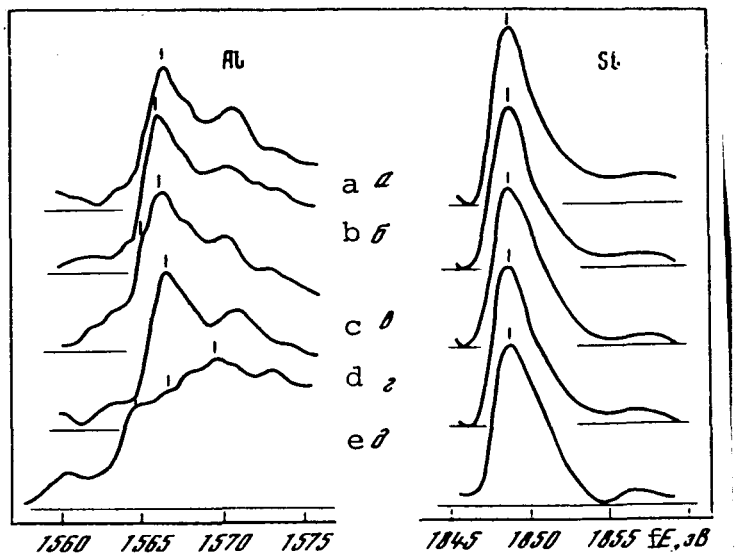

Fig. 37. K spectra of quantum yield of various glassy formations: ordinate, reduced intensity; abscissa, quantum yield energy; a. "Pele's Hair"; b. moldavite; c. Irigizite; d. basaltic glass; e. lunar black glass [47]

Key: f. E, eV

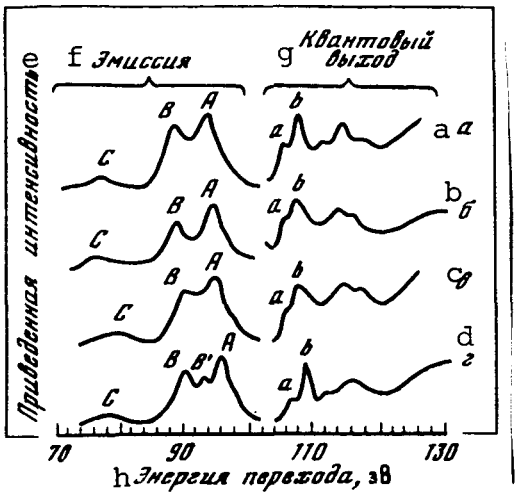

Fig. 38. $L_{II,III}$ spectra spectra of silicon: a. fused silica; b. indochinite; c. moldavite; d. Irgizite **[47]**

Key: e. reduced intensity; f. emission; g. quantum yield; h. transition energy, eV

The $L_{II,III}$ emission spectrum of /91
silicon in tektites is close in its double peaked configuration of the energy splitting of the maxima Δ(A-B) to the spectrum of quartz (Δ=5.5 eV) and the spectrum of breccia (Δ=4.8 eV). In moldavites, Δ=5.3 eV, but it is only 5.0 eV in Irgizites. This is evidence of a reduction in the degree of /92
covalence of the Si-O bond compared with that of quartz, but it is nevertheless higher here than in the breccias. The increase in ionicity of the Si-O bond is due to some increase in the distance between them and, besides, the quite discreet nature of coupling of the silicon-oxygen tetrahedra together and of their separateness. Such small energy splitting is evidence of a sharp difference of tektites in general and of Irgizites in particular from crystalline and glassy silicates, and it characterizes the formation of structures similar to chains with slight internal distortion of the tetrahedra.

The high energy maximum in the Irgizite spectra is slightly drawn out, and inner maximum B', inconspicuous in moldavite and indochinite and absent in lechatelierite and quartz glass, developed in the transition energy region (92.6 eV). This inner maximum formed in a strong inter-tetrahedral interaction of various tetrahedra with each other $[SiO_4]^{4-}$; $[AlO_4]^{5-}$, $[FeO_4]^{6-}$, **[62, 47, 54]**, which did not however distort their internal structure.

The quantum yield spectra of silicon in tektites, by the great splitting of maxima of a and c and their energy location, indicate its tetrahedral coordination. In the case of octahedral surroundings, these maxima would fuse together. In other words, the high degree of geometric idealization of tetrahedral groups $[SiO_4]^{4-}$, $[AlO_4]^{5-}$ and $[FeO_4]^{6-}$ characteristic of silicate melts at ultrahigh temperatures is characteristic of tektites in general and of Irgizites in particular. This results in their structural equivalence. Structural unification of the tetrahedra has the result that an extremely homogeneous substance is formed which, with a high silica content, makes tektites structurally analogous to pure quartz glass with its anomalously low thermal expansion and high heat conductivity, which is additionally provided by an acute deficit of alkali ions, which determine the heat conductivity effect in glasses.

c-2

IRON IN CALCINED CLAYS, ZHAMANSHINITES AND IRGIZITES

Nuclear gamma resonance (Mossbauer) spectra were taken of a number of samples sequentially replacing each other from calcined clays to Zhamanshinite impactites to Irgizite tektites, both undisturbed and subjected to melting and annealing (Fig. 39). In addition, the central parts of the spectra were taken with a stretched out velocity scale (Fig. 40), which permitted details of the spectra to be brought out.

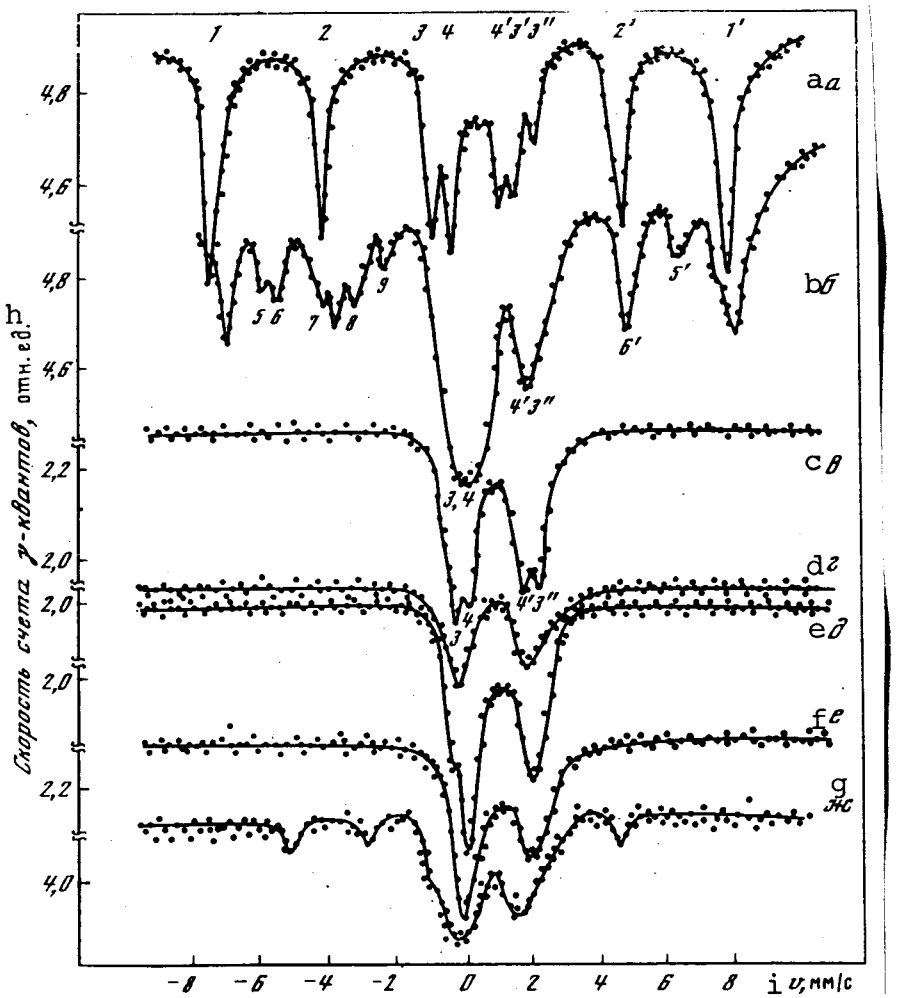

Fig. 39. Mossbauer spectra of samples from Zhamanshin natural landmark **[62]**: a. calcined clay; b. scoria; c, d. Zhamanshinites; e. Irgizites; f. Irgizite after heating to 950°C; g. Irgizite after melting at 1350°C.

Key: h. quantum count rate, rel. units; i. v, mm/s

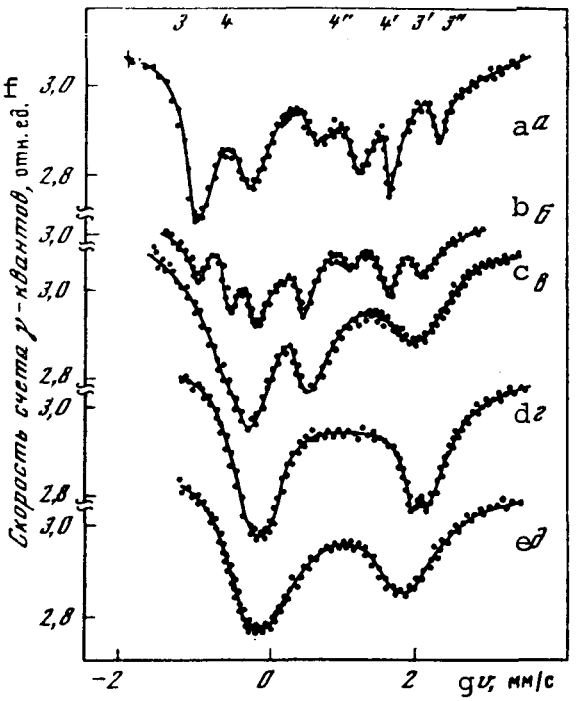

Fig. 40. Central portion of Mossbauer spectra of samples from Zhamanshin natural landmark with stretched out scale of movement rate of quantum source; designations same as in Fig. 39 **[62]**.

Key: f. quantum count rate, rel. units; g. v, mm/s

In Tertiary clays which are reddened because of calcining at the contact with Zhamanshinites, there is much trivalent iron, which is contained primarily in hematite (Fig. 39a, lines 1,2,3,3',2',1'; Fig. 40a, lines 3, 3'). The presence of hematite is indicated by the large effective magnetic field, which reaches 5.15 kOe. Besides, there is a subordinate amount of iron in calcined clays in the composition of silicates, but it is there basically in the divalent state (Fig. 39a, lines 3,4,4',3') and as an impurity in the trivalent state (Fig 39a, lines 4,4'). The ratio of the area of the spectrum which corresponds to hematite to the area of the silicate component is on the order of 3. This indicates prevalence of iron in the trivalent state in hematite over the divalent iron in silicates. It is evident from the Fig. 39 and 40 curves how sequentially hematite disappears initially and then trivalent iron in silicates in proportion to the change from calcined clays to Zhamanshinites and Irgizites. /93

The Zhamanshinite spectrum differs noticeably from the calcined clay spectra. In the least reworked Zhamanshinites, which contain xenoliths of reddened, swollen clays (see Fig. 39, 40a), trivalent iron still is present partly in oxides and partly in hydroxides (most resolved lines 5,6,7,8,9,5') but the silicate component still is predominant (lines 3,4,4',3'). In the majority of Zhamanshinites analyzed however (see Fig. 39, 40c, d), there either is no trivalent iron at all or it is present only in the silicates, without forming an independent compound with oxygen. It is thus evident from the series of spectra that, with change from calcined clays to Zhamanshinites, upon formation of the melt, trivalent iron is reduced from the oxides and then from the silicates, and all the iron is divalent and is entirely in the silicates in Zhamanshinites. /94

The Irgizite spectrum (see Fig. 39, 40e') is an asymmetric doublet with considerable 3-4 times broadening of the components compared with the apparatus line width. The left peak is more intense than the right peak, while the areas of both peaks are equal. The latter circumstance permits these two peaks to be considered a doublet with $\delta E \simeq 0.75$ and $\Delta E = 1.8$ mm/s, which is

characteristic of divalent iron, and not as the sum of unresolved spectra from the ions of di- and trivalent iron. Irgizites thus contain only divalent iron. Analogous spectra were observed in other previously studied tektites, indochinites, phillippinites, /95 etc. [92, 93].

The total absence of trivalent iron in tektites is particularly important, since it fundamentally separates from volcanic glasses, industrial slag and the majority of artificial glasses, although chemical analyses of tektites [130] showed only substantial prevalence of divalent over trivalent iron, which was validly considered a specific trait of tektites, differientiating them from ordinary rock. However, even such an amount of trivalent iron was previously considered to be the result of oxidation in the analysis process and not a property of tektites [13]. The total absence of trivalent iron in tektites and impactites is evidence of reducing conditions, which are characteristic the ultrahigh temperatures in a meteorite explosion. Evidently as a result of these conditions, in Irgizites and Zhamanshinites, titanium reduced to the trivalent state, which predetermined the formation of blue tektites and blue veins in Zhamanshinites, as well as chromium reduced to the divalent form, which were determined by Yu. P. Dikov, were formed.

The Mossbauer spectrum parameters of the silicate component (see Table 13) vary negligibly and correspond to the presence of divalent iron in octrahedral, although highly distorted coordination, in silicate chain type structures, in which the degree of distortion increases considerably toward Irgizites. This is reflected by broadening and fusing of the spectral lines. We note that, in well decrystallized and therefore ordered chain and insular silicates, in accordance with the two structural positions of divalent iron, the spectra consist of two doublets with distinct narrow lines $\Gamma_{1/2}$ 35 mm/s, in which [92] the slower the pyroxenes cooled during crystallation, the more ordered they are and the better resolved are these doublets in the spectra. In unordered substances such as glass, specific structural positions with long range order do not exist. In connection with this, the spectra are not resolved, but are the superposition of a large number of spectra with similar but different parameters, which causes line broadening. In exactly the same way (see Table 13), in the transition from pyroxenes to synthesized glasses of pyroxene composition or to the lunar regolith, only average parameters δE and ΔE are observed for the entire spectrum. This picture is reflected in the spectra of samples from Zhamanshin Crater (see Fig. 39, 40). For calcined clays, the spectrum of the silicate portion is represented by two doublets. Distinct splitting of the spectral lines also is observed in some of the least reworked Zhamanshinites. In the majority of Zhamanshinites and in all Irgizites however, there is no separation of the spectra in positions M_1 and M_2, and they are doublets with broadened lines. The latter reflects the existence in Irgizites of regions of only short range order, similar to that of the chain type of structure.

Still another difference of the tektite spectra from the spectra of crystalline chain silicates is asymmetry of the doublet component, caused by the fact that, in rapid cooling from high temperature in formation of the vitreous state, the closest metal-oxygen bonds are distinguished by both a diversity of distances and /96
a diversity of bond angles. Asymmetry of the spectra also was a characteristic feature of tektites, previously noted for indochinites, australites, phillippinites, etc. **[93]**. The decrease in magnitude of isomeric shifts of δE in Irgizites compared with pyroxenes (see Table 13) represents a higher degree of covalence of the Me-O bond, which also makes tektites unique formations. Yet even among tektites, Irgizites have a minimum isomeric shift, δE=0.71-0.79 m/s vs. Ø.88-Ø.92 m/s for indochinites and moldavites. A substantial increase of covalence of the bond of iron with oxygen is evidence that the normal octahedral coordination of iron, in chain silicates for example, is distorted because of the reduction of the distance of the bond with oxygen, and part of the iron-oxygen polyhedra is reformed into $[FeO_4]^{6-}$ tetrahedra, iron does not play the normal part of cation, but it forms an anion together with oxygen, a tetrahedron of $[SiO_4]^{4-}$, $[AlO_4]^{5-}$ type. Actually, the isomeric shift in Irgizites δE=Ø.71-Ø.79 mm/s which is close to that of staurolite, for iron has a tetrahedral surround of oxygen as well as other high spin tetrahedral compounds of divalent iron. The tetrahedral surround of iron is formed with a severe deficiency of silica for saturation of the cations, which can be with high alkalinity of the melt. The octahedral surround of iron is distorted in this case and it also forms a tetrahedron. Yet, there is a severe deficit of alkali in tektites. The unusual behavior of iron therefore requires a different explanation. It should most likely be sought in the formation of short range order under high temperature conditions, when the anion function of the tetrahedral cations (silicon, aluminum and iron) is unified.

In such a melt (with anion abundance) of negatively charged tetrahedra and with a significant deficit of cations, the only cation capable of stabilizing such a stressed structure is calcium, of which there actually is unusually much in tektites (3-4%). However, high calcium glasses are extremely stable chemically, they do not decrystalize, have low viscosity at high temperatures, and have high heat conductivity and low surface tension. They differ in this from alkali glasses, which are viscous even at high temperatures and therefore usually do not form drops, but pumice.

Apparently because of the octahedral surround and the cation bond with oxygen, iron is extremely stable in tektites. After annealing at T=950°C and open cooling in air, neither oxidation nor the liberation of metallic iron occurred. The spectrum of such a calcined Irgizite (see Fig. 39, 40f) is practically identical to the spectrum of Irgizite before annealing (see Fig. 39, 40e). Only by annealing indochinites in a hydrogen atmosphere at 950°C for twelve hours, was negligible liberation of metallic iron noted **[93]**. After softening at 1350°C, when the Irgizites were converted to an extremely viscous mass and open cooling in air, the value of

effect ε decreased sharply (from 4-6% in the initial state to 8% after softening). The central part of the spectrum remains similar, but it became "smeared out" and small peaks appeared on /97
the limbs in the region of velocities characteristic of the metallic iron lines, which were thus singled out. However, calculation of the areas of the spectra shows that the assumption of the appearance of metallic iron and a reduction of the number of divalent iron ions because of this does not entirely fit into the observed decrease in the effect. It evidently reflects abrupt disordering in tektites upon softening and as a consequence an increase in the root mean displacement of the iron atoms in the structure.

It follows from the studies, the results which are presented above, that first there is no trivalent iron in tektites. All the iron is divalent. More than that, titanium and chromium can be present in reduced forms. In this case, a covalent bond of iron with oxygen and a tetrahedral surround are formed. Second, tektites are distinguished by extreme mixing and unification of the tetrahedral $[SiO_4]^{4-}$, $[AlO_4]^{5-}$ and $[FeO_4]^{6-}$ oxy groups. The features specified which are characteristic of low viscosity melts at ultrahigh temperatures should disappear in slow hardening. In impactites therefore, which harden slowly, an octahedron surround of iron forms and pyroxene microliths are present in them. The iron is partly oxidized and forms magnetite. More than that, the $[SiO_4]^{4-}$ and the $[AlO_4]^{5-}$ tetrahedra are combined in skeleton structures connecting with alkali elements, and plagioclase microliths form. There is none of this in tektites.

The causes of fixation in tektites of a structure characteristic of only an ultrahigh temperature melt should be sought in extremely rapid hardening, practically quenching, which probably occurred as they fell to the surface of the earth. In rapid cooling of the majority of glasses with a high alkali content, they crack and disintegrate. An exception, because of increased heat conductivity and stability, is only alkali free, high silicon, high calcium glasses, the structures of which are similar to the structure of pure quartz glass. Tektites are just such noncracking glasses.

CONCLUSION: GENETIC CAUSES OF TEKTITE UNIFORMITY

Tektites, independently of site and geologic age, have a /98
stable unified composition, an excess of silica (70-75%), unusually much Al_2O_3, CaO, and FeO for acid terrestrial magmas and severely deficient K_2O and Na_2O (tektites fundamentally differ from other terrestrial glasses by this). Their structural and chemical features are still more unusual and unique. The question of their origin probably lies precisely in the unity of composition and structure of tektites. Such specific limitations on variation of composition and its specificity undoubtedly is evidence of unity of the features of their formation.

The majority of investigators after L.J. Spencer **[125]** think that the formation of tektites most likely is the result of an explosion caused by the impact of a gigantic meteorite. The temperature reaches several thousand degrees in the inner zone of such an explosion, and both the meteorite and substantial masses of earth matter are not only melted but are vaporized. The pressure in the inner zone of the explosion exceeds hundreds of kilobars and reaches megabars and, upon removal of it, additional melting of the target rock and formation of specific minerals occur.

However, none of the known tektites are connected unambiguously in space with known meteor craters. The only exception is the Irgizite tektites described here from Zhamanshin meteor crater. In the region of the crater, the upper 200 m is made up of sedimentary rocks of Mesozoic and Cenozoic ages, which underlie dislocated igneous and metamorphic basement rocks. The 5.5 km diameter crater is surrounded by an eroded wall up to 3 km wide. From seismic data and calculation, the crater depth is 0.7 km, the amount of material ejected is 10^9 tons and the mass of remelted matter is 10^7-10^8 tons. The upper part of the wall is formed of allogenic breccia, which is made up of mixed loose Mesozoic and Cenozoic formations and fragments of the basement rock. Impact glasses of diverse composition and structure occur among the breccias and directly in the bedrock. They form a specific series from the target rock to hardened impact melts. Reddened calcined clays, black scorias, porous and dense glasses, lumps of lechatelierite and finally Irgizite tektites, which have hardened in the form of glassy drops and sprays, although differentiated from impactites by a quite sharp difference in properties, composition and structure, are found here. The Irgizites are from 1-3 mm to 2-3 mm in size, and the weight is approximately 0.6 g. Their surfaces are shiny, lustrous and frequently contain minute glassy globules adhering to them. The Irgizite glass has a 1.509 index of refraction, and it is devoid of microliths and flow structure due to impurities. The Irgizites are /99 concentrated only in an area of 1-2 km^2 in the southeast of the crater. Their total number is 10^7-10^8 and the total weight is tens of tons. The ages of the Irgizites and impactites, determined by geological, geomorphological, paleomagnetic, isotope and fission track methods, are $(0.9\text{-}0.85)\cdot 10^6$ years **[46, 48]**. The ages of the tektites and microtektites from the Australasian scattering field, like the age of Darwin Crater in Tasmania, is $0.7\cdot 10^6$ years, i.e., all these formations may prove to be synchronous. All the above mentioned permits Irgizites to be considered a standard for study of the question of tektite formation and the problem of differentiation of the matter of the planet in the early stages of genesis of the planet connected with it.

The droplets are divided into two separate groups by chemical composition **[42, 43, 57]**: of basic composition containing only 54.4% silica, similar to Zhamanshinite impactites; acid, characteristic of Irgizites which correspond to tektites in composition.

Irgizites fundamentally differ from igneous rocks by a low alkali and increased CaO and MgO content, as well as by the presence of only divalent iron, a substantial portion of which forms tetrahedra with oxygen **[62, 47, 54]**.

The vaporization of mobile elements, among which alkalis are the most noticeable, which is characteristic of extremely high temperature melts, results in a radical change of their composition **[41-43, 145]**. This was established for the lunar regolith **[77]**. Irgizites evidently are the result of such evolution. The reduced amount of alkalis and the increased K/Na ratio are evidence of their thorough high temperature reworking. More than that, it is not excluded that, at the time of the explosion in the fireball, matter was in a state of silicate aerosol or even partly as vapors, which later were combined into larger silicate drops. This was proposed in the study of moldavites **[85]**. The microgranular structure of Irgizites is evidence in favor of this hypothesis. In observations in the scanning electron microscope and in delicate microchemical studies, it was determined that Irgizites were formed from minute (less than a micron) spherical particles, sometimes consisting of 80-90% silica and the glass cementing them, which is rich in aluminum and alkalis, which possibly condensed in the process of subsequent cooling of the fireball. These phenomena naturally resulted in the mixing of matter and unification of the glass composition. The primary glasses were most likely sprays and even fragments of hardened glass which escaped from the crater.

There may be traces of melting in glass of any origin, and the features of chemical composition also ambiguously indicate the genesis of tektites. The most fundamental features of tektites, which are practically unreproducible under other conditions than high temperature explosion, consist of their microstructure, the state of grouping of the atoms, of the atoms themselves and of /100 their electron shells. This was studied by Yu.P. Dikov by X-ray spectroscopy methods **[47, 54]**.

The quantum yield K spectra (see Fig. 37) and $L_{II,III}$ emission spectra of the silicon of Irgizites and other tektites (see Fig. 38) were taken.

A 10-15% narrowing of the maximum of the quantum yield K spectra of silicon and aluminum compared with albite glasses, as well as constant location of the maxima of 1848.8 eV for silicon and 1566.9 eV for aluminum are characteristic of different tektites. This is evidence of the idealization and separateness of the tetrahedra, i.e., of the absence of crystallization effects in tektites. Tektites are therefore characterized by an extremely high degree of vitrification and minimum interaction of dissimilar structural units, which is characteristic of a high temperature melt and could only be preserved at ordinary temperatures as a result of the very rapid cooling of quenching.

The $L_{II,III}$ emission spectrum of tektite silicon is distinguished by a pronounced double peaked configuration in the high energy portion, similar to the lechatelierite and artificial quartz glass spectra. There are differences in the spectra however. First, the reduction of energy splitting of the basic maxima indicates an increase of ionicity of the Si-O bond and a reduction of the distances between them, as well as of quite discrete coupling of the silicon and oxygen tetrahedra and of their separateness. Second, the high temperature maximum in the Irgizite spectra is slightly drawn out, and internal maximum B developed in a strong interaction of different tetrahedra with each other, which did not distort their internal structure.

The quantum yield spectrum of silicon in tektites, by the large splitting of a and c maxima and their energy position, indicate only tetrahedral coordination and its covalent bonding with oxygen. In other words, for tektites in general and Irgizites in particular, unification of different tetrahedral oxy groups $[SiO_4]^{4-}$, $[AlO_4]^{5-}$ and $[FeO_4]^{6-}$, which are structurally indistinguishable, is characteristic. In this case, the interaction of the tetrahedra does not affect the interaction of the ions within the tetrahedra or the configurations of the tetrahedra themselves, which practically do not interact with cations. This nature of the bond with a high silica content makes tektites structurally similar to pure quartz glass with its anomalously low thermal expansion. The latter would increase sharply if Na and K (which were vaporized from the tektites) would actively interact with the tetrahedra. The cations present evidently lost electrons at high temperatures and their atoms apparently acquired the configuration of inert gas atoms and do not distort the tetrahedra.

A scheme of formation of tektites in the explosion at the time of impact of a gigantic meteorite can be constructed from the characteristics found of atomic and molecular structure of tektites. The explosion should have been sufficiently strong for the melting which occurred to result in the formation of substantial volumes of melt. The crater in such an explosion should have been at least 1-3 km and the explosion energy more than 10^{25} ergs.

The initial material should be quite rich in SiO_2, which is close to granitoids. The initial material for Irgizites in Zhamanshin Crater could have been sedimentary rocks and metamorphic schists. /101

At the time of an explosion, the target rocks are melted and mixed and partly ejected, and they are therefore subjected to selective vaporization of the mobile elements. In distinction from igneous melts, the temperature of which is approximately a thousand degrees, impact melts are heated to several thousand degrees. The following occur in this case:

1. dehydration and unification of the melt;
2. selective vaporization of mobile elements, primarily alkalis;
3. change of trivalent iron to divalent;
4. shortening of the Fe-O bond distance and formation of tetrahedral surroundings;
5. mixing and unification of tetrahedral oxy groups;
6. idealization of the tetrahedra and formation of extremely isotropic glass **[136]**.

Far from all the features listed can form however in complex melt masses, and a finely divided state of matter in the region in the explosion is necessary for their formation. The molten, vaporized and shock wave ejected matter mixes in the turbulent cloud. Substantial selective vaporization, thorough mixing and unification of the target and meteorite matter are possible only in the finely divided state. Silicate aerosols and vapors in the incandescent cloud can be transported considerable distances from the explosion site. During cooling of the cloud, condensation of the silicate vapors and conglomeration, accretion of the droplets as a result of electrostatic forces occurred, after which the droplets fell to the ground like a silicate rain or shower. They could have fallen out at different places at different distances. Upon falling to the earth, the glassy drops rapidly hardened and probably at just that time acquired their partly fused shape. The features of tektites disappear upon slow hardening and in impactites, therefore, which harden relatively slowly, the octahedral surroundings of the iron forms even if partly and pyroxene microliths are present. The iron is even partly oxidized and forms magnetite. More than that, the $[SiO_4]^{4-}$ and $[AlO_4]^{5-}$ tetrahedra in impactites are joined in a skeleton structure and, by combining with alkalis, form feldspar microliths (there is none of this in conventional tektites).

QUENCHING

The abovementioned features of high temperature melts can be preserved only by instantaneous cooling. It occurs when tektites fall out of the fireball and pass through the atmosphere. Precisely because of quenching, tektites have the properties of a high temperature melt. In rapid cooling however, the majority of the glasses formed in the explosion, especially those with a high alkali content, crack and disintegrate because of the low thermal expansion. Only alkali free high silica glasses, the structure of which is similar to the structure of quartz glass, have high heat conductivity, low thermal expansion and are preserved in rapid cooling. Tektites are just such crack resistant glasses.

None of the intraplanet processes, which are distinguished by long and gradual evolution, provide the conditions necessary for the development of tektites: extremely high temperatures; low pressure; short time; one time action. Tektites could only be formed and preserved by a combination of quite unique events successively replacing each other, which led to multistage separation and unification of tektite structure and composition:

the impact of a gigantic meteorite among high silica rocks; differentiation in the melting process; selective vaporization; transport of silicate vapors and aerosol; their partial condensation and separation in the quenching process at the time of impact on the surface of the earth.

PLATE 1

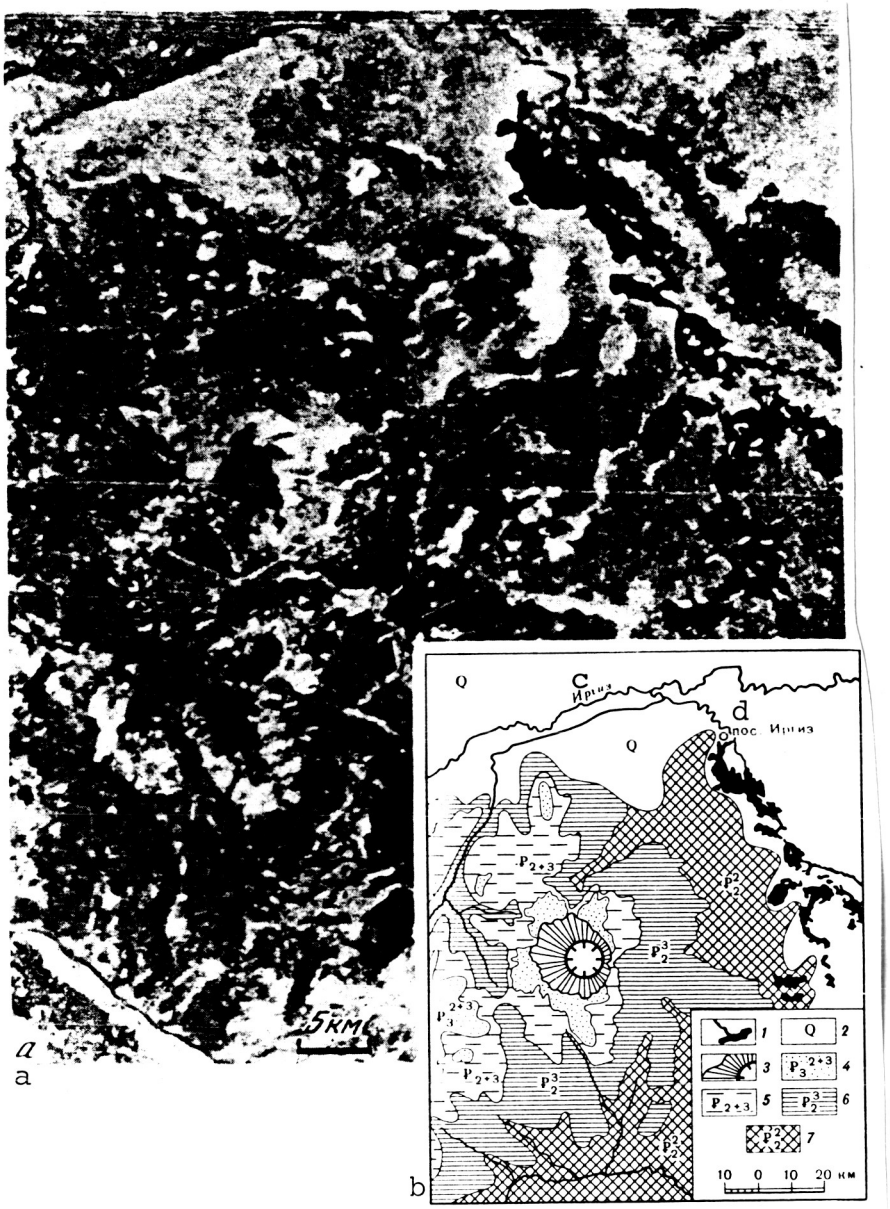

Zhamanshin meteor crater region: a. Photograph made in 1975 summer from Salyut-4 orbital space station by cosmonauts P.I. Klimuk and V.I. Sevast'yanov [46]; b. diagram of geologic-geographic interpretation of the space photograph; 1. rivers and lakes; 2. Quaternary deposits; 3. crater rim and wall deposits; 4. Chagray and Chiliktin series of Middle and Upper Oligocene; 5. Chegan series of Upper Eocene-Lower Oligocene; 6. Saksaul series of Upper Eocene; 7. Tasaran series of Middle Eocene.

Key: c. Irgiz; d. Irgiz settlement

PLATE 2

a. Superposition of allogenic breccia, dark due to presence of Paleozoic rock fragments, on light Tertiary clays; southeastern part of wall, Irgizite field; b. aerial photographs; dark is hills remaining of allogenic breccia; light is Tertiary deposits underlying it in northwestern part of wall.

PLATE 3

a. Block of Paleozoic rock split and raised to surface in northwestern part of crater; b. stratum of split Paleozoic sandstones (southern vicinity of crater); c. brecciated quartz vein containing planar elements, isotropized quartz, coesite and stishovite; d. brecciated Paleozoic limestones.

PLATE 4

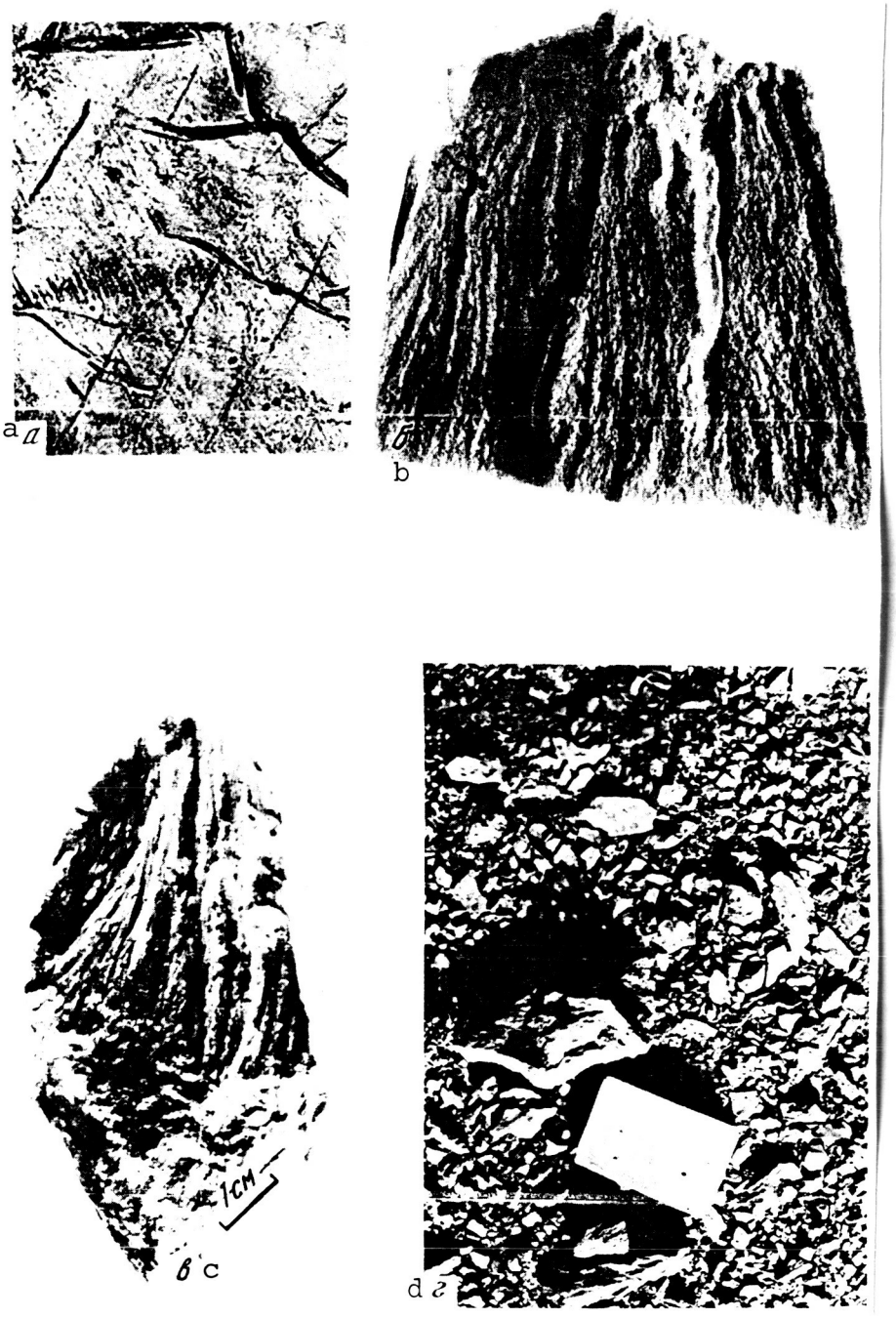

a. Planar elements in quartz (N. Short photograph); b. "horsetail" type chip from Upper Paleozoic volcanogenic sedimentary rock from southeastern part of wall; c. shatter cone of Paleozoic limestone rubble from Upper Paleozoic conglomerate; d. typical surface of north wall, clay and sand blown out of its allogenic breccia and surface enriched in fragments of Lower Paleozoic rock, among which shatter cones and "horsetail" type chips are seen.

PLATE 5

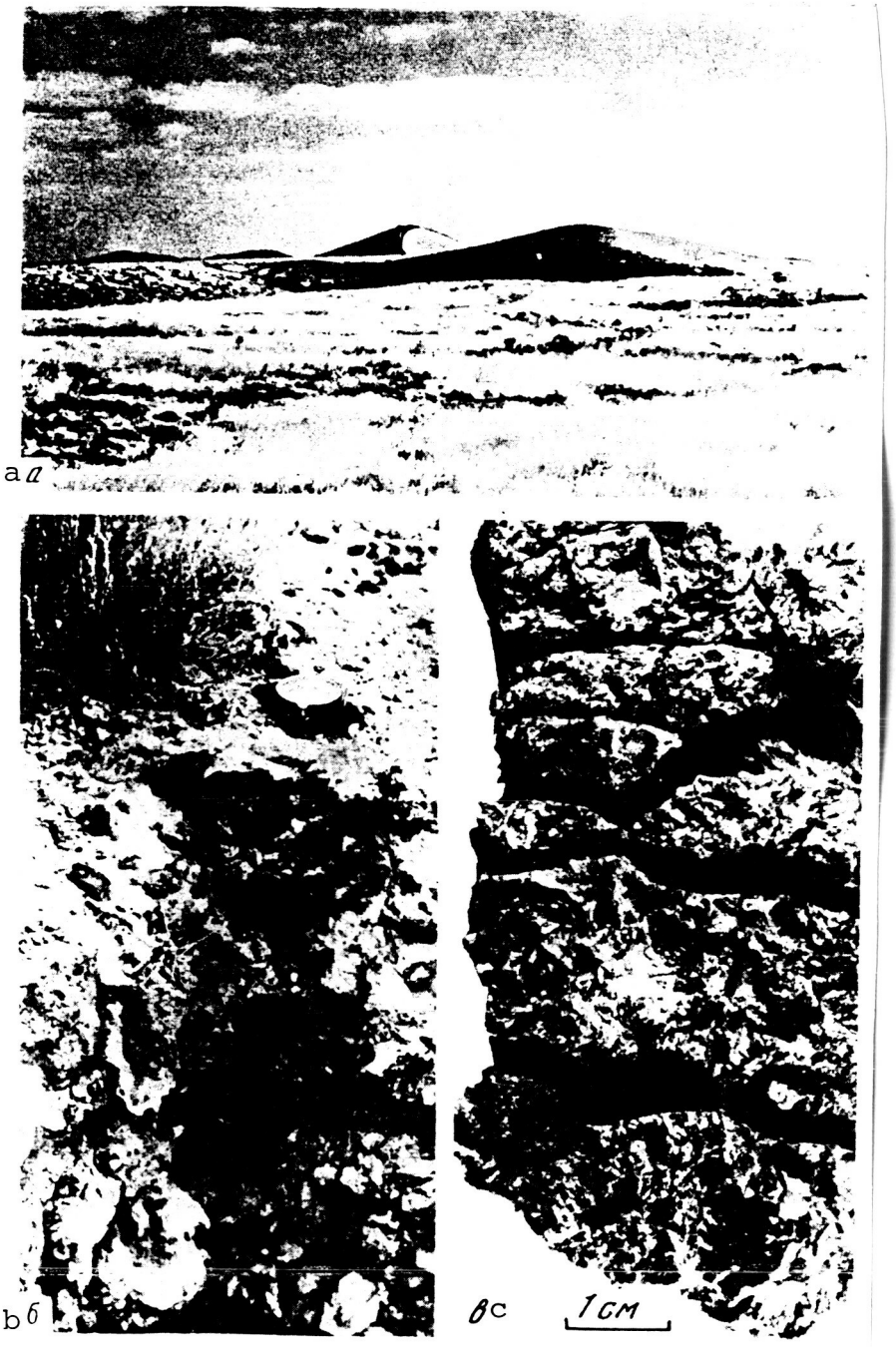

a. West side of cone shaped hill on east slope of crater turned toward crater, covered with dark ignimbrite-like Zhamanshinites, bedded on light Tertiary clays (view from south); b. melt (Zhamanshinite) penetrating fracture in Tertiary clays (north side of crater); c. Zhamanshinite bomb with disintegrated "breadcrust" (full size).

PLATE 6

a. Aerial photograph of three separate circular structures south of Zhamanshin Crater, probably of impact origin; b. aerial photograph of circular structure south of Zhamanshin Crater, probably of impact origin; c. aerial photograph of two contacting circular structures southeast of Zhamanshin Crater [46].

PLATE 7

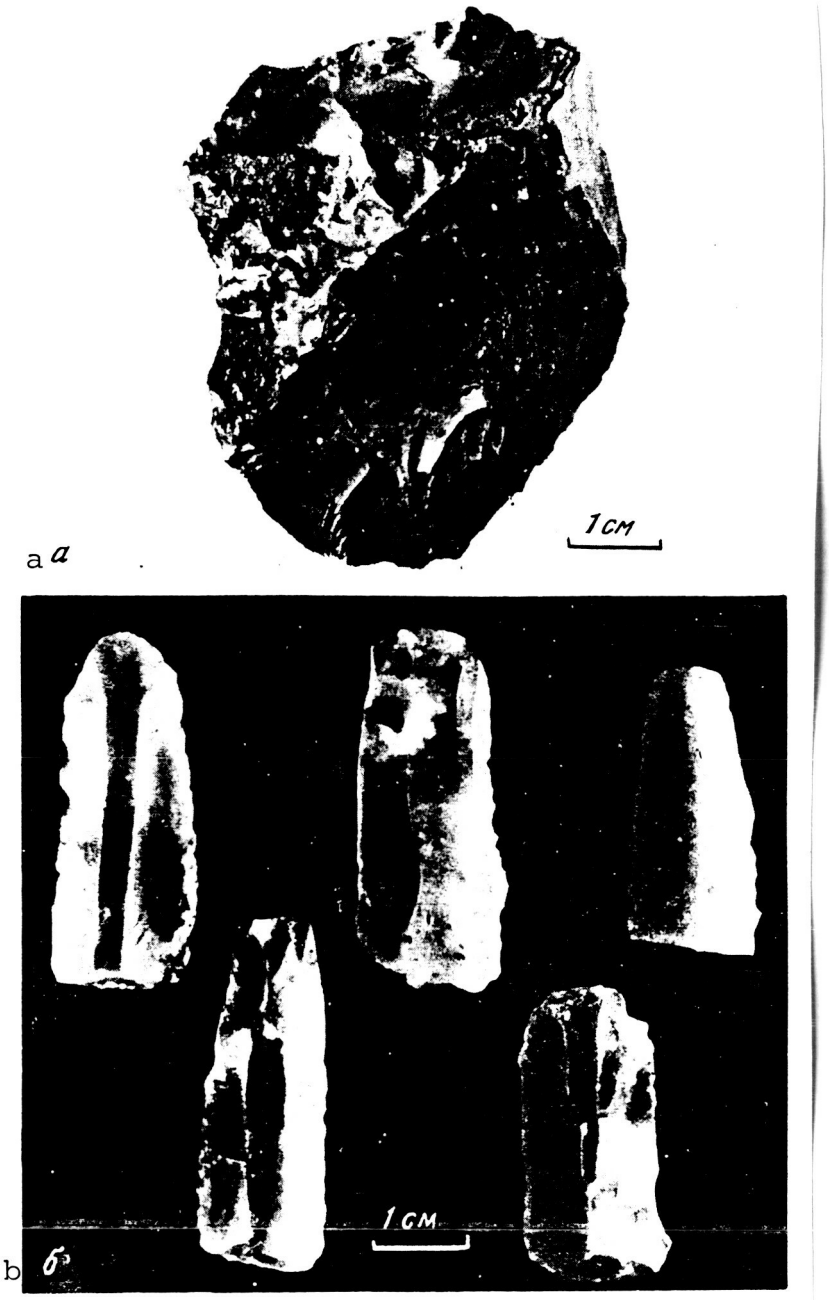

Stone tools found in Zhamanshin Crater: a. Paleolithic chopper; b. Neolithic flint spear tips and scrapers.

PLATE 8

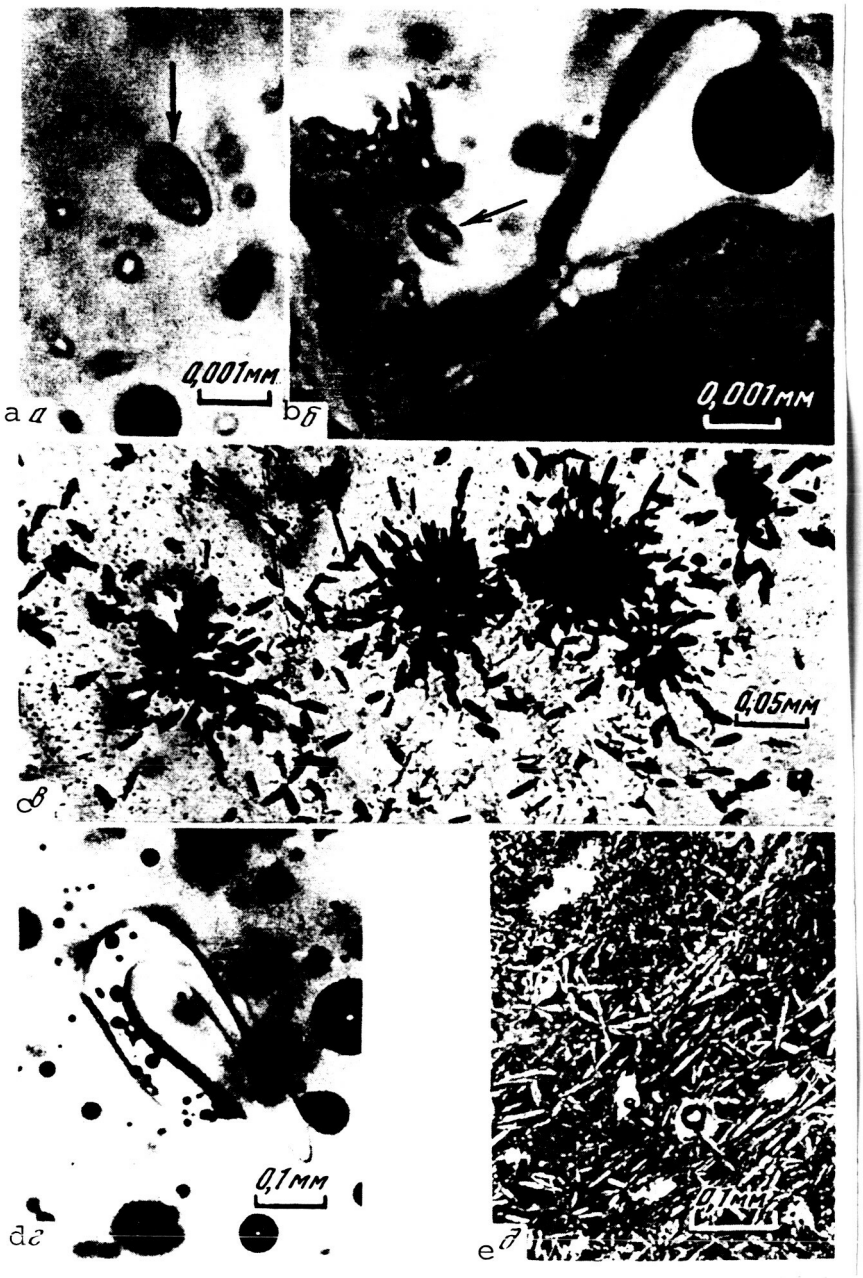

a,b. Tracks of spontaneous fission of uranium in Zhamanshinite, V. P. Perelygin microphotograph; c. local track clusters in Dacron film applied to Zhamanshinite after irradiation with thermal neutrons reflect local increase of uranium content (V.P. Perelygin microphotograph); d. lechatelierite inclusion in Zhamanshinite (Yu.F. Pogrebnyak microphotograph); e. dark, basalt-like impactites with plagioclase microliths and bubbles (N. Short micrograph).

PLATE 9

Microphotograph of polished section of drop-shaped 10 mm long irgizite with flow texture, due to nonuniform distribution of brown color; bubbles (white), ore inclusions (black) and light glass particles captured during growth process are seen; they are spherical along edges but deformed inside the irgizite.

PLATE 10

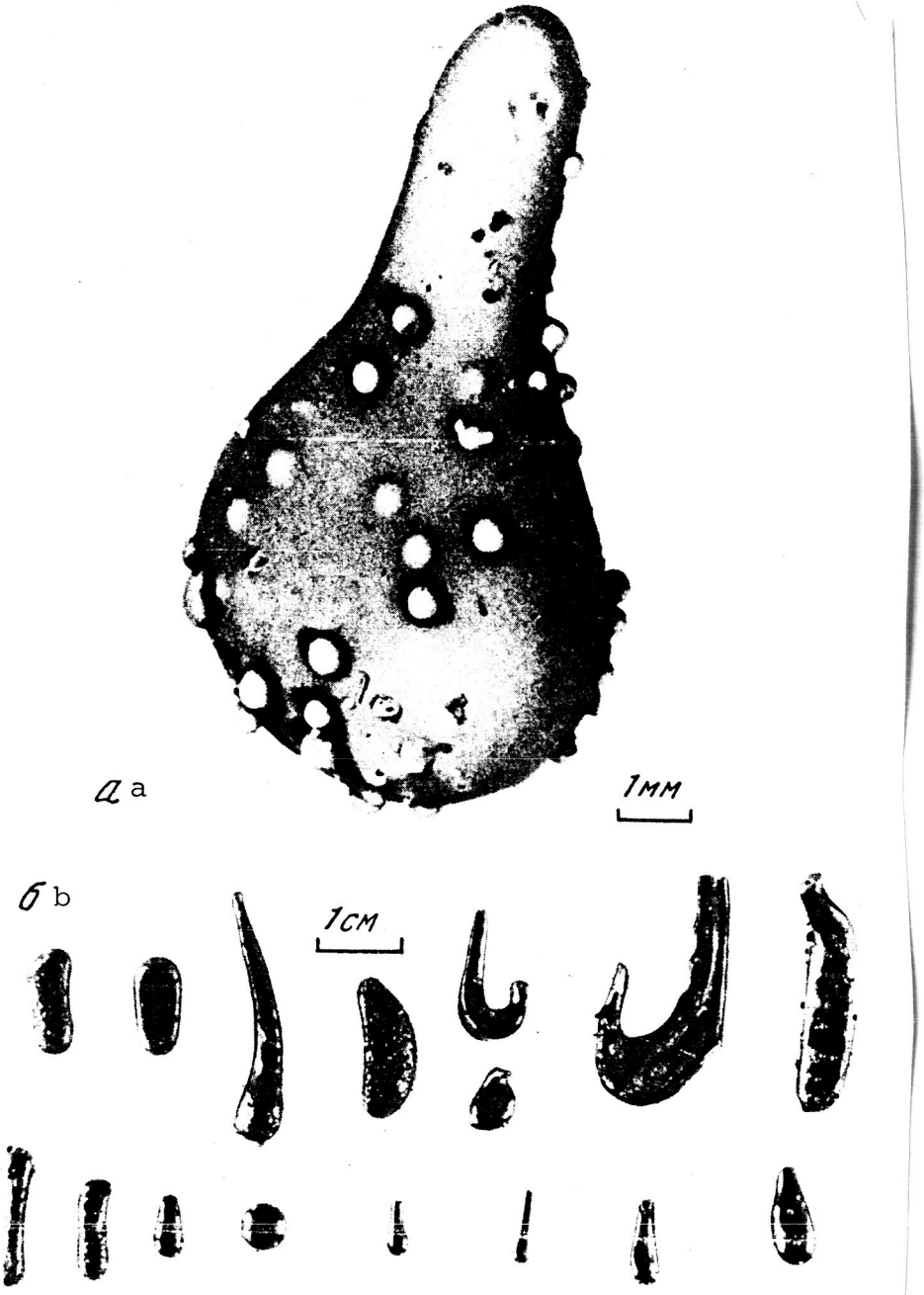

a. Drop-shaped irgizite with spherical particles captured during formation process; sputtered with magnesia before photographing, highly magnified; b. drop-shaped irgizites with shiny surfaces, full size.

PLATE 11

Irgizites (sputtered with magnesia before photographing): a-d. round, drop-shaped and dumbbell shapes with smooth surfaces; e-i. complex shapes with spherical glassy droplets which adhered and were captured during formation.

PLATE 12

Irgizites (sputtered with magnesia before photographing): a,b. complex crumpled shapes with adhering glass droplets; c. twisted conical fragments with internal sculpture found by dissolving; d-f. large fragments with twisted surfaces.

PLATE 13

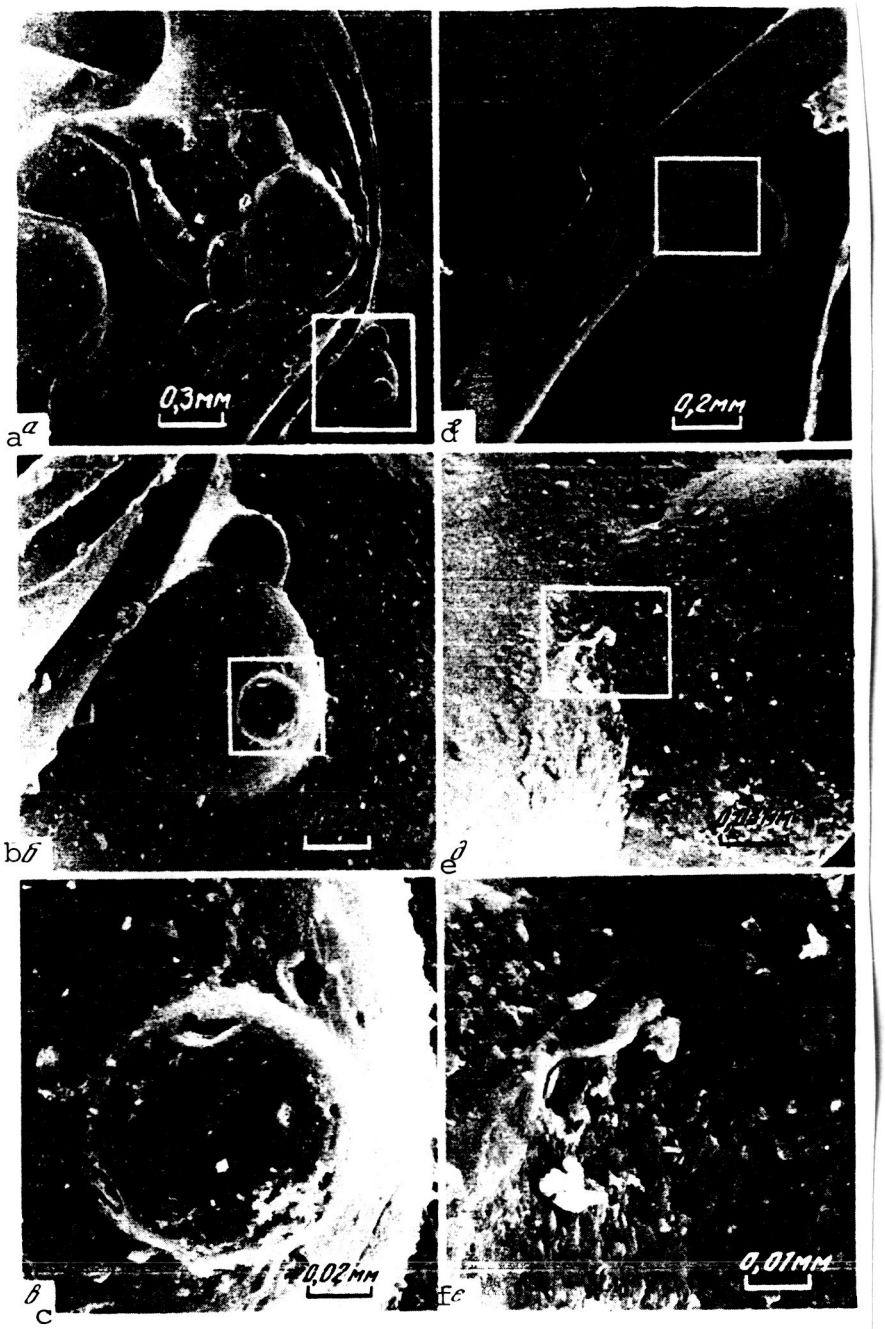

Scanning microphotographs of Irgizites of complex shapes and glassy fibers and spherical droplets adhering to them: spherical droplet (a) to which tiny spherical droplets (b) have adhered; their surfaces disturbed by microcraters (c); two spherical droplets adhered to fiber (d); glass is flaked at point of adhesion (e,f).

PLATE 14

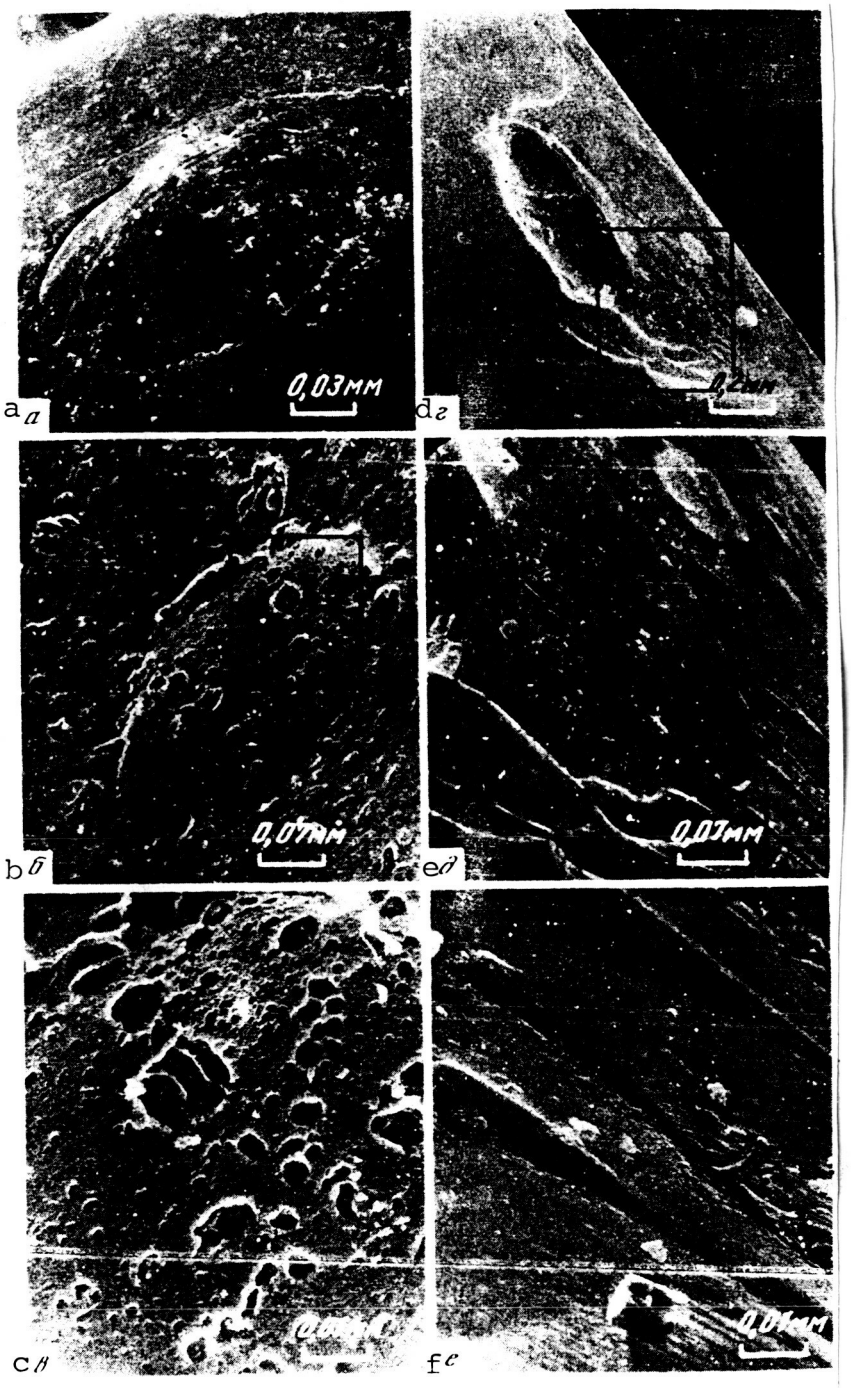

Scanning microphotographs of glassy spheres (a,b) captured by Irgizite in formation process; particles captured by it (c) seen on surface of sphere; scanning microphotographs of craters formed after hardening of Irgizites by cracking; conchoidal fractures formed along its edges (e,f).

PLATE 15

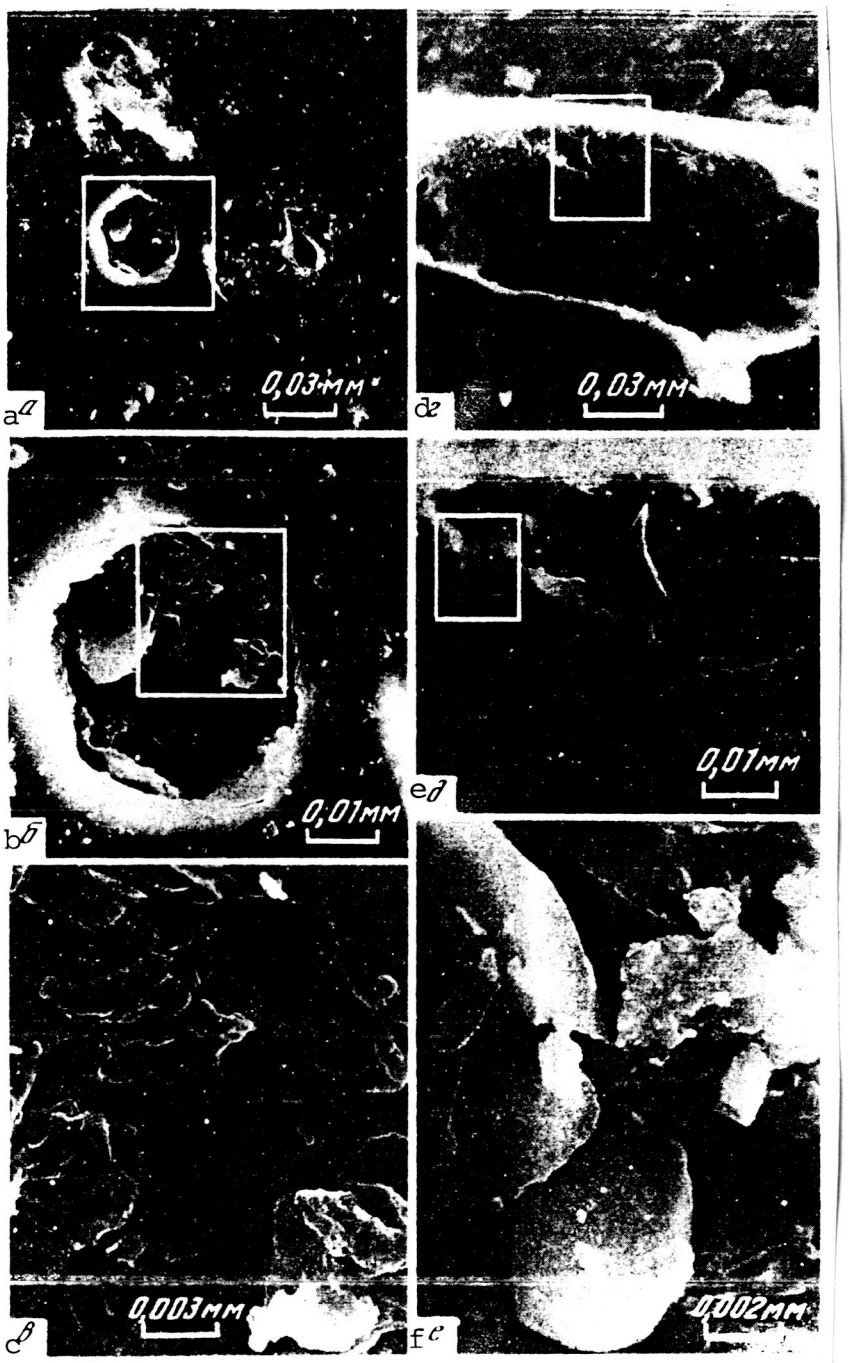

Scanning microphotographs of Irgizites and microcraters on their surfaces formed by explosion of bubbles in initial hardening of glass; in plan view microphotograph (a), glass in microcrater at start of hardening and flaked off (b,c); in perspective view photograph (d) of another microcrater, glass was partly viscous in explosion and formed fibers, but hardened in places and formed conchoidal chips (e); process accompanied by flaking (f).

PLATE 16

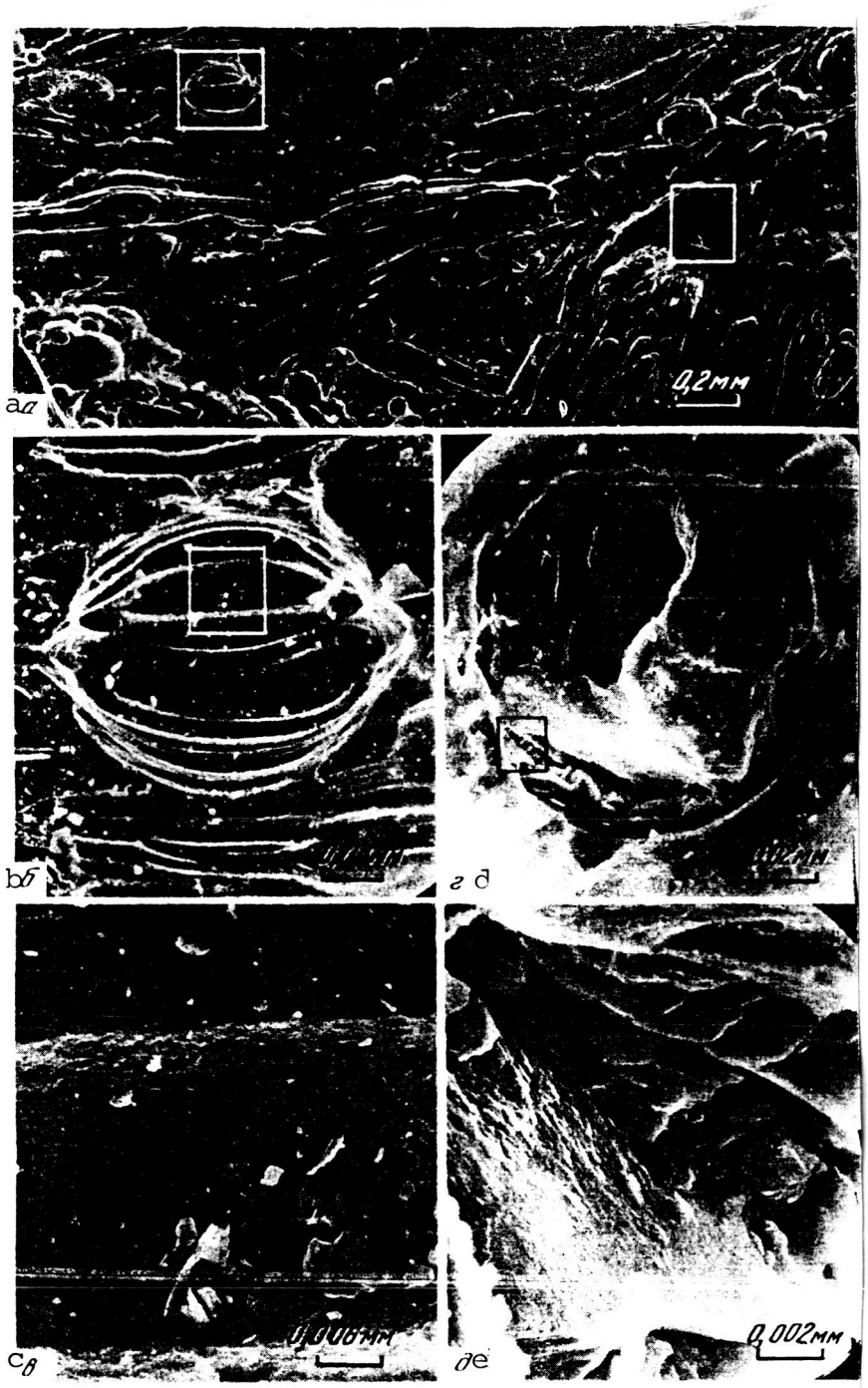

Irgizite with heavily dissolved surface, which brought out details of its inner structure (a): visible are captured spherical droplets, fibrous structure, fibers bend around bubble (b), their surfaces slightly flaked (c), foreign particles also captured (d). at contact with glass cracked (e).

REFERENCES

1. Aaloe, A.O., "Impact meteor craters," Meteoritika 31, 68-73 (1972).

2. Aaloe, A.O., A.I. Dabizha, B. Karnaukh and V. Starodubtsev, "Geophysical studies in Main Kaali Crater," Izv. AN ESSR. Khimiya, geoloogiya 25/1, 58-65 (1976).

3. Aaloe, A.O., V.A. Korchemagin, Ye.G. Osadchiy and V.I. Tsvetkov, "Some features of fracturing in the craters of the Sikhote-Alin meteor shower," DAN SSSR 215/2, 409-412 (1974).

4. Andrieux, P. and J.F. Clark, "Application of electrical prospecting methods to study of Holleford Crater," Canadian J. Earth Sci. 6/6, 1325-1337 (1969).

5. Baldwin, R.B., "Relationships among crater parameters," in the book Vzryvnyye kratery na Zemle i planetakh [Explosive Craters on the Earth and Planets], Mir Press, Moscow, 1968, p. 222-246.

6. Barringer, D.M., "Coon Mountain and its crater," Proc. Acad. Natur. Sci. 57, 861-866 (1905).

7. Beals, C.S., "The identification of ancient craters," Ann. N.Y. Acad. Sci. 123, 904-914 (1965).

8. Beals, C.S. and M.J.S. Innes, "Identification of ancient meteor craters," Meteoritika 25, 3-39 (1964).

9. Benevolenskiy, A.M., "The role of cumulative processes in the formation of circular lunar mountains," Byul. VAGO 30(37), 20-27 (1962).

10. Bjork, R.L., "Analyses of the formation of meteor craters," J. Geophys. Res. 66/10, (1961).

11. Boon, J.D. and C.C. Albritton, "Established and supposed examples of meteoritic craters and structures," Field and Lab. 5/1, (1936); 5/2, 53-64 (1937); 6/2, 44-56 (1938).

12. Boytsova, Ye.P., Ye.A. Mazina, B.M. Mikhaylov and N.K. Ovechkin, "Geology of the southwestern part of the Turgay Depression," Tr. VSEGEI. Nov. ser. 5, 156 pp (1955).

13. Chao, E., "Petrographic properties of tektites," in the book Tektity [Tektites], Mir Press, Moscow, 1966, pp. 78-136.

14. Chao, E.C.T., "Pressure and temperature histories of impact metamorphosed rocks -- based on petrographic observation," Neues Jahrb. Miner. 108/3, 209-246 (1968).

15. Charters, A.C., "High-speed impact," Sci. Amer. 203/4, 128-140 (1960).

16. Classen, J., "Discovery of new tektite occurrence," Naturwiss. Rndsch. 29/5, 172 (1976).

17. Classen, J., "Catalogue of 230 certain, probable, possible and doubtful impact structures," Meteoritics 12/1, 61-68 (1977).

18. Crook, K.A.W. and P.J. Cook, "Origin of Gosses Bluff," J. Geol. Soc. Austral. 13/2, 495-516 (1966).

19. Dabizha, A.I., "New interpretation of meteor crater structure," Astron. vestn. 11/2, 23-77 (1977).

20. Dabizha, A.I., "'Deficient' mass of terrestrial and lunar craters," DAN SSSR 241/3, 559-562 (1978).

21. Dabizha, A.I., M.S. Anuchin, V.V. Fedynskiy and V.R. Melikhov, "Circular structures of central part of Russian platform," Meteoritika 34, 88-91 (1975).

22. Dabizha, A.I. and V.V. Fedynskiy, "Characteristics of the gravity fields of astroblems," Meteoritika 36, 113-119 (1977).

23. Dabizha, A.I. and B.A. Ivanov, "Geophysical model of meteor crater structure and some questions of crater formation mechanics," Meteoritika 37, 160-167 (1978).

24. Dabizha, A.I., M.S. Krass and V.V. Fedynskiy, "Evolution of meteor craters as structures of the planetary crust," Astron. vestn. 10/1, 6-18 (1976).

25. Danon, I., "Metals, alloys and inorganic compounds," in the book Khimicheskiye primeneniya myessbauerovskoy spektroskopii [Chemical Applications of Mössbauer Spectroscopy], Mir Press, Moscow, 1970, p. 130-212.

26. David, E.G.H., "Flight of tectites from meteorite impact," Z. Naturforsch. 21a, 1133-1137 (1978).

27. Dence, M.R., R.A.F. Grieve and P.B. Robertson, "Terrestrial impact structures: principal characteristics and energy considerations," in the book Impact and Explosion Cratering, Pergamon Press, New York, 1977, p. 247-275.

28. Dick, W. and H. Gris, "Nuclear war destroyed an ancient planet -- survivors landed on Earth," National Enquirer, 14 Oct. 1975.

29. Dietz, R.S., "Astroblems: ancient structures on the earth, formed by meteorite impacts," in the book Vzryvnyye kratery

na Zemle i planetakh [Explosive Structures on the Earth and Planets], Mir Press, Moscow, 1968, p. 153-173.

30. Dietz, R.S., "Elgygytgyn crater, Siberia: probable source of Australasian tectite field (and bediasites from Popigai)," Meteoritics 12/2, 145-157 (1977).

31. Dikov, Yu.P., I.A. Brytov, Yu.N. Romashchenko and S.P. Dolin, Osobennosti elektronnogo stroyeniya silikatov [Characteristics of Electronic Structure of Silicates], Nauka Press, Moscow, 1979, 128 pp.

32. Dikov, Yu.P., A.A. Levin, E.J. Debolski, S.P. Dolin and G.A. Brytov, "Molecular orbitals of Si_2O_5 and mixed (B, Al? P, $Si)_n$ on clusters: an approach to the electronic structure and X-ray spectroscopy data of silicates," J.Phys. and Chem. Miner. 1/1, 27-41 (1977).

33. Ehmann, W.D., W.B. Stroube Jr., M.Z. Ali and T.I.M. Hossain, "Zhamanshin crater glasses: chemical composition and comparison with tectites," Meteoritics 12/3, 212-214 (1977).

34. Engelhardt, W.V., "Meteor craters," Naturwissenschaften 61/10, 13-42 (1974).

35. Engelhardt, W.V., J. Arndt, D. Stöffler et al, "Diaplectic glasses in breccia of Nordlinger Ries as indication of impact metamorphosis," Contribs. Mineral. and Petrol. 15/1, 93-102 (1967).

36. Ernston, K., "The structure of Ries Crater from geoelectric depth soundings," Z. Geophys. 40/5, 639-659 (1974).

37. Fedynskiy, V.V., A.I. Dabizha and I.T. Zotkin, "Size and age distribution of cosmogenic structures of the earth," DAN SSSR 238/5, 1087-1090 (1978).

38. Firsov, L.V., "Meteoritic origin of Puchezh-Katun Crater," Geotektonika 2, 106-118 (1965).

39. Fleischer, R.L. and P.B. Price, "Fission track evidence of the simultaneous origin of tektites and other natural glasses," Geochim. et cosmochem. acta 28/3, 755-760 (1964).

40. Fleischer, R.L., P.B. Price and R.M. Walker, "Nuclear tracks in solids," in the book Principles and Application, Univ. Calif. Press, Berkeley, 1975, p. 350-352.

41. Florenskiy, K.P., "Initial stage of differentiation of the substance of the earth," Geokhimiya 8, 909-917 (1965).

42. Florenskiy, P.V., "Zhamanshin meteor crater (Northern Aral region) and its tektites and impactites," Izv. AN SSSR. Ser. geol. 10, 73-86 (1975a).

43. Florenskiy, P.V., "Irgizites, tektites of the Zhamanshin meteor crater (Northern Aral region)," Astron. vestn. 9/4, 237-243 (1975b).

44. Florenskiy, P.V., "First find of tektites in the USSR," Priroda 1, 85-87 (1976).

45. Florenskiy, P.V., "First find of tektites in the USSR: (Zhamanshin meteor crater. Northern Aral region)," Meteoritika 36, 120-122 (1977).

46. Florenskiy, P.V., A.I. Dabizha, A.O. Aaloe et al, "Geological and geophysical characteristics of Zhamanshin meteor crater: (from materials of 1977 expedition)," Meteoritika 38, 86-98 (1979a).

47. Florenskiy, P.V., Yu.P. Dikov and T.S. Gendler, "Structural and chemical features of tektites as a result of their melting and quenching," Meteoritika 37, 152-159 (1978).

48. Florenskiy, P.V., V.P. Perelygin, M.L. Bazhenov et al, "Combined determination of age of Zhamanshin meteor crater," Astron. vestn. 13/3, 178-186 (1979b).

49. Florenskiy, P.V., Ye.I. Zabelin, S.V. Mochalov and Yu.G. Pimenov, "Nonuniformity of distribution of circular structures of the Moon by their diameters," in the book Problemy geologii Luny [Problems of Geology of the Moon], Nauka Press, Moscow, 1969, p. 206-228 (Tr. GIN AN SSSR, Issue 204).

50. Florensky, P.V., "The first tektite deposit in a meteoritic crater (Zhamanshin, North Aral regions, USSR)," in the book Symposium on Planetary Cratering Mechanics, Flagstaff, Lunar Sci. Inst. NASA, Houston, Texas, 1976a, p. 33-35.

51. Florensky, P.V., "The Zhamanshin meteorite crater (The Northern Near-Aral, USSR), and its tektites and impactites," NASA Techn. transl. F-16765, suppl. and correct., 1976b.

52. Florensky, P.V., "The Zhamanshin meteorite crater (The Northern Aral region, USSR) and its tektites and impactites," Chem. Erde 36/1, 83-95 (1977a).

53. Florensky, P.V., "The Zhamanshin meteorite crater (Northern Aral Sea region) and its tektites and impactites," Intern. Geol. Rev. 19, 526-538 (1977b).

54. Florensky, P.V., "Structural chemical peculiarities of the

tektite -- the result of melting and quenching," Chem. Erde 37/2, 109-118 (1978).

55. Florensky, P.V., N. Short, S.R. Winzer and K. Fredricsson, "The Zhamanshin structure: geology and petrography," Meteoritics 12/3, 227-228 (1977).

56. Foster, G.E., "The meteor crater story," Publ. Meteor Crater Enterprises, Flagstaff, 1978, 44 pp.

57. Fredricsson, K., A. de Gasparis and W. Ehmann, "The Zhamanshin structure: chemical and physical properties of selected samples," Meteoritics 12/2, 229-230 (1977).

58. Fudali, R.F., D.P. Gold and J.J. Gurney, "The Pretoria Salt Pan: astrobleme or cryptovolcano?" Geology 81/4, 495-507 (1973).

59. Garetskiy, R.G. and O.Ye. Gorshenin, "Discovery of Upper Cretaceous deposits in Zhamanshin natural landmark (Irgiz River basin in Northern Aral region)," DAN SSSR 148/5, 1152-1156 (1963).

60. Garetskiy, R.G. and V.I. Shraybman, Glubina zaleganiya i stroyeniye skladchatogo fundamenta severnoy chasti Turanskoy plita [Depth of Occurrence and Structure of Folded Basement of Northern Part of Turan Plate], USSR Academy of Sciences Press, Moscow, 1960, 85 pp (Tr. GIN AN SSSR, Issue 44).

61. Gault, D.E., W.L. Quaide and V.K. Oberbeck, "Modelling meteorite craters in the laboratory. I. Mechanics of formation," Trans. Amer. Geophys. Union 47/1, 148 (1966).

62. Gendler, T.S., P.V. Florenskiy and R.N. Kuz'min, "State of iron ions as indicator of Irgizite tektite formation conditions," Astron. vestn. 11/3, 179-185 (1977).

63. Gentner, W., T. Kirsten, D. Storzer and G.A. Wagner, "K-Ar and fission track dating of Darwin Crater glass," Earth and Planet. Sci. Lett. 20/2, 204-210 (1973).

64. Gilbert, G.K., "The origin of hypotheses, illustrated by the discussion of a topographic problem," Science, N.S. 3, 1-13 (1896).

65. Glass, B.P., "Zhamanshin crater: possible source of the Australasian tectites? (abstract)," Geology 7/7, 351-353 (1979).

66. Glass, B.P. and R.A. Borlow, "Mineral inclusion in Muong Nong-type indochinites: implications concerning parent material and process of formation," Meteoritics 14/1, 55-68 (1979).

67. Gorshkov, A.P., "Plutonic structure of Malyy Semyachik volcano

in Kamchatka from gravimetric data," Geologiya i geofizika 4, 103-108 (1973).

68. Green, G., "Geological sciences as applied to studies of the Moon," in the book Novoye o Lune [The Latest About the Moon], USSR Academy of Sciences Press, Moscow-Leningrad, 1963, pp. 126-196.

69. Gretskaya, T.A., "Tektites," in the book BSE [Great Soviet Encyclopedia], 3rd ed, Sovetskaya entsiklopediya Press, Moscow, 1976, vol. 25, p. 369-370.

70. Halliday, J. and A.A. Griffin, "Summary of drilling at the West Hawk Lake Crater," J. Roy. Astron. Soc. Canada 61/1, 1-8 (1967).

71. Hartmann, W.K., "Terrestrial and lunar flux of large meteorites in the last two billion years," Icarus 4/2, 157-165 (1965).

72. Hartmann, W.K., "Early lunar cratering," Icarus 5/14, 406-418 (1966).

73. Hartung, J.B. and Pivolo, "A possible source in Cambodia for Australasian tektites," Meteoritics 14/1, 153-160 (1979).

74. Heide, K. and H.-G. Schmidt, "Thermal outgassing behavior and gas content of Irgizites," Chem. Erde 37/3, 271-273 (1978).

75. Hutchison, R., "Meteorite research old and new," Nature 268/8, 69-70 (1977).

76. Innes, M.J.S., "The use of gravity methods to study the underground structure and impact energy of meteorite craters," J. Geophys. Res. 66/7, 2225-2239 (1961).

77. Ivanov, A.V., K.P. Florenskiy, M.A. Nazarov and I.D. Shevale skiy, "Some manifestations of volatilization and condensation processes in formation of lunar regolith particles," DAN SSSR 221/2, 458-561 (1975).

78. Journal of Geophysical Research 76/23, 5380-5798 (1971).

79. Kahle, H.G., "Estimation of the disturbed mass in Nordlinger Ries," Z. Geophys. 35, 317-345 (1969).

80. King, E.A. and J. Arndt, "Water content of Russian tectites," Nature 269/5623(9), 48-49 (1977).

81. Kiryukhin, L.G. and P.V. Florenskiy, "Paleozoic rocks of the Northern Aral region," Izv. AN SSSR. Ser. geol. 9, 135-140 (1968).

82. Kiryukhin, L.G., P.V. Florenskiy and Yu.S. Sobolev, "The Zhamanshin puzzle," Priroda 3, 70-77 (1969).

83. Kiselev, L.I. and A.I. Bachin, "The geological position of the ultrabasic rocks of the Irgiz region (Southwestern Turgay)," in the book Geologiya Turgayskogo Progiba i Priaral'ya. -- Tr. VSEGEI. Nov. ser. [Geology of the Turgay Depression and the Northern Aral Region: Proceedings of All-Union Scientific Research Institute of Geology, New Series], vol. 129, 1967, p. 113-121.

84. Kohen, A., "Hypotheses of tektite formation as a result of an asteroid or comet impact: Tektite dispersion field," in the book Tektity [Tektites], Mir Press, Moscow, 1966, p. 226-293.

85. Konta, J. and L. Mraz, "Volatility of oxides from silicate melt and the origin of moldavites," Mineral. Mag. 40/309, 70-78 (1975).

86. Kostik, G.A and B.V. Piliya, "Quaternary volcanic glasses of the Zhamanshin natural landmark in the Irgiz region," Izv. AN SSSR. Ser. geol. 2, 145-148 (1973).

87. Krinov, Ye.L., "Meteor craters on the surface of the earth," Meteoritika 22, 3-30 (1962).

88. Kuznetsov, I.I., K.R. Plekhanova and A.A. Lapisheva, "Cenozoic volcanic rocks of the southwestern part of the Turgay depression," Sov. geologiya 2, 142-146 (1974).

89. Kvasha, L.G. and G.S. Gorshkov, "Vector diagram of chemical composition of tektites and terrestrial lavas," Meteoritika 20, 193-203 (1961).

90. Lichkov, B.L., "Natural waters of the earth and lithosphere," Zap. geogr. o-va AN SSSR. Nov. ser. 19, 164 pp (1960).

91. Malahoff, A. and G.P. Woolard, "Magnetic measurements of the Hawaiian Ridge and their volcanological implications," Bull. Volcanol. 29, (1966).

92. Malysheva, T.V., Effekt Myessbauera v geokhimii i kosmokhimii [The Mössbauer Effect in Geochemistry and Astrochemistry], Nauka Press, Moscow, 1975, 166 pp.

93. Marzlof, J.G., J.T. Dehr and J.F. Salmon, "The Mössbauer study of tectites, pyroxene and olivine," in the book Mössbauer Effect and Its Application in Chemistry, Academic Press, New York, 1965.

94. Masaitis, V.L., "Extreterrestrial impact in the USSR," Meteoritics 12/3, 305 (1977).

95. Masaytis, V.L., Geologicheskiye posledstviya padeniy kraterobrazuyushchikh meteoritov [Geological Consequences of the Impacts of Crater Forming Meteorites], Nedra Press, Leningrad, 1973, 19 pp.

96. Masaytis, V.L., "Basic outlines of the geology of USSR astroblems," in the book Meteoritnyye struktury na poverkhnosti Zemli i planet [Meteorite Structures on the Surfaces of the Earth and Planets], Nauka Press, Moscow, 1979, p. 173-191.

97. Masaytis, V.L., M.A. Mashchak, A.I. Raykhlin et al, "Meteorite craters and astroblems in the territory of the USSR," DAN SSSR 240/15, 1191-1193 (1978).

98. Masaytis, V.L., M.V. Mikhaylov and T.V. Selivanovskaya, Popigayskiy meteoritnyy krater [Popigay Meteor Crater], Nauka Press, Moscow, 1976, 124 pp.

99. Meen, V.L., "Chubb crater, Ungava, Quebec," J. Roy. Astron. Soc. Canada 44/5, 169-180 (1950).

100. Meteoritnyye struktury na poverkhnosti planet [Meteorite Structures on the Surfaces of Planets], V.V. Fedynskiy and A.I. Dabizha (ed), Nauka Press, Moscow, 1979, 240 pp.

101. Mekhanika obrazovaniya voronok pri udare i vzryve [Mechanics of Crater Formation by Impact and Explosion], Mir Press, 1977, 228 pp.

102. Mukhamedzhanov, A.K. and K.P. Stanyukovich, "Theories of lunar craters," Kosm. issled. 4/3, 403-413 (1966).

103. O'Keefe, J.A., Tektites and Their Origin, Amsterdam-Oxford-New York, 1976, 254 pp.

104. O'Keefe, J.A., "The tektite problem," Sci. Amer. 239/2, 115-125 (1978).

105. Palme, H., R. Wolf and R.A.F. Grieve, "New data on meteoritic material at terrestrial impact crater," in the book Lunar and Planetary Science. IX. 1978. Abstr., Houston, Texas, 1978, p. 856-858.

106. Parfenova, O.V., O.J. Yakovlev and V.D. Popovich, "Compositional variations produced by impact explosion event: some additional data and result," in the book Lunar and Planetary Science. IX. 1978. Abstr., Houston, Texas, 1978, p. 865-867.

107. Pashkovskiy, V.G., L.M. Shkerin and V.M. Lodygin, "Change of physical and mechanical properties of rocks as a result of a meteorite impact," Meteoritika 32, 150-152 (1973).

108. Perelygin, V.P., S.P. Tret'yakova and I.I. Zvara, "Recording nuclear fission with the aid of amorphous media," Pribory i tekhnika eksperimenta 4, 70-72 (1964).

109. Pervyye panoramy lunnoy poverkhnosti [First Panoramas of the Lunar Surface], Nauka Press, Moscow, 1966, 80 pp.

110. Philpotts, J.A., S. Schuhmann, S.R. Winzer and R.K.L. Lum, "The Zhamanshin structure: lithophile trace element abundances and strontium isotope systematics. Abstr.," Meteoritics 12/3, 338 (1977).

111. Pohl, J. and G. Angenheister, "Anomalies of Earth's magnetic field and magnetization of rocks in Nordlinger Ries, the Ries," Geol. bavarica 61, 327-336 (1969).

112. Pullen, M.W., "Geologic aspects of radio wave transmission, Report of Investigations," Dept. Registr. and Educ. Div. State Geol. Surv. No. 162, 1953, p. 111.

113. Raykhlin, A.I. and T.V. Selivanovskaya, "Breccias and impactites of explosive meteor craters and astroblems," in the book Meteoritnyye struktury na poverkhnosti Zemli i planet [Meteorite Structures on the Surfaces of the Earth and Planets], Nauka Press, Moscow, 1979, p. 65-80.

114. Regan, R.D. and W.J. Hinze, "Gravity and magnetic investigations of Meteor Crater, Arizona," J. Geophys. Res. 80/5, 776-788 (1977).

115. Robertson, R.V. and A.F. Grieve, "The astroblems of Canada," Priroda 9, 70-77 (1973).

116. Rode, O.D., A.V. Ivanov, M.A. Nazarov et al, Atlas mikrofotografiy poverkhnosti chastits lunnogo regolita [Atlas of Microphotographs of the Surfaces of Lunar Regolith Particles], Academia Press, Prague, 1979, 164 pp.

117. Rodin, G., Seysmologiya yadernykh vzryvov [Seismology of Nuclear Explosions], Mir Press, Moscow, 1974, 190 pp.

118. Sabaneyev, P.F., "Some results of modelling of lunar craters," in the book Novoye o Lune [The Latest About the Moon], USSR Academy of Sciences Press, Moscow-Leningrad, 1963, p. 314-324.

119. Sears, D.W., "The nature and origin of meteorites: Monographs on Astronomical Subjects 5," Adam Hilder, Bristol, 1978, p. 53-54.

120. Shnettsler, K. and U. Pinson, "Chemical composition of tektites," in the book Tektity [Tektites], Mir Press, Moscow, 1966, p. 137-188.

121. "Shock metamorphism of natural materials," B.M.French and N.M. Short (ed), in the book Proceedings of the First Conference Held, NASA, Goddard Space Flight Center, Greenbelt, Maryland, April 14-16, 1966, Mono Book Co., Baltimore, 1968, 644 pp.

122. Shoemaker, E.M., "Impact mechanics with the example of the Arizona Crater," in the book Vzryvnyye kratery na Zemle i planetakh [Explosive Craters on the Earth and Planets], Mir Press, Moscow, 1968, p. 184-221.

123. Short, N.M., "Impact processes in geology," in the book Vzryvnyye kratery na Zemle i planetakh [Explosive Craters on the Earth and Planets], Mir Press, Moscow, 1968, p. 30-67.

124. Sjogren, W.L., R.N. Winberly and W.R. Wollenhaupt, "Lunar gravity: Apollo 17," Moon 9/1, 115-128 (1974); 11/1/2, 35-40, 41-52 (1974).

125. Spencer, L.J., "Origin of tektites," Nature 131, 117-118; 132, 571 (1933).

126. Stanyukovich, K.P. and V.V. Fedynskiy, ""Destructive action of meteorite impacts," DAN SSSR 2, 129-132 (1947).

127. Stauffer, P.H., "Anatomy of the Australasian tektite strewnfield and the probable site of its source crater," in the book Third Regional Conference on Geology and Mineral Resources of South-east Asia, Bangkok, 14-18 Nov. 1978, p. 285-289.

128. Storzer, D. and G.A. Wagner, "Fission track dating of meteorite impacts," Meteoritics 12/3, 368-369 (1977).

129. Taylor, S.R. and S.M. McLennan, "Chemical relationships among irghizites, zhamanshinites, Australasian tektites and Henbury impact glasses," Geochim. et cosmochem. acta 43/9, 1551-1565 (1979).

130. Tektity [Tektites], J.A. O'Keefe (ed), Mir Press, Moscow, 1966, 303 pp.

131. Tilghman, B.C., "Coone Butte, Arizona," Proc. Acad. Nat. Sci. 57, 887-914 (1905).

132. Trifonov, V.G. and P.V. Florenskiy, "Geologic comparison of the Earth and the Moon," in the book Problemy geologii Luny [Problems of the Geology of the Moon], Nauka Press, Moscow, 1969, p. 274-285 (Tr. GIN AN SSSR, issue 204).

133. Vakhrameyev, V.A. and A.L. Yanshin, "The Paleozoic in the Northern Aral region," DAN SSSR 30/9, 818-821 (1941).

134. Val'ter, A.A. and Ye.P. Gurov, "Established and supposed extent of explosive meteor craters on the Earth and their preservation in the Ukrainian shield," in the book Meteoritnyye struktury na poverkhnosti Zemli i planet [Meteorite Structures on the Surfaces of the Earth and Planets], Nauka Press, Moscow, 1979, p. 126-148.

135. Val'ter, A.A. and V.A. Ryabenko, Vzryvnyye kratery Ukrainskogo shchita [Explosive Craters of the Ukrainian Shield], Naukova dumka Press, Kiev, 1977, 156 pp.

136. Vdovenko, V.M., A.S. Krivokhatskiy, V.G. Savonenko and A.N. Komarov, "Artificial analogs of tektites," Radiokhimiya 10/6, 688-695 (1968).

137. Vishnevskiy, S.A. and N.A. Pal'chik, "Coesite in Zahmanshin structure breccias," DAN SSSR 243/5, 1269-1272 (1978).

138. Vishnevskiy, S.A., R. Rost and Yu.A. Dolgov, "Gases in inclusions from Ries (FRG) impact glasses and finding of high pressure polymorphs of carbon," DAN SSSR 241/3, 695-698 (1978).

139. Vlodavets, V.I., "International symposium on volcanology in Japan in 1962," in the book Chetvertichnyy vulkanizm nekotorykh rayonov SSSR [Quaternary Volcanism of Some Regions of the USSR], Nauka Press, Moscow, 1965, p. 136-150.

140. Vysokoskorostnyye udarnyye yavleniya [High Velocity Shock Phenomena], R. Kinslow (ed), Mir Press, Moscow, 1973, 533 pp.

141. Vzryvnyye kratery na Zemle i planetakh [Explosive Craters on the Earth and Planets], Mir Press, Moscow, 1968, 266 pp.

142. Wasilewski, P.J., "Shock remagnetization associated with meteorite impact of planetary surfaces," Moon 6, 264-292 (1973).

143. Wegener, A., Proiskhozhdeniye Luny i yeye kraterov [Origin of the Moon and Its Craters], Gosizdat Press, Moscow, 1923, 48 pp.

144. Whipple, F.L., "Origins of meteoritic materials (survey papers)," in the book Physics and Dynamics of Meteors, L. Kresak and P. Millman (ed), 1968, p. 481-485.

145. Yakovlev, O.A., O.V. Parfenov and V.N. Arkhangel'skaya, "Composition change of rocks in formation of impact melts," DAN SSSR 240/4, 934-937 (1978).

146. Yanshin, A.L., Geologiya Severnogo Priaral'ya: Materialy k poszaniyu geologicheskogo stroyeniya SSSR [Geology of the Northern Aral Region: Materials for Identification of the

Geologic Structure of the USSR], issue 15(19), MOIP, Moscow, 1953, 736 pp.

147. Yokoyama, J. and A. Tajama, "Gravity survey on the Kuttuyaro Caldera by means of a worden gravimeter," Nature 4663, 739-790 (1959).

148. Zel'dovich, Ya.B. and Yu.P. Rayzer, Fizika udarnykh voln i vysokotemperaturnykh gidrodinamicheskikh yavleniy [The Physics of Shock Waves and High Temperature Hydrodynamic Phenomena], Nauka Press, Moscow, 1966.

149. Zeylik, B.S. and E.Yu. Seytmuratova, "Meteor structure in Central Kazakhstan and its magma controlling role," DAN SSSR 218/1, 67-70 (1974).

150. Zotkin, I.T. and V.I. Tsvetkov, "Searches for meteor craters on the Earth," Astron. vestn. 4/1, 55-65 (1970).

151. Zybin, M.I., I.V. Melekestsev, A.A. Tarakanovskiy and E.N. Erlikh, "Quaternary calderas of Kamchatka," in the book Vulkanizm i glubiny Zemli [Volcanism and the Interior of the Earth], Nauka Press, Moscow, 1971, p. 55-66.